COMPARATIVE PHYTOCHEMICAL, SPECTROSCOPIC ANALYSIS, AND NETWORK PHARMACOLOGY OF *Ficus sur* AND *Justicia secunda*: IMPLICATIONS ON SICKLE CELL ANAEMIA

BY

AGU, CHIAMAKA MARTINA
GOU/U22/BCH/310

BIOCHEMISTRY
DEPARTMENT OF CHEMICAL SCIENCE
FACULTY OF NATURAL SCIENCE AND ENVIRONMENTAL STUDIES
GODFREY OKOYE UNIVERSITY, ENUGU

JULY, 2026

COMPARATIVE PHYTOCHEMICAL, SPECTROSCOPIC ANALYSIS, AND NETWORK PHARMACOLOGY OF *Ficus sur* AND *Justicia secunda*: IMPLICATIONS ON SICKLE CELL ANAEMIA

BY

AGU, CHIAMAKA MARTINA
GOU/U22/BCH/310

BIOCHEMISTRY
DEPARTMENT OF CHEMICAL SCIENCE
FACULTY OF NATURAL SCIENCE AND ENVIRONMENTAL STUDIES
GODFREY OKOYE UNIVERSITY, ENUGU

A PROJECT RESEARCH REPORT SUBMITTED TO THE DEPARTMENT OF CHEMICAL SCIENCE, FACULTY OF NATURAL SCIENCE AND ENVIRONMENTAL STUDIES, GODFREY OKOYE UNIVERSITY, ENUGU, IN PARTIAL FULFILMENT OF THE REQUIREMENTS FOR THE AWARD OF BACHELOR OF SCIENCE (B.Sc.) DEGREE IN BIOCHEMISTRY.

SUPERVISOR: DR. EJIKEME. C

JULY, 2026

APPROVAL

This research titled "Comparative Phytochemical, Spectroscopic analysis, and Network Pharmacology of *Ficus sur* and *Justicia secunda*: Implications on Sickle Cell Anaemia" has been assessed and approved by the Committees of Department of Chemical Sciences and Faculty of Natural Sciences and Environmental Studies, Godfrey Okoye University, Enugu, Nigeria.

Dr. Ejikeme C.	.....	.....
Supervisor	Signature	Date
Dr. Anosike Joy .C.	.....	.....
HOD, Department of Chemical Sciences	Signature	Date
Prof. Chidi Uhuegbu	.....	.....
Dean, FNSES	Signature	Date
	.....	.....
External Examiner	Signature	Date

CERTIFICATION

This is to certify that this research titled "Comparative Phytochemical, Spectroscopic analysis, and Network Pharmacology of *Ficus sur* and *Justicia secunda*: Implications on Sickle Cell Anaemia" was carried out by AGU, CHIAMAKA MARTINA (Registration Number: GOU/U22/BCH/310) under supervision in the Department of Biochemistry, Godfrey Okoye University, Enugu. It has been read and approved as meeting the requirements for the award of the degree of Bachelor of Science (B.Sc.) in Biochemistry.

Dr. Ejikeme C.	.....	.....
Supervisor	Signature	Date
Dr. Anosike Joy .C.	.....	.....
HOD,	Signature	Date
Department of Chemical Sciences		

DEDICATION

To the Almighty God, the Source of all wisdom and knowledge, whose grace sustained me through every step of this journey.

ACKNOWLEDGEMENTS

I give all glory and honour to Almighty God, whose grace, wisdom, and strength carried me through the entire duration of this research. This work would not have been possible without Him.

I wish to express my deepest and most sincere gratitude to my project supervisor, Dr. Ejikeme C., for her exceptional guidance, patience, intellectual rigour, and unwavering commitment to excellence throughout the course of this research. Her insightful direction shaped the scientific quality of this work in ways I am profoundly grateful for.

I owe an immeasurable debt of gratitude to my co-supervisor, Dr. Ijoma, who introduced me to the world of computational biochemistry and guided me through every stage of the network pharmacology, molecular docking, and bioinformatics analyses that form the heart of this study. His mentorship, patience, and technical expertise were indispensable, and I am deeply grateful for the countless hours he invested in teaching me.

My profound appreciation goes to Mrs. Amara Nnadikwe, our Laboratory Technician, who was present from the very first day of laboratory work to the very last. She guided me through every bench procedure with remarkable dedication, skill, and patience, ensuring every experiment was conducted properly and safely. Her practical wisdom and personal investment in this project went far beyond professional duty, and I am truly grateful for everything she did.

I also extend my sincere appreciation to the Head of Department of Chemical Sciences, Godfrey Okoye University, Enugu, and to all the lecturers of the Department whose teaching, encouragement, and academic support throughout my undergraduate programme provided the foundation upon which this research was built.

Finally, I am profoundly grateful to the family of Ogbuefi and Lolo Joseph Uwaezuoke Onaga, for their unwavering support, prayers, and constant belief in me from the very beginning of my university journey to the end. I am equally grateful to my mother, who believed in me every step of the way and constantly reminded me that I could do it. This work is a living testimony to your love, sacrifice, and faith in me. Thank you.

ABSTRACT

Sickle cell anaemia (SCD) is the most prevalent monogenic haemoglobinopathy in Nigeria, yet definitive treatment remains largely inaccessible, sustaining reliance on ethnomedicinal "blood-building" plants such as *Ficus sur* Forssk. and *Justicia secunda* Vahl. This study integrated phytochemical screening, proximate analysis, FTIR spectroscopy, atomic absorption spectroscopy (AAS), and network pharmacology with molecular docking to identify drug-like compounds from both leaf extracts and characterise the blood-related molecular targets they engage, interpreted specifically in the context of SCD. Ethanolic Soxhlet extraction gave yields of 7.04% (*F. sur*) and 8.56% (*J. secunda*). Qualitative screening confirmed alkaloids, flavonoids, tannins, saponins, phenols, terpenoids, and reducing sugars in both extracts, with steroids/triterpenoids unique to *F. sur* and cardiac glycosides to *J. secunda*. FTIR-ATR spectra showed characteristic O–H, aromatic C=C/N–H, and C–O–C glycosidic bands consistent with polyphenolic and flavonoid glycosides. AAS quantified twelve elements, with *F. sur* showing markedly higher calcium (280.56 vs 80.16 mg/L) and comparable iron content (2.60 vs 2.54 mg/L) to *J. secunda*; lead and cadmium were undetected in both. Of sixty literature-reported compounds screened for drug-likeness, nine met criteria and eight proceeded to network pharmacology, yielding 32 compound–target interactions dominated by the Fanconi anaemia DNA-repair pathway (15/32 genes; FDR = 1.03×10^{-30}). Molecular docking of 22 compound–target complexes identified piperine–BRCA2 ($\Delta G = -8.4$ kcal/mol) and apigenin–ATM (-8.2 kcal/mol) as strongest interactions, while caffeic acid and p-coumaric acid from *F. sur* directly engaged the haem-binding pockets of HBA1 and HBA2. These findings provide the first mechanistically grounded, compound-level evidence linking both plants' traditional anti-sickling use to antioxidant protection, genomic-stability support, and direct haemoglobin structural engagement, supporting their potential as complementary phytotherapeutic adjuncts for sickle cell anaemia management pending experimental validation.

TABLE OF CONTENTS

LIST OF TABLES

LIST OF FIGURES

CHAPTER ONE

INTRODUCTION

1.1 Background to the Study

Sickle cell anaemia (SCD) is the most common monogenic blood disorder worldwide and the single most significant inherited haemoglobinopathy in sub-Saharan Africa. The disease arises from a single point mutation in the beta-globin (HBB) gene (GAG→GTG, Glu6Val), producing abnormal haemoglobin S (HbS) that polymerises under deoxygenated conditions, distorting the erythrocyte into the characteristic rigid, sickle shape. These sickled cells are mechanically fragile, prone to premature intravascular and extravascular haemolysis, and capable of occluding microvascular beds, producing the twin clinical hallmarks of the disease: chronic haemolytic anaemia and recurrent, painful vaso-occlusive crises. Nigeria carries the single largest global burden of SCD, with an estimated 150,000 children born annually with the homozygous (HbSS) genotype and an estimated national carrier (HbAS) prevalence of approximately 20-30% in some populations, making the disease a major paediatric and public health priority. Definitive disease-modifying treatment (hydroxyurea, chronic transfusion, and curative haematopoietic stem cell transplantation) remains costly, logistically demanding, and largely inaccessible to most Nigerian patients, who instead rely heavily on supportive and traditional management. *Ficus sur* Forssk. (Moraceae) and *Justicia secunda* Vahl (Acanthaceae) are two such ethnomedicinal plants, independently and widely documented across Nigerian, Cameroonian, and Caribbean traditional medicine as "blood-building" remedies, with several traditional and folkloric records explicitly naming sickle cell anaemia among the conditions they are used to manage. Despite this ethnomedicinal pedigree, neither plant has been investigated using an integrated, compound-level approach that identifies which of their many constituent phytochemicals are even viable drug candidates, and what molecular machinery those surviving candidates actually engage. This study addresses that gap by

combining phytochemical screening, FTIR spectroscopy, atomic absorption spectroscopy, and computational network pharmacology with molecular docking, to identify the drug-like compounds of both plants and characterise the blood-related molecular targets they engage, interpreted specifically in the context of sickle cell anaemia pathology.

1.2 Statement of the Problem

Despite the extensive ethnomedicinal record linking *F. sur* and *J. secunda* to the management of anaemia and, specifically in several documented sources, sickle cell anaemia, neither plant has been subjected to an integrated, compound-first investigation capable of identifying which of their phytochemical constituents are pharmacologically viable as drug candidates and which human molecular targets those candidates engage. Existing studies on both plants are fragmented: phytochemical screening, in vivo haematological assays, and isolated structural characterisation have each been reported individually, but no study has combined gravimetric extraction, qualitative phytochemical screening, comparative FTIR functional-group profiling, validated AAS mineral analysis, in silico ADME-based virtual screening, network pharmacology, and molecular docking within a single comparative investigation of both species. Consequently, the specific compounds responsible for the traditionally reported anti-sickling and haematinic effects of *F. sur* and *J. secunda*, and the molecular targets through which they might act, remain scientifically undefined. This creates a critical gap between traditional ethnomedicinal use and an evidence-based, mechanistically grounded case for the development of either plant as an adjunct phytotherapeutic for sickle cell anaemia.

1.3 Aim and Objectives of the Study

1.3.1 Aim

To conduct an integrated phytochemical, FTIR spectroscopic, atomic absorption spectroscopic, and network pharmacological investigation of *Ficus sur* Forssk. and *Justicia secunda* Vahl, in order to identify their drug-like bioactive compounds and characterise the blood-related

molecular targets they engage, with specific interpretation of findings in the context of sickle cell anaemia.

1.3.2 Specific objectives

The objectives of this study were to:

i. Qualitatively screen the leaf extracts of both plants for phytochemical constituents by conventional methods.

ii. Comparatively determine the functional group profiles of both extracts using FTIR-ATR, and compare the elemental mineral content (Fe, Zn, Cu, Mn, Ca, Mg, Na, K, Pb and Cd) of both extracts by flame Atomic Absorption Spectroscopy (AAS).

iii. Identify the bioactive compounds of both plants from the literature and subject them to in silico Absorption, distribution, metabolism and excretion (ADME)-based virtual screening to eliminate compounds that are not drug-like, retaining only pharmacologically viable candidates.

iv. Predict the human molecular targets of the surviving drug-like compounds, cross-reference these against blood- and anaemia-associated genes, construct the resulting compound-target-pathway network, and confirm the strongest predicted interactions by molecular docking, reporting binding free energies (ΔG, kcal/mol).

v. Interpret the combined phytochemical, spectroscopic, mineral, and network pharmacological data to identify the specific compounds and molecular targets of both plants most relevant to the pathophysiology of sickle cell anaemia.

1.4 Scope of the Study

This study is limited to a comparative investigation of the phytochemistry, FTIR functional-group spectroscopy, mineral elemental composition, and computational network pharmacology and molecular docking of leaf extracts of *F. sur* and *J. secunda*. In vitro and in vivo pharmacological validation, clinical testing, and isolation of pure compounds are outside the

scope of this study; all bioactivity claims relating to sickle cell anaemia in this work are derived from literature evidence and in silico/computational prediction, and are presented as testable hypotheses for future experimental validation rather than as established clinical efficacy.

1.5 Significance of the Study

This study produced several novel scientific contributions: the first simultaneous, directly comparable phytochemical and FTIR spectroscopic profile of *F. sur* and *J. secunda* leaf extracts under identical experimental conditions; the first quantitative AAS elemental profile of *J. secunda*; and the first network pharmacology and molecular docking analysis to identify the specific drug-like compounds of either plant and the blood-related molecular targets they engage, interpreted in the context of sickle cell anaemia. By narrowing focus from generic anaemia to sickle cell anaemia specifically, the study provides a more clinically actionable, mechanistically grounded scientific basis for the continued ethnomedicinal use of both plants among populations living with this disease, particularly in Nigeria, where the burden of sickle cell anaemia is the highest in the world.

1.6 Limitations of the Study

This study has limitations. Network pharmacological predictions are statistical and computer-based, and molecular docking provides estimated rather than experimentally measured binding affinities; in vitro and in vivo experimental validation is outside the scope of this study. The molecular docking tool used assumes rigid or semi-flexible receptor conformations and may not fully capture the dynamic behaviour of proteins in solution. Sickle cell anaemia is a complex, multi-system disease, and the molecular targets discussed in this study, while biologically relevant, represent only a subset of the full pathophysiological picture; clinical extrapolation from these findings should therefore be made with appropriate caution pending experimental confirmation.

CHAPTER TWO

LITERATURE REVIEW

2.1 Overview of Sickle Cell Anaemia as a Global and Public Health Problem

Sickle cell anaemia (SCD, HbSS genotype) is the most prevalent monogenic disorder of haemoglobin worldwide, caused by a single adenine-to-thymine substitution in codon 6 of the beta-globin (HBB) gene, which replaces glutamic acid with valine and produces structurally abnormal haemoglobin S (HbS). Under deoxygenated conditions, HbS molecules polymerise into long, rigid fibres that distort the erythrocyte into the characteristic sickle shape. Sickled cells are mechanically fragile and are removed prematurely from circulation by both intravascular and extravascular haemolysis, producing chronic haemolytic anaemia, while their rigidity and abnormal adhesion to vascular endothelium precipitate microvascular occlusion, the second hallmark of the disease, manifesting clinically as recurrent painful vaso-occlusive crises, acute chest syndrome, stroke, and progressive multi-organ damage. The disease is most prevalent in sub-Saharan Africa, where the sickle-cell trait (HbAS) confers partial resistance to severe falciparum malaria and has therefore been maintained at high frequency by balancing natural selection. Nigeria carries the largest absolute burden of SCD of any country in the world, with an estimated 150,000 children born with the HbSS genotype annually and carrier (HbAS) prevalence reported at approximately one in four in some Nigerian populations. The disease imposes a substantial burden of childhood mortality, recurrent hospitalisation, chronic organ damage, and economic hardship on affected families, while definitive disease-modifying interventions, hydroxyurea therapy, regular blood transfusion, and curative haematopoietic stem cell transplantation, remain largely inaccessible to most patients in low-resource settings because of cost, infrastructure, and donor availability constraints. This treatment gap is a central driver of the continued and widespread reliance on ethnomedicinal "blood-building"

plant remedies among Nigerian SCD patients and their caregivers, which this study takes as its point of departure.

Anaemia has far-reaching implications, beyond the haematology lab. In pre-school children, anaemia caused by iron deficiency retards cognitive development, interferes with schoolwork, slows linear growth, and reduces the strength of the immune response: some of these effects are partially irreversible when anaemia develops in the first two years (Kassebaum and GBD 2013 Anaemia Collaborators, 2016). In reproductive-age women, anaemia is a key risk factor for maternal death, preterm birth, low birth weight and infant morbidity. In the workforce, anaemia's impact on stamina and productivity in physiological anaemia reduces income and entrench poverty. The world's anaemia burden has declined from 28.2% in 1990 to 24.3% in 2021 (GBD 2021 anaemia, 2023) despite several, well-tolerated, effective pharmaceutical haematinics (ferrous sulphate, ferrous fumarate, folic acid, and cyanocobalamin); this is modest progress given the multi-aetiology nature of this complex syndrome. The expense, poor patient adherence, and limited availability of pharmaceuticals in resource-limited settings have compounded the problem. This is where traditional and emerging scientific evidence for the haematinic activity of *Ficus sur* Forssk. and *Justicia secunda* Vahl is scientifically and clinically relevant.

2.2 Ethnopharmacological Use of Medicinal Plants for Anaemia and Sickle Cell Anaemia Management in Africa

Across sub-Saharan Africa, plant-based remedies remain a primary or adjunct source of haematinic and anti-sickling therapy for populations with limited access to definitive SCD care. Justicia carnea Lindl., a close congener of *J. secunda*, is among the most extensively studied African anti-anaemic plants, with documented network-pharmacological evidence of anti-anaemic mechanisms (Abdullahi *et al*., 2023). In Cote d'Ivoire, Kone *et al*. (2012) catalogued numerous plant species used traditionally in the management of anaemia, several explicitly

recommended for sickle cell patients. The specific traditional use of *F. sur* and *J. secunda* for sickle cell anaemia, rather than anaemia in general, is independently documented across at least two geographically distinct ethnomedicinal traditions: the NMPPDB (2024) records *F. sur* among plants traditionally used for sickle cell anaemia in Nigeria, while Koffi *et al*. (2013) report that fresh *J. secunda* leaf juice is used in Cameroon and Cote d'Ivoire specifically to manage sickle cell disease. This convergent, independent ethnomedicinal targeting of sickle cell anaemia specifically, rather than anaemia as an undifferentiated category, by traditional healers in geographically separate regions is a strong signal that both plants may contain anti-sickling or erythroprotective phytochemicals worthy of rigorous scientific characterisation, and provides the direct ethnopharmacological rationale for the present study's narrowed focus on sickle cell anaemia.

2.3 *Ficus sur* Forssk. (Moraceae): Taxonomy, Authentication, Botanical Description, Distribution, and Ethnomedicinal Uses

Ficus sur Forssk. (family Moraceae) has been reported by various researchers as *Ficus sur* Thunb. and *Ficus quibeba* Ficalho. The most recent botanical thinking, as exemplified by Plants of the World Online (POWO), recognises *Ficus sur* Forssk. as the correct name, while *Ficus sur* Thunb. is a synonym. This is a significant distinction and has been adhered to in this study. The botanical material used in this work was nomenclaturally authenticated by Felix I. Nwafor, Plant Taxonomist Curator of University of Nigeria Herbarium (UNN), Department of Plant Science and Biotechnology, Faculty of Biological Sciences, University of Nigeria, Nsukka, on March 2026. The accession number of the voucher specimen at UNN was UNN/11770, family MORACEAE, scientific name *Ficus sur* Forssk. The certificate was issued to Nnadikwe, Amara, Godfrey Okoye University, Enugu. The UNN is registered on Index Herbariorum, the world's herbarium database. Full scientific classification is detailed in Table 2.1.

Table 2.1: Scientific classification of *Ficus sur* Forssk. (syn. *Ficus sur* Thunb.)

Classification Level	Taxon
Kingdom	*Plantae*
Division	*Magnoliophyta*
Class	*Magnoliopsida*
Order	*Rosales*
Family	*Moraceae*
Genus	*Ficus L.*
Accepted Species Name	*Ficus sur Forssk.*
Synonym	*Ficus capensis Thunb.; Ficus guineensis (Miq.) Stapf; Ficus ituriensis De Wild.; Ficus mallotocarpa Warb.; Ficus riparia (Miq.) A.Rich.; Ficus thonningiana (Miq.) Miq.*
Species ID (NMPPDB)	*NMP-069 | WFO ID: wfo-0000687678*
NCBI Taxonomy ID	*3090068*
Voucher (This study)	*UNN/11770, UNN, Nsukka — issued March 2026*

Source: NMPPDB (2024); POWO (2024); University of Nigeria Herbarium Authentication Certificate (2026).

Ficus sur is a medium to large deciduous tree that typically attains heights of 10–20 metres, with a broadly spreading crown and a rough, greyish-brown bark that releases white latex when cut. The leaves are large, simple, alternate, and ovate to broadly elliptic in shape, measuring 10–25 cm in length, with entire to slightly wavy margins. The plant displays cauliflory, bearing its small rounded figs (1–2 cm diameter) directly on the main trunk and branches rather than on leafy shoots. These figs ripen from green to orange-red and serve as food for frugivorous birds and mammals. The species is distributed across sub-Saharan Africa from Senegal and Nigeria westward to Ethiopia and Somalia, and southward through the Great Lakes region to South Africa. In Nigeria it grows naturally in lowland rainforests, derived savannah, gallery forests, and disturbed secondary vegetation, at elevations of up to 1,800 m above sea level (NMPPDB, 2024; Coates Palgrave, 2002). In Nigerian traditional medicine, the aqueous leaf decoction is the most commonly administered preparation, given orally to anaemic patients, post-partum women, and individuals recovering from chronic illness. Traditional practitioners across Igbo, Yoruba, and Hausa communities consistently describe it as a 'blood builder'—reinforced by the reddish colouration of the aqueous extract—a description independently documented in Ghana, Cameroon, Uganda, and South Africa (Menezes and collaborators, 2022).

2.3.1 Local names and ethnolinguistic distribution in Nigeria

The diversity of vernacular designations for *F. sur* across Nigerian linguistic groups reflects its wide geographic distribution and the independent ethnomedicinal recognition it has received across culturally distinct communities. Table 2.2 presents the documented local names across major Nigerian tribes and selected other African regions.

Table 2.2: Local names of *Ficus sur* Forssk. across Nigerian linguistic groups and other African regions

Local Name	**Language/Tribe**	**Region/Country**
Opoto	Yoruba	Southwestern Nigeria
Anwerenwa	Igbo	Southeastern Nigeria
Farin Baure	Hausa	Northern Nigeria
Ogbaikolo	Igala	North-Central Nigeria (Kogi State)
Akoro	Nsukka Igbo	Enugu State, SE Nigeria
Etai	Igbo (dialectal)	Southeastern Nigeria
Umvubu	Zulu	KwaZulu-Natal, South Africa
Mkuyu	Swahili	East Africa (Kenya, Tanzania)
Cape Fig / Broom Cluster Fig	English	Pan-African (common names)

Source: NMPPDB (2024); Burkill (1985); Lawal *et al*. (2016).

Figure2.1: *Ficus sur* Forssk. (syn. *Ficus sur* Thunb.), showing characteristic cauliflorous fig clusters (syconia) borne directly on the main branches, ripening from green to orange-red — a diagnostic feature of the species. Family: Moraceae. Voucher: UNN/11770, University of Nigeria Herbarium, Nsukka (2026).

Source: Nigerian Medicinal Plants and Phytochemicals Database — NMPPDB (2024). Available at: nmppdb.com.ng/species-details?specy=ficus-capensis [Accessed: April 2024].

2.3.2 Ethnopharmacological uses

F. sur has a wide spectrum of uses across its geographical range. Traditional uses reported in NMPPDB (2024) include anaemia, sickle cell anaemia, leprosy, leukoderma, wounds, oedema, respiratory infections, diarrhoea and dysentery, tuberculosis, epilepsy, rickets, sexually transmitted diseases, gonorrhoea and infertility. In southern-west Nigeria, Yoruba healers use root bark decoctions as primary haematinic medicines; they apply the leaf latex topically for warts and ringworm. Traditional midwives in the southeast Nigeria use root bark as a post-partum haemopoietic tonic (Akomolafe *et al*., 2016). Northern Nigerian Hausa practitioners administer the leaves orally to adjunct-treat malaria (Esievo *et al*., 2018). Validated scientific uses include antidiarrheal effects (root decoctions, South Africa); anti-ACE, anti-AChE and anti-arginase activity in erectile dysfunction (IC50 value for ACE = 52.17 μg/mL; Akomolafe *et al*., 2016); anti-diabetic activity (150 mg/kg body weight; Ezeigwe *et al*., 2020); in vitro promotion of wound healing (bark paste; Shi *et al*., 2018); and potent anti-anaemic activity on phenylhydrazine-treated anaemic rats (Okafor *et al*., 2021; Saidu *et al*., 2020).

2.3.3 Phytochemical constituents of *Ficus sur*

Phytochemical studies of *F. sur* have consistently shown a broad spectrum of secondary metabolites in leaves, bark, roots and fruits. Studies and analysis show the total phenol content of 15.4 to 48.6 mg gallic acid equivalents (GAE) per gram of extract and total flavonoids of 8.2-23.7 mg quercetin equivalents (QE) per gram of extract, with consistently higher values obtained in methanol than in water (Mgbemena *et al*., 2022; Owolabi *et al*., 2022). The molecular formulae of the twenty bioactive compounds identified from research articles (Akomolafe *et al*., 2016; Lawal *et al*., 2016; Esievo *et al*., 2018; Harmander Singh *et al*., 2022; NMPPDB, 2024) are listed in Table 2.3. Figures 2.1(a)–2.1(t) depict their two-dimensional structures.

Table 2.3: Bioactive compounds identified from *Ficus sur* Forssk. with molecular formulae and literature sources

No.	Compound Name	Molecular Formula	Primary Source(s)
1	Lupeol	$C_{30}H_{50}O$	Akomolafe *et al*. (2016); NMPPDB (2024)
2	β-Sitosterol	$C_{29}H_{50}O$	Lawal *et al*. (2016); NMPPDB (2024)
3	β-Amyrin	$C_{30}H_{50}O$	Lawal *et al*. (2016)
4	α-Amyrin	$C_{30}H_{50}O$	Akomolafe *et al*. (2016); Harmander Singh *et al*. (2022)
5	Xanthotoxin	$C_{12}H_8O_4$	Esievo *et al*. (2018)
6	Campesterol	$C_{28}H_{48}O$	Lawal *et al*. (2016)
7	Stigmasterol	$C_{29}H_{48}O$	Lawal *et al*. (2016); Harmander Singh *et al*. (2022)
8	Quercetin	$C_{15}H_{10}O_7$	Harmander Singh *et al*. (2022); NMPPDB (2024)
9	Rutin	$C_{27}H_{30}O_{16}$	Harmander Singh *et al*. (2022); NMPPDB (2024)
10	Ellagic Acid	$C_{14}H_6O_8$	Harmander Singh *et al*. (2022); NMPPDB (2024)
11	Gallic Acid	$C_7H_6O_5$	Akomolafe *et al*. (2016); NMPPDB (2024)
12	Kaempferol	$C_{15}H_{10}O_6$	Harmander Singh *et al*. (2022)
13	Chlorogenic Acid	$C_{16}H_{18}O_9$	Harmander Singh *et al*. (2022); NMPPDB (2024)
14	Catechin	$C_{15}H_{14}O_6$	Esievo *et al*. (2018)
15	Phytol	$C_{20}H_{40}O$	Lawal *et al*. (2016)
16	Limonene	$C_{10}H_{16}$	Esievo *et al*. (2018)
17	β-Ionone	$C_{13}H_{20}O$	Lawal *et al*. (2016)
18	Caffeic Acid	$C_9H_8O_4$	Harmander Singh *et al*. (2022); NMPPDB (2024)
19	4,4,24-Trimethylcholesta-8-en-3β-ol	$C_30H_{52}O$	Lawal *et al*. (2016)
20	Ferulic Acid	$C_{10}H_{10}O_4$	Harmander Singh *et al*. (2022); NMPPDB (2024)

Source: Akomolafe *et al*. (2016); Lawal *et al*. (2016); Esievo *et al*. (2018); Harmander Singh *et al*. (2022); NMPPDB (2024).

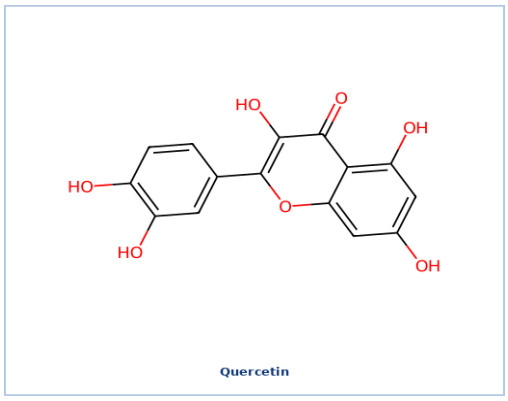

Figure 2.1(a): Lupeol ($C_{30}H_{50}O$). Lupane triterpenoid; anti-inflammatory (NF-κB/COX/LOX), anti-sickling, hepatoprotective.

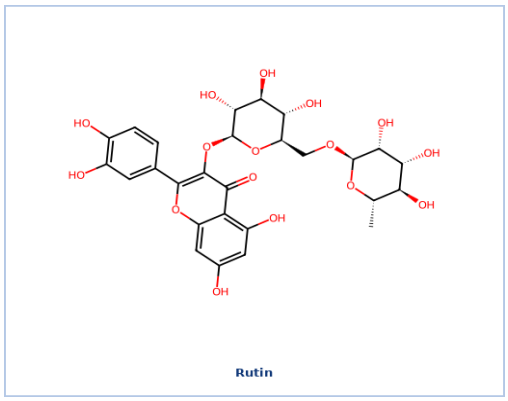

Figure 2.1(b): Quercetin ($C_{15}H_{10}O_7$). Flavonol; potent antioxidant, Fe^{2+}chelator, reported inhibitor of HbS polymerisation and membrane lipid peroxidation in sickle erythrocytes.

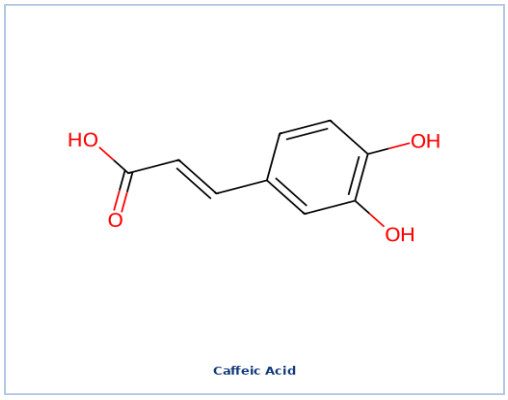

Figure 2.1(c): Rutin ($C_{27}H_{30}O_{16}$). Quercetin-3-O-rutinoside; iron absorption enhancer, antioxidant, erythroprotective.

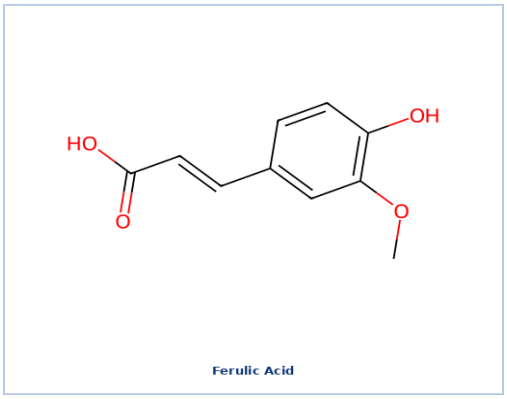

Figure 2.1(d): Caffeic acid ($C_9H_8O_4$). 3,4-Dihydroxycinnamic acid; $Fe^{3+} \rightarrow Fe^{2+}$ reducer, HIF-PHD modulator, Fe^{2+} chelator; retained after ADME-based virtual screening and docked against HBA1.

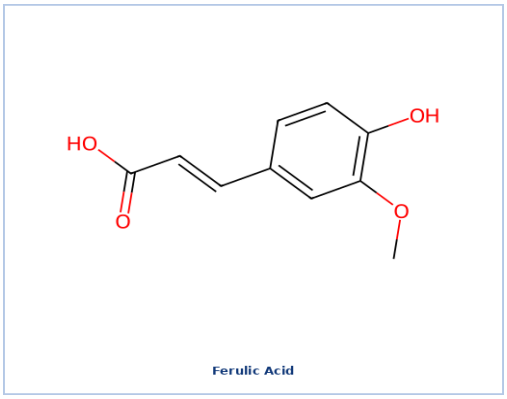

Figure 2.1(e): Ferulic acid ($C_{10}H_{10}O_4$). 4-Hydroxy-3-methoxycinnamic acid; iron bioavailability enhancer; retained after ADME-based virtual screening and docked against SMAD3.

Terpenoid fraction

Of the literature-reported phytochemicals of *F. sur*, this study focuses on five compounds of greatest pharmacological and mechanistic relevance to sickle cell anaemia (Table 2.3; Figure 2.1(a)-(e)). Lupeol (compound 1, $C_{30}H_{50}O$), a pentacyclic triterpenoid, demonstrates anti-inflammatory activity through inhibition of NF-κB and COX/LOX pathways together with directly reported anti-sickling activity, of particular relevance given that chronic vaso-occlusion-driven inflammation is a central feature of sickle cell pathophysiology. Quercetin (compound 8, C15H10O7) and rutin (compound 9, $C_{27}H_{30}O_{16}$) are potent antioxidant flavonoids: quercetin is a strong Fe^{2+} chelator and reported inhibitor of HbS polymerisation and membrane lipid peroxidation in sickle erythrocytes, while rutin enhances iron absorption and limits erythrocyte haemolysis. Caffeic acid (compound 18, $C_9H_8O_4$) and ferulic acid (compound 20, $C_{10}H_{10}O_4$) are hydroxycinnamic acid antioxidants that mitigate the oxidative stress driving both HbS polymerisation and chronic haemolysis; both were independently confirmed as drug-like after ADME-based virtual screening and carried forward to network pharmacology and molecular docking (Chapter Four), where caffeic acid was found to engage the haem-binding pocket of HBA1 and ferulic acid the TGF-β mediator SMAD3. The remaining fifteen leaf-derived compounds listed in Table 2.3, comprising additional terpenoids, phytosterols, and phenolics, are not given individual structural (2D structure) treatment in this section but, together with ten further compounds reported from other parts of *F. sur* (bark, root, and fruit), formed part of the full thirty-compound pool subjected to virtual screening in Chapter Four.

Phytosterol fraction

Flavonoid and phenolic acid fraction

2.3.4 Pharmacological activities of *Ficus sur*

The multi-institutional haematinic data on *F. sur* is substantial and consisent. Ezeigwe *et al*. (2020) reported treatment with the aqueous leaf suspension (200 mg/kg) displaying significantly increased haemoglobin (Hgb), PCV, and RBC to levels comparable to the normal control group in anaemic rats induced by phenylhydrazine hydro-chloride - establishing in vivo haematinic activity. Okafor *et al*. (2021) replicated these observations with the ethanolic leaf extract at 200 and 400 mg/kg for 14 days, with results approaching ferrous sulphate at 400 mg/kg. Obeagu (2021) performed histopathological studies demonstrating no damage to liver, kidney, and intestine of anaemic rats at therapeutic doses, confirming the safety of *F. sur*. Shaibu *et al*. (2025) reported the phytochemical and acute toxicity testing of the methanol leaf extract in adult Wistar rats using the LD50 model, (LD50>5,000 mg/kg), which is an excellent safety profile, with the presence of alkaloids, flavonoids and phenols being confirmed. The significant antioxidant effects (DPPH radical scavenging, ABTS decolourisation, FRAP) of *F. sur* leaf extracts reported in numerous independent studies is pharmacologically relevant to the haematinic activity of the leaves in preventing haemolysis and erythrocyte damage. Owolabi *et al*. (2022) demonstrated potent antibacterial properties of the methanol and water extracts against *Staphylococcus aureus, Escherichia coli, Klebsiella pneumoniae* and *Pseudomonas aeruginosa*, which is significant for infectious anaemia. The review of Ayodele *et al*. (2021) on the chemical composition and pharmacological activity of the essential oils of 14 Ficus species show that *F. sur* and other species produce anti-inflammatory terpenoids. Also, Saidu *et al*. (2020), found higher EPO levels in the serum of extract-treated animals, indicating an increase in renal EPO, and Iniaghe *et al*. (2009) showed the initial haematological evidence for the aqueous leaf extract.

2.4 *Justicia secunda* Vahl (Acanthaceae): Taxonomy, Botanical Description, Distribution, and Ethnomedicinal uses

Justicia secunda Vahl (Symb. Bot. 2: 7, 1791) belongs to the family Acanthaceae, which comprises approximately 250 genera and 2,500 species distributed across tropical and subtropical regions. This is the largest genus of the family with 600 species. Common names for the plant include a reference to its "blood" nature: "Blood Root" or "Blood Herb" in Nigeria and Ghana; Sanguinaria and Hierba de la sangre in Colombia or Venezuela; "Cristo's Blood" and "St John's Bush" in the Caribbean; and "Craboo weed" in Barbados. The blood name(s) across cultures and continents are pharmacologically relevant as they reflect independent ethnopharmacological recognition (Bulo, 2024). The full taxonomic name is given in Table 2.4.

Table 2.4: Scientific classification of *Justicia secunda* Vahl

Classification Level	Taxon
Kingdom	*Plantae*
Division	*Magnoliophyta*
Class	*Magnoliopsida*
Order	*Lamiales*
Family	*Acanthaceae*
Genus	*Justicia L.*
Species	*Justicia secunda Vahl, 1791*
Synonyms	*Dianthera secunda (Vahl) Griesb.; Rhacodiscus secundus (Vahl) Bremek.; Ecbolium secundum (Vahl) Kuntze*
Key Reference (This study)	*Oyewale et al. (2024), Adv. Tradit. Med. 24:531–540. DOI: 10.1007/s13596-023-00716-z*

Source: Oyewale *et al*. (2024); Koffi *et al*. (2013); Fotso Wabo *et al.* (2023).

J. secunda is a small erect perennial herb or subshrub growing to 30–90 cm in height. Its most distinctive feature is the deep red-purple colouration of the abaxial (lower) leaf surface, produced by constitutively expressed anthocyanin pigments, while the adaxial surface is dark, glossy green. The leaves are simple, opposite, ovate to lanceolate, 4–12 cm long, with entire margins and a prominent midrib. The plant produces small tubular red to pink flowers in terminal and axillary spikes and reproduces readily by stem cuttings. It is widely cultivated across West and Central Africa, the Caribbean, and South America as an ornamental and medicinal plant. Its ethnomedicinal use as a haematinic has been documented across Nigeria, Ghana, Cameroon, Côte d'Ivoire, Barbados, Jamaica, Venezuela, and Colombia—one of the most geographically extensive cross-cultural pharmacological validations in the tropical medicinal plant literature (Irinmwinuwa and Afonne, 2022; Bayengue *et al*., 2025).

2.4.1 Local names and ethnolinguistic distribution in Nigeria

Table 2.5 presents the documented vernacular names of *J. secunda* across Nigerian and West African linguistic groups, alongside international designations. The cross-linguistic convergence on blood-referencing terminology across Yoruba (*Ewe eje* — blood leaf), Igbo (*Akwukwo olu* — red leaf), and Hausa (*Ja jini* — red blood) independently documents the plant's primary medicinal application across divergent linguistic communities.

Table 2.5: Local names of *Justicia secunda* Vahl across Nigerian and West African linguistic groups

Local Name	Language/Tribe	Region/Country
Ewe eje	Yoruba (lit. "blood leaf")	Southwestern Nigeria
Akwukwo olu / Akwukwo mmiri eje	Igbo (lit. "red/blood leaf")	Southeastern Nigeria
Ja zafi / Ja jini	Hausa (lit. "red blood")	Northern Nigeria
Tete Rouge	Francophone (lit. "red tete")	Côte d'Ivoire; Cameroon
Insulina / Sanguinaria	Spanish/Venezuelan	Venezuela; Colombia
St John's Bush / Blood Root	English Creole	Trinidad; Jamaica; Barbados
Cristo's Blood	English Creole	Caribbean (general)
Blood Plant / Red Justicia	English	Pan-tropical (common names)

Source: Koffi *et al*. (2013); Fotso Wabo *et al*. (2023); Oyewale *et al*. (2024); Bulo (2024); TRAMIL (2014).

Figure 2.3: *Justicia secunda* Vahl (Acanthaceae), showing the characteristic terminal racemose inflorescence bearing vivid crimson tubular bilabiate flowers, with opposite elliptic-lanceolate leaves showing prominent reticulate venation. Family: Acanthaceae. **Source:** C. Delnatte, reproduced in Oyewale *et al*. (2024), Advances in Traditional Medicine, 24: 531–540. doi:10.1007/s13596-023-00716-z. Used with permission.

2.4.2 Ethnopharmacological uses

The vernacular name "Blood Plant" provides insight. In the Caribbean, leaf preparations address IDA, amenorrhoea and hemorrheic recovery after childbirth, formally established by the TRAMIL network in the Caribbean Herbal Pharmacopoeia (TRAMIL, 2014; Weniger *et al*., 1993). In Cameroo and Côte D'Ivoire, fresh leaf juice treats sickle cell disease and IDA (Koffi *et al*., 2013). In Nigeria and Ghana, it is finding its way into the urban herbal market as an iron supplement (Fotso Wabo *et al*., 2023; Oyewale *et al*., 2024). The pioneering pharmacological study by Oyewale *et al*. (2024) in Advances in Traditional Medicine (Springer, DOI: 10.1007/s13596-023-00716-z) documented LD50 > 5,000 mg/kg bwt and its ability to significantly ($p < 0.05$) increase PCV, RBCs and Hgb at 10 and 100 mg/kg bwt doses, confirming its efficacy and high safety margin. Bayengue *et al*. (2025) also reported haematinic efficacy and antiplasmodial activity against chloroquine-resistant Plasmodium falciparum (IC50: 5.74-100.26 μg/mL), revealing that a single plant extract meets three simultaneous causes of tropical anaemia: haemopoiesis deficiency, infection and inflammation.

2.4.3 Phytochemical constituents of *Justicia secunda*

Phytochemical analyses of *J. secunda* have been carried out via LC-MS, GC-MS, GC-FID and UV-visible spectrophotometry. The most extensive profiling of the plant was reported by Swiatek *et al*. (2023), who identified more than 50 compounds in five different solvent extracts; the methanol extract and water infusion had the highest total phenolic contents (58.07 and 36.34 mg GAE/g respectively) and the highest total flavonoid contents (13.07 and 8.52 mg rutin equivalents/g respectively). Bako *et al*. (2024) quantified the most abundant compounds in the ethanol extract of the leaf by GC-FID; namely, spartein (28.10 μg/mL), rutin (15.6 μg/mL), and naringin (12.4 μg/mL). Remarkably, Uchegbu *et al*. (2023) detected the cofactor vitamin B12 (methylcobalamin) in the alkaloid fraction by GC-MS, a discovery of potential clinical significance as vitamin B12 for red blood cell (RBC) maturation is almost never found

in natural materials. Theiler *et al*. (2014) used the plant-derived secondary metabolites secundarellones A-C and justisecundoside A, which have never been previously isolated from any other plant. Twenty bioactive compounds and their formulae are listed in Table 2.6.

Table 2.6: Bioactive compounds identified from *Justicia secunda* Vahl with molecular formulae and literature sources

No.	Compound Name	Molecular Formula	Primary Source(s)
1	Secundarellone A	$C_{18}H_{16}O_7$	Theiler *et al*. (2014)
2	Secundarellone B	$C_{18}H_{16}O_7$	Theiler *et al*. (2014)
3	Secundarellone C	$C_{18}H_{16}O_7$	Theiler *et al*. (2014)
4	Justisecundoside A	$C_{21}H_{20}O_{10}$	Theiler *et al*. (2014)
5	Luteolin	$C_{15}H_{10}O_6$	Koffi *et al*. (2013); Oyewale *et al*. (2024)
6	Luteolin-7-O-glucoside	$C_{21}H_{20}O_{11}$	Koffi *et al*. (2013); Swiatek *et al*. (2023)
7	Apigenin	$C_{15}H_{10}O_5$	Koffi *et al*. (2013); Swiatek *et al*. (2023)
8	Quindoline	$C_{19}H_{14}N_2$	Fotso Wabo *et al*. (2023)
9	Aurantiamide Acetate	$C_{28}H_{30}N_2O_5$	Fotso Wabo *et al*. (2023)
10	Rutin	$C_{27}H_{30}O_{16}$	Swiatek *et al*. (2023); Bako *et al*. (2024)
11	Diosmetin	$C_{16}H_{12}O_6$	Swiatek *et al*. (2023)
12	2-Caffeoyloxy-4-hydroxyglutaric Acid	$C_{14}H_{14}O_9$	Swiatek *et al*. (2023)
13	Auranamide	$C_{27}H_{28}N_2O_4$	Fotso Wabo *et al*. (2023)
14	Kaempferol-3-O-coumaroylglucoside	$C_{30}H_{26}O_{13}$	Koffi *et al*. (2013)
15	Naringenin-7-O-rutinoside	$C_{27}H_{32}O_{14}$	Koffi *et al*. (2013)
16	Columbamine	$C_{20}H_{22}NO_4$	Swiatek *et al*. (2023); Uchegbu *et al*. (2023)
17	Quercetin-7-O-glucoside-3-O-rutinoside	$C_{33}H_{40}O_{21}$	Swiatek *et al*. (2023)
18	Apigenin-7-O-neohesperidoside	$C_{27}H_{30}O_{14}$	Koffi *et al*. (2013)
19	Luteolin-7-O-rutinoside (Scolymoside)	$C_{27}H_{30}O_{15}$	Swiatek *et al*. (2023)
20	Spinasterol	$C_{29}H_{48}O$	Koffi *et al*. (2013)

Source: Theiler *et al*. (2014); Koffi *et al*. (2013); Fotso Wabo *et al*. (2023); Swiatek *et al*. (2023); Bako *et al*. (2024).

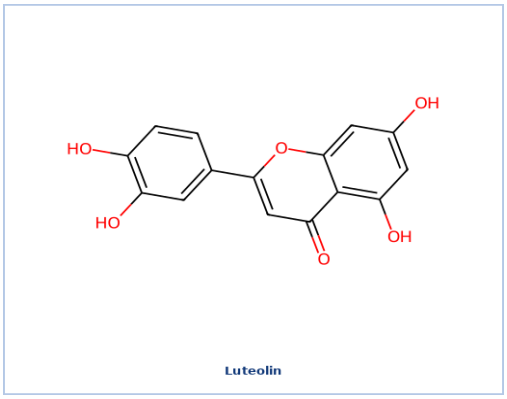

Figure 2.4(a): Luteolin ($C_{15}H_{10}O_6$). Potent flavonoid antioxidant; reported to reduce oxidative haemolysis and membrane lipid peroxidation in stressed erythrocytes; retained after ADME-based virtual screening.

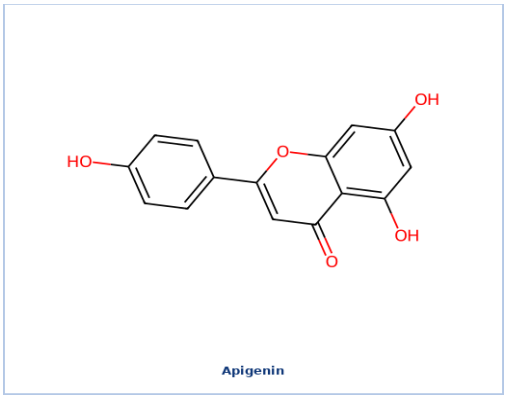

Figure 2.4(b): Apigenin ($C_{15}H_{10}O_5$). Flavone; antioxidant, reported to reduce reactive-oxygen-species-mediated membrane damage in erythrocytes; retained after ADME-based virtual screening.

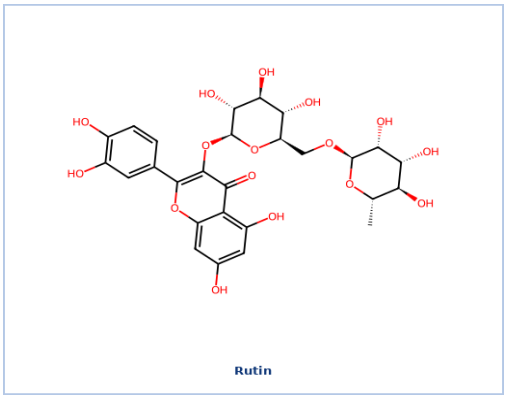

Figure 2.4(c): Rutin ($C_{27}H_{30}O_{16}$). Iron absorption enhancer, erythroprotective; shared marker with *F. sur*; retained after ADME-based virtual screening.

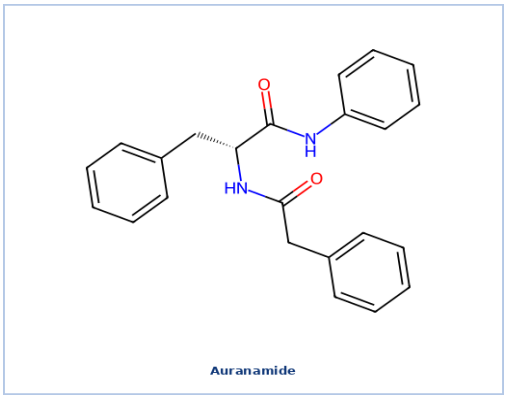

Figure 2.4(d): Auranamide ($C_{27}H_{28}N_2O_4$). Cinnamamide derivative; 72.4% HbS polymerisation inhibition at 2 mg/mL.

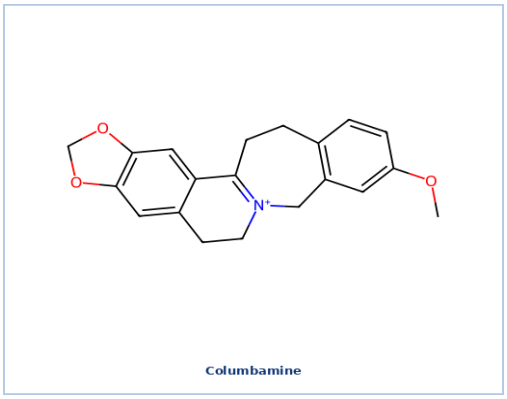

Figure 2.4(e): Columbamine ($C_{20}H_{22}NO_4$). Isoquinoline alkaloid; 58.3% anti-sickling inhibition at 2 mg/mL; antimicrobial.

Secundarellones and plant-specific compounds

The most pharmacologically distinctive compounds in *J. secunda* are secundarellones A, B, and C (compounds 1–3) and justisecundoside A (compound 4), which are unique to this plant and have not been identified in any other species. The secundarellones, first isolated and characterised by Theiler *et al*. (2014) using HR-MS and NMR, demonstrate inhibition of HbS polymerisation and stabilisation of RBC membranes—mechanisms distinct from conventional haematinic pharmacology in that they protect already-formed erythrocytes from structural deformation and haemolysis characteristic of sickle cell anaemia.

Flavone fraction

Of the literature-reported phytochemicals of *J. secunda*, this review focuses on five compounds of greatest pharmacological and mechanistic relevance to sickle cell anaemia (Table 2.6; Figure 2.4(a)-(e)). Luteolin (compound 5, $C_{15}H_{10}O_6$) and apigenin (compound 7, $C_{15}H_{10}O_5$) are potent flavonoid antioxidants capable of limiting the oxidative stress that drives both HbS polymerisation and the chronic haemolysis characteristic of sickle erythrocytes, with additional anti-inflammatory activity relevant to the vaso-occlusive inflammatory component of the disease; both were confirmed as drug-like after ADME-based virtual screening and carried forward to network pharmacology and molecular docking (Chapter Four). Rutin (compound 10, $C_{27}H_{30}O_{16}$), shared with *F. sur*, similarly enhances iron absorption and antioxidant protection, and was likewise retained after virtual screening. Auranamide (compound 13, $C_{27}H_{28}N_2O_4$) and columbamine (compound 16, $C_{20}H_{22}NO_4$) are, by contrast, compounds with directly reported anti-sickling bioactivity rather than antioxidant action: auranamide has been reported to inhibit HbS polymerisation by 72.4% at 2 mg/mL, and columbamine to inhibit erythrocyte sickling by 58.3% at the same concentration, making both among the most direct experimental evidence for the anti-sickling potential of *J. secunda* identified in this review. The remaining fifteen leaf-derived compounds listed in Table 2.6, including the plant-unique

secundarellones A-C and justisecundoside A, are not given individual structural (2D structure) treatment in this section but, together with ten further compounds reported from other parts of *J. secunda* (whole-plant and stem extracts), formed part of the full thirty-compound pool subjected to virtual screening in Chapter Four.

Alkaloid fraction

The alkaloid fraction comprises quindoline (compound 8), aurantiamide acetate (compound 9), auranamide (compound 13), and columbamine (compound 16). Columbamine, an isoquinoline protoberberine alkaloid, demonstrates antimicrobial activity against drug-resistant bacterial pathogens and anti-inflammatory properties relevant to the attenuation of hepcidin-mediated iron sequestration. Auranamide achieved 72.4% HbS polymerisation inhibition at 2 mg/mL, surpassing para-hydroxybenzoic acid at equimolar concentration (Koffi *et al*., 2013). Notably, Uchegbu *et al*. (2023) identified methylcobalamin (vitamin B12) within the alkaloid profile of *J. secunda* by GC-MS—a finding of exceptional clinical significance, as vitamin B12 is an essential cofactor for RBC maturation that is almost never found in plant-derived materials and whose deficiency independently causes megaloblastic anaemia.

2.4.4 Pharmacological activities of *Justicia secunda*

The haematinic evidence base for *J. secunda* is among the strongest available for any African medicinal plant. Irinmwinuwa and Afonne (2022) investigated the haemopoietic activity of four solvent fractions of the leaf extract in phenylhydrazine-induced anaemic mice using 16 treatment groups, demonstrating that all four fractions produced significant increases in haemoglobin, PCV, and RBC count ($p < 0.05$). Critically, the n-hexane, ethyl acetate, and n-butanol fractions produced haemopoietic effects superior to both ferrous sulphate and vitamin B12 standards at the doses tested ($p < 0.001$)—a finding with important implications for the development of the plant as a superior alternative or complementary haematinic. Bayengue *et al*. (2025) confirmed haematinic efficacy of the traditional leaf beverage in phenylhydrazine-

induced anaemic rats co-infected with *Plasmodium berghei*, demonstrating restoration of haematological parameters to near-normal levels after 14 days, alongside antiplasmodial activity (IC50: 5.74–100.26 μg/mL against chloroquine-resistant *P. falciparum*) and antibacterial activity against 14 drug-resistant strains—addressing three co-occurring causes of tropical anaemia in a single preparation.

Swiatek *et al*. (2023) demonstrated antioxidant IC_{50} values of 0.69–4.0 mg/mL in DPPH assays, alongside antiviral activity against influenza A virus, and selective cytotoxic activity against MCF-7 (breast cancer) and HeLa (cervical cancer) cell lines, confirming a broad pharmacological portfolio extending well beyond strictly haematinic applications. Fotso Wabo *et al*. (2023) provided the most mechanistically detailed molecular validation: extract upregulated *EPOR* (fold change 2.8), *GATA-1* (3.1), *KLF1* (2.5), *SCL/TAL-1* (2.2), and *NF-E2* (1.9) gene expression in K562 cells at 100 μg/mL, confirming direct transcriptional engagement with the erythropoietic programme. Oyewale *et al*. (2024) additionally demonstrated SOD elevation, HDL increase, LDL reduction, and absence of hepatotoxic or nephrotoxic effects at therapeutic doses.

2.5 Studies on Combined Preparations of *Ficus sur* and *Justicia secunda*

A small but scientifically important body of literature has examined preparations combining both study plants, providing direct experimental justification for their comparative individual characterisation. Uchegbu *et al*. (2023) developed a functional tea from a statistically optimised blend of *F. sur* and *J. secunda* leaves using response surface methodology with a three-level factorial design, arriving at an optimal formulation ratio of 48% *Ficus sur* to 52% *Justicia secunda*. The optimised blend demonstrated a nutritional and phytochemical profile that is exceptional by the standards of any known haematinic plant preparation: iron content of 489.11 mg/g; total flavonoid content of 83.64 mg QE/100 g; vitamin C content of 1,003.14 mg/100 g; and pyridoxine (vitamin B6) content of 357.31 mg/100 g. The alkaloid profile characterised by

GC-MS included tetrahydrorhombiofoline (35%), columbamine (20.10%), laudanosine (11.50%), salsoline (8.22%), methylcobalamin/vitamin B12 (7.98%), quinine (5.89%), and quinidine (3.21%)—a combination addressing multiple haematinic mechanisms simultaneously through different bioactive classes.

Fasuan and Uchegbu (2024) further characterised the physicochemical, phenolic, antioxidant, and functional group properties of the blended teas and conducted haematological evaluation in fed animals, confirming blood-boosting activity and reporting antioxidant values of 6,464.95 μmol Trolox equivalents/100 g (DPPH) and 40.13 mmol Fe^{2+}/100 g (FRAP).

This series of research shows *F. sur* and *J. secunda* are pharmacologically complementary rather than duplicative herbs - *F. sur* contributes the terpenoid/phytosterol resource that provides anti-inflammatory and anti-sickling effects, but *J. secunda* provides the chromene/alkaloid resource that provides haem-protective effects and EPO gene induction. This complementarity justifies the comparative individual characterisation of each plant, which is the aim of this current study.

2.6 Fourier-Transform Infrared (Ftir) Spectroscopy in the Characterization of Medicinal Plant Extracts

Fourier-Transform Infrared (FTIR) spectroscopy, is a non-invasive method that identifies the functional group content of complex systems by absorption of infrared light by molecular bonds. Spectrum peaks corresponding to vibrational stretching and bending motions of functional groups occur at characteristic wavenumbers (absorbance/spectrum peaks are plotted against wavenumbers on the x-axis) and the resultant spectrum is a fingerprint of the chemical identity of the sample (Singh *et al.*, 2022). The technique allows identification of all major functional group classes in a single analysis (without separation of individual analytes) and is well suited to comparative profiling of complex multi-compound samples, such as extracts of *F. sur* and *J. secunda*. In plant extracts, the most pharmacologically significant absorption

bands are: the broad O-H stretching band at 3,200-3500 cm^{-1} (polyphenols, flavonoids, tannins), C-H aliphatic stretching at 2850-2930 cm^{-1} (terpenoids and fatty acids), C=O stretching at 1700-1750 cm^{-1} (flavonoids, phenolic acids, secundarellone lactones), C=C aromatic ring stretching at 1500-1600 cm-1 (flavonoid and phenolic compounds), N-H bending at about 1550 cm-1 (confirms alkaloids) and C-O-C stretching at 1000-1300 cm^{-1} (cardiac glycosides and flavonoid glycosides; Shamim *et al*., 2022; Dev and Mukadam, 2025). The fingerprint region (600-1,500 cm^{-1}) is definitive for molecular discrimination of closely-related compounds, and is used in comparative profiling. Singh *et al*. (2022) combined FTIR spectroscopy with high-resolution LC-MS for characterisation of a polyherbal formulation and showed that C=O and C=N aggregations identified by FTIR were directly assignable to compounds identified by mass spectrometry, confirming that FTIR is indeed accurate for phytochemical profiling of complex extracts. Sarmah *et al*. (2025) characterised three ethnomedicinal herbs by FTIR, of the view that FTIR spectral analysis provides valuable information for identifying plant extracts with potential therapeutic uses. Patle *et al*. (2021) quantified phenolics and flavonoids in Dillenia pentagyna using FTIR, noting that functional groups in the 1,000-1,750 cm^{-1} region corresponded completely to flavonoids in the plant extract. Fasuan and Uchegbu (2024) used FTIR for the blended Ficus/Justicia functional tea, finding absorption peaks that indicated the presence of the hydroxyl, carbonyl and aromatic groups that are generally associated with high phenolic and flavonoid content and provided direct FTIR evidence for the present study. The World Health Organisation (WHO, 2011) officially recognises FTIR fingerprints as acceptable for purposes of quality assurance in herbal material identification and batch-to-batch consistency.

2.7 Atomic Absorption Spectroscopy (AAS) in the Mineral Profiling of Medicinal Plants

Atomic Absorption Spectroscopy (AAS) is the canonical method for quantitative elemental analysis of biological and pharmaceuticals products with the principle that ground-state atoms

selectively absorb electromagnetic radiation at specific wavelengths, which vary between elements and are in proportion to the analyte concentration, according to the Beer-Lambert's equation (Welz and Sperling, 1999; Hina *et al*., 2023). With herbal medicine used as haematinic supplements, AAS provides the direct chemical proof of the mineral-mediated aspects of haematinic action that qualitative phytochemical analyses do not. The pharmacological relevance for each targeted mineral is: iron (Fe) as the central atom for haemoglobin's porphyrin ring, and the limiting mineral in IDA; zinc (Zn) as cofactor for erythroid differentiation enzymes (and Zn deficiency independently suppresses haematopoiesis); copper (Cu), as structural element of caeruloplasmin and intestinal hephaestin, is required for $Fe^{2+} \rightarrow Fe^{3+}$ oxidation for transferrin binding, so Cu deficiency limits iron utilisation in the presence of sufficient iron stores; manganese (Mn), a cofactor for mitochondrial superoxide dismutase, prevents oxidative haemolysis; calcium (Ca) and magnesium (Mg) regulate erythrocyte membrane fluidity and cation import-export; sodium (Na) and potassium (K), maintain the electrical gradient required for erythrocyte volume regulation. Lead (Pb) and cadmium (Cd) form the chemically essential safety check parameters, with Pb in particular inhibiting enzymes involved in haem biosynthesis (aminolaevulinic acid dehydratase and ferrochelatase), leading to an IDA-like anaemia (WHO, 2007; Zvèrina *et al*., 2023). Hina *et al*. (2023) showed that wet acid digestion (using nitric: perchloric acids) yielded more precise and accurate AAS results than dry ashing in plants. Zvèrina *et al*. (2023) developed a high-resolution continuum source graphite furnace AAS for simultaneous determination of the Zn and Fe in plants with detection limits of 0.01-0.1 µg/mL and satisfactory accuracy for certified reference materials. Radha *et al*. (2021) have used AAS for nutritional and mineral composition of medicinal plants from Western Himalayas, with Fe, Zn, Cu and Mn reporting combined with pertinent pharmacological insights. Olusegun *et al*. (2023) established baseline AAS data for *F. sur* root bark: Fe: 18.4 mg/100 g DW; Cu: 1.2

mg/100 g DW; Zn: 2.8 mg/100 g DW; Mn: 3.1 mg/100 g DW. There is no systematic literature on AAS determination of *J. secunda* mineral elements, and this study now provides information on Fe, Zn, Cu, Mn, Ca, Mg, Na, K, Pb, and Cd (target analytes) content using validated flame AAS.

2.8 Network Pharmacology: Principles, Workflow, and Application to Haematinic Plant Research

Network pharmacology is a network-based computational strategy that models the effects of multi-component therapeutic agents by creating and evaluating networks of interactions between bioactives and the protein targets that they bind, leading to network pathways. The strategy recognises that the majority of diseases are the result of the dysfunction of multiple components of complex networks of interactions, rather than just the malfunction of a single gene or protein, and that the therapeutic effects of multi-component plant-based agents result from the simultaneous interaction of multiple targets on multiple nodes in the disease network to produce a synergistic effect (Noor *et al*., 2022, Hopkins, 2008). As such, network pharmacology is the ideal approach to guide pharmaceutical studies on haematinic plants like *F. sur* and *J. secunda*, whose multi-component phytochemicals number 20 each, and include terpenoids, phytosterols, flavonoids, flavonoid glycosides, phenolic acids, alkaloids, and plant-specific chromenes.

The workflow applied in this study proceeds as follows: (i) bioactive compounds retrieved from peer-reviewed literature are submitted to ADME evaluation using SwissADME, retaining compounds satisfying Lipinski's Rule of Five (MW < 500 Da; logP < 5; H-bond donors < 5; H-bond acceptors < 10); (ii) protein targets are predicted using SwissTargetPrediction at a probability threshold of 0.5 with human species as reference; (iii) disease-associated targets for anaemia, erythropoiesis, and haemoglobin synthesis are retrieved from GeneCards, OMIM, and DisGeNET; (iv) compound–disease target overlap is mapped by Venn diagram analysis;

(v) a PPI network is constructed using STRING at a confidence threshold of 0.700 and visualised in Cytoscape; (vi) hub targets are identified using the CytoHubba plugin with the Maximal Clique Centrality algorithm; and (vii) GO and KEGG pathway enrichment analyses are performed using DAVID and Enrichr with an adjusted *p*-value threshold of < 0.05 after Benjamini-Hochberg correction. Molecular docking of top-ranked phytochemical candidates against hub targets is performed using AutoDock Vina to validate predictions at the structural level (Kim *et al*., 2024).

He *et al*. (2021) applied the complete network pharmacology workflow to Danshen (Salvia miltiorrhiza), identifying 115 compound–target interactions and converging on a small number of disease-relevant signalling pathways, illustrating that the virtual-screening-led, compound-first strategy adopted in this study, narrowing a large literature-derived compound list down to a small set of drug-like candidates before target prediction, is a validated and reproducible approach for identifying mechanistically plausible bioactive principles in multi-component herbal preparations. In the present study, this workflow is applied to *F. sur* and *J. secunda* with the specific objective of identifying which of their surviving drug-like compounds engage molecular targets of relevance to sickle cell anaemia.

2.9 Molecular and Pathophysiological Basis of Sickle Cell Anaemia

Sickle cell anaemia arises from a single, well-characterised molecular lesion, the substitution of valine for glutamic acid at the sixth position of the beta-globin chain (HBB, Glu6Val), which produces haemoglobin S (HbS). Under conditions of low oxygen tension, HbS molecules polymerise into rigid fibres that deform the erythrocyte into the sickle shape characteristic of the disease. This single mutation sets in motion a cascade of secondary pathophysiological processes, oxidative stress, erythrocyte membrane damage, chronic haemolysis, vaso-occlusion, and inflammation, several of which present plausible points of pharmacological

intervention by plant-derived phytochemicals, and against which the molecular targets identified by network pharmacology and docking in this study (Chapter Four) are interpreted.

2.9.1 Oxidative stress and antioxidant defence in sickle erythrocytes

Repeated cycles of HbS polymerisation, sickling and unsickling generate substantial intracellular oxidative stress in sickle erythrocytes, through autoxidation of HbS and the release of free haem and iron, which catalyse the formation of reactive oxygen species. This chronic oxidative burden damages the erythrocyte membrane, accelerates premature haemolysis, and contributes to the vascular endothelial dysfunction that underlies vaso-occlusive crises. Plant-derived antioxidant phenolics and flavonoids, several of which are present in both *F. sur* and *J. secunda* (Sections 2.3.3 and 2.4.3), are therefore of direct mechanistic interest as agents capable of scavenging these reactive oxygen species and limiting downstream membrane and vascular damage.

2.9.2 Erythrocyte membrane stabilisation and anti-sickling activity

The sickle erythrocyte membrane is intrinsically more fragile and mechanically unstable than the normal biconcave erythrocyte membrane, owing to HbS polymer-induced cytoskeletal distortion, lipid peroxidation, and altered membrane cation transport. Compounds capable of integrating into or stabilising the erythrocyte lipid bilayer, such as the phytosterols and triterpenoids identified in *F. sur* (Section 2.3.3), or of directly inhibiting HbS polymer formation, as reported for several *J. secunda* compounds including auranamide and columbamine (Section 2.4.3), represent two distinct but complementary anti-sickling mechanisms of direct relevance to this disease.

2.9.3 Vaso-occlusion, inflammation, and the haemoglobin subunit genes

Sickled erythrocytes adhere abnormally to vascular endothelium and activate circulating leukocytes and platelets, producing a chronic low-grade inflammatory and pro-thrombotic state

that drives recurrent vaso-occlusive crises. Compounds capable of directly engaging the haemoglobin subunit genes themselves (HBA1, HBA2, HBB), or of suppressing pro-inflammatory signalling (for example through NF-κB or COX/LOX pathway inhibition, as reported for several terpenoids in *F. sur*), present two further mechanistic routes by which the plants under study could plausibly support the sickle cell disease phenotype, independent of any classical iron-haematinic action.

2.9.4 Genomic stability under chronic haemolytic regenerative stress

Because chronic haemolysis in sickle cell disease imposes a sustained, elevated demand on the bone marrow to continuously regenerate the erythroid progenitor pool, the genomic stability of these rapidly dividing progenitor cells is of particular physiological importance; impairment of DNA-repair capacity in this compartment, as occurs in the Fanconi anaemia pathway, is independently associated with bone marrow failure. Compounds capable of supporting genomic stability in actively regenerating haematopoietic progenitor cells may therefore confer a secondary protective benefit in the setting of chronic haemolytic stress, a hypothesis explored further from the network pharmacology findings of this study in Chapter Five.

2.10 Molecular Docking and Admet Profiling in the Validation of Phytochemical Pharmacology

Molecular docking is a structure-based computational method that predicts the binding conformation and thermodynamic binding affinity (expressed as the binding free energy, ΔG, in kcal/mol) of a small-molecule ligand within the three-dimensional active site of a target protein. In this study, docking served as the confirmatory step of the network pharmacology pipeline: compounds and targets identified by target-prediction software (SwissTargetPrediction) were re-evaluated by docking each surviving drug-like ligand against the three-dimensional structure of its predicted target protein using AutoDock Vina, with the

resulting ΔG values used to rank the strength of each compound-target interaction and identify the most promising candidates for further study.

ADMET evaluation using SwissADME assesses oral bioavailability and drug-likeness through Lipinski's Rule of Five (molecular weight < 500 Da; logP < 5; hydrogen-bond donors < 5; hydrogen-bond acceptors < 10). Compounds that fail these criteria are generally poorly absorbed or poorly soluble and are unlikely to succeed as oral drug candidates regardless of their intrinsic biological activity; this is the specific basis on which the present study filtered the full literature-derived compound lists of both plants down to the small subset of drug-like candidates carried forward to target prediction and docking. Sharma *et al*. (2019) and Aguilar-Tola *et al*. (2020) have each validated this combined ADMET-filtering-plus-docking strategy in unrelated plant systems, supporting its reliability as a virtual screening approach prior to experimental validation.

2.11 Gap in Knowledge

The foregoing review establishes that *Ficus sur* Forssk. (Voucher No. UNN/11770, authenticated March 2026, University of Nigeria Herbarium) and *Justicia secunda* Vahl are ethnomedicinally credible candidate phytotherapeutics for sickle cell anaemia, independently and repeatedly named in traditional medicine sources as remedies for the condition, and individually supported by fragmented phytochemical and in vivo haematological evidence. However, several specific scientific gaps remain.

Gap 1: No investigation has subjected both plants simultaneously to a comparative, multi-platform analytical approach encompassing phytochemical screening, FTIR spectroscopy, AAS mineral profiling, and network pharmacology within a single study.

Gap 2: A comprehensive, validated AAS mineral profile covering all haematologically relevant elements has not been reported quantitatively for *J. secunda*, and no study has directly compared the elemental profiles of both plants under identical analytical conditions.

Gap 3: The functional group architectures of the leaf extracts of both plants have not been comparatively characterised by FTIR and related to their respective phytochemical profiles in any published comparative study.

Gap 4: No study has applied a virtual-screening-led, compound-first network pharmacology workflow, eliminating non-drug-like compounds before target prediction, to the literature-reported phytochemicals of either plant, and none has examined the resulting molecular targets specifically in relation to sickle cell anaemia pathology rather than anaemia in general.

Gap 5: There is no molecular docking study confirming the binding of the specific drug-like compounds identified from either plant (including the plant-unique secundarellones A-C and justisecundoside A from *J. secunda*) to their predicted blood-related molecular targets, nor has any study reported binding free energies for these interactions.

Gap 6: No study has integrated FTIR, AAS, and network pharmacological/docking evidence within a single mechanistic framework and interpreted the resulting findings specifically in the context of sickle cell anaemia, as opposed to generic anaemia.

The present study addresses all of these gaps within an integrated experimental and computational framework, providing the most comprehensive and mechanistically grounded scientific characterisation of *F. sur* and *J. secunda* as candidate phytotherapeutics for sickle cell anaemia produced to date.

CHAPTER THREE

MATERIALS AND METHODS

3.1 Study Design

This study was a comparative in vitro and in silico investigation conducted in the Department of Biochemistry, Godfrey Okoye University, Enugu. FTIR spectroscopic fingerprinting and AAS elemental analysis were carried out at the Central Science Laboratory, University of Nigeria, Nsukka. The investigation comprised: (i) plant collection, authentication, and extract preparation; (ii) qualitative phytochemical screening; (iii) proximate compositional analysis; (iv) FTIR spectroscopic fingerprinting; (v) AAS elemental analysis; and (vi) in silico network pharmacological analysis with molecular docking validation. Both species were processed simultaneously under identical conditions throughout.

3.2 Materials and Equipment

All chemicals were of analytical grade (Sigma-Aldrich, USA; BDH Chemicals, UK), including ethanol, chloroform ($CHCl_3$), HCl, H_2SO_4, $FeCl_3$, lead acetate, NaOH, Dragendorff's/Mayer's/Wagner's/Hager's reagents, Fehling's solutions A and B, Folin–Ciocalteu reagent, $AlCl_3$, Na_2CO_3, acetic anhydride, gallic acid and quercetin standards, HNO_3, $HClO_4$, and certified multi-element AAS standards. Deionised water (≥18.2 MΩ·cm) was used throughout. Equipment included: Soxhlet apparatus (Pyrex, UK); rotary evaporator (BÜCHI R-300); analytical balance (Mettler-Toledo XSE205, ±0.1 mg); Thermo Scientific iCE 3000 Series FAAS (SOLAAR V11.10 software, Central Science Laboratory, UNN); FTIR-ATR spectrometer; UV-Vis spectrophotometer (Shimadzu UV-1800); muffle furnace, drying oven, water bath, and standard glassware.

3.3 Plant Material Collection and Authentication

Fresh, mature leaves of *Ficus sur* Forssk. (syn. *Ficus sur* Thunb.; Moraceae) and *Justicia secunda* Vahl (Acanthaceae) were collected from Enugu State, Nigeria (March 2026, 07:00–

09:00 h) and processed within 24 hours. *F. sur* was authenticated by Felix I. Nwafor, University of Nigeria Herbarium (UNN), March 2026 (Voucher No. UNN/11770; MORACEAE). *J. secunda* was correspondingly identified by a registered plant taxonomist with a voucher specimen deposited for reference.

3.4 Preparation of Plant Material

Leaves were washed, rinsed with distilled water, and air-dried under shade (25–30°C, 21 days) to prevent photodegradation of heat-labile metabolites. Dried leaves were pulverised to a uniform powder and stored in airtight amber containers at room temperature until extraction.

3.5 Preparation of Plant Extracts

Fifty grams (50 g) of powdered leaf material of each species were independently extracted with 70% ethanol (v/v; 300 mL) by Soxhlet apparatus at 78–80°C for 8 hours (≥10 siphon cycles), chosen for its broad-spectrum extraction of both polar and moderately polar phytoconstituents (Azmir *et al.*, 2013). In addition, fifty grams (50 g) of *J. secunda* and eighteen grams (18 g) of *F. sur* (the latter reflecting available authenticated material after the 50 g ethanolic allocation) were separately extracted with chloroform (CHCl3; 60–62°C, 8 h) for non-polar constituents. All filtrates (Whatman No. 1) were concentrated by rotary evaporation (35–40°C) and dried to constant weight in a pre-weighed vial. Percentage extraction yield was calculated for each of the four extracts (Table 3.1) as:

$$\% \text{ Yield} = (W_1 / W_2) \times 100 \quad \text{(Equation 3.1; Azmir } et\ al.\text{, 2013)}$$

where W_1 = mass of dry extract obtained (g) and W_2 = mass of the initial powdered plant material subjected to extraction (g), for each of the four solvent/species combinations in Table 3.1. Extracts were stored at 4°C in sealed amber vials.

Table 3.1: Summary of extraction parameters for both study plants

Plant species	Extract type	Mass (g)	Solvent	Temp. (°C)	Duration (h)	Purpose
Ficus sur	70% Ethanolic	50	70% EtOH	78–80	8	Phytochem.; FTIR; AAS; in silico
Ficus sur	Chloroform	18	$CHCl_3$	60–62	8	Non-polar/GC-MS
Justicia secunda	70% Ethanolic	50	70% EtOH	78–80	8	Phytochem.; FTIR; AAS; in silico
Justicia secunda	Chloroform	50	$CHCl_3$	60–62	8	Non-polar/GC-MS

3.6 Qualitative Phytochemical Screening

The 70% ethanolic extracts of both species were screened in triplicate for major phytoconstituent classes using standard colorimetric and precipitation tests (Shaikh & Patil, 2020; Harborne, 1973; Trease & Evans, 2002; Sofowora, 1993). Results were recorded as present (+) or absent (−). Table 3.2 summarises the tests, reagents, and positive-result criteria.

Table 3.2: Qualitative phytochemical screening tests and positive-result criteria

Phytoconstituent	Test	Procedure (brief)	Positive Indication
Alkaloids	Dragendorff's / Mayer's / Wagner's	0.5 g extract + 1% HCl, filtrate + reagent	Orange-red / creamy-white / brown precipitate
Flavonoids	Shinoda; lead acetate	Extract + Mg ribbon + conc. HCl; extract + 10% $Pb(OAc)_2$	Pink/crimson colour; yellow precipitate
Tannins	$FeCl_3$ test	Filtrate + 5% $FeCl_3$	Blue-black (hydrolysable) / blue-green (condensed)
Saponins	Froth test	Extract + water, vigorous shaking, 15 min	Persistent froth, stable to olive oil
Steroids/Triterpenoids	Liebermann–Burchard	Extract + acetic anhydride + conc. H_2SO_4	Blue-green (steroids) / red-purple (triterpenoids)
Cardiac glycosides	Keller–Kiliani	Extract + glacial acetic acid + $FeCl_3$ + conc. H_2SO_4	Brown ring; blue acetic acid layer
Phenols	$FeCl_3$ test	Ethanol extract + 10% $FeCl_3$	Dark green / bluish-black
Terpenoids	Salkowski	Chloroform extract + conc. H_2SO_4	Reddish-brown / golden-yellow interface
Anthraquinones	Bornträger's	Boiled extract + H_2SO_4, benzene layer + NH_3	Pink/violet/red ammoniacal layer
Reducing sugars	Fehling's test	Extract + Fehling's A & B, boiled	Brick-red precipitate

3.7 Proximate Compositional Analysis

Proximate composition of the powdered leaf samples was determined in triplicate following AOAC (2016) methods, summarised in Table 3.3.

Table 3.3: Proximate analysis parameters and methods (AOAC, 2016)

Parameter	**Method (brief)**
Moisture	Oven-drying at 105°C to constant weight; % loss on drying
Ash	Furnace incineration at 550°C for 6 h
Crude protein	Macro-Kjeldahl (digestion, distillation, titration); N × 6.25
Crude fat	Soxhlet extraction with petroleum ether (60–80°C), 16 h
Crude fibre	Sequential acid (1.25% H_2SO_4) and alkali (1.25% NaOH) digestion; loss on ignition
Carbohydrate (by difference)	100 − (% moisture + protein + fat + fibre + ash)
Energy value	Atwater factors: (4×protein) + (4×carbohydrate) + (9×fat), kcal/100 g

The full working formulas applied to each of the AOAC (2016) procedures summarised in Table 3.3 were as follows.

Moisture content was determined by loss on drying of 2 g of powdered sample at 105°C to constant weight:

$$\% \text{ Moisture} = [(W_2 - W_3) / (W_2 - W_1)] \times 100 \quad \text{(Equation 3.2)}$$

where W_1 = weight of empty crucible (g), W_2 = weight of crucible + sample before drying (g), and W_3 = weight of crucible + sample after drying (g).

Ash content was determined by incinerating 2 g of sample in a muffle furnace at 550°C for 6 h:

$$\% \text{ Ash} = [(W_3 - W_1) / (W_2 - W_1)] \times 100 \quad \text{(Equation 3.3)}$$

where W_1 = weight of empty crucible (g), W_2 = weight of crucible + sample before ashing (g), and W_3 = weight of crucible + ash after ashing (g).

Crude protein was determined by the macro-Kjeldahl method (digestion in concentrated H_2SO_4 with a catalyst, alkaline distillation into standard acid, and back-titration):

$$\% \text{ N} = [(V_1 - V_2) \times N_a \times 14.01 \times 100] / (W \times 1000) \quad \text{(Equation 3.4)}$$

$$\% \text{ Crude protein} = \% \text{ N} \times 6.25 \quad \text{(Equation 3.5)}$$

where V_{11} = titre volume for the sample (mL), V_{22} = titre volume for the reagent blank (mL), N_a = normality of the standard acid used for titration, W = weight of sample digested (g), and 6.25 is the standard nitrogen-to-protein conversion factor (equivalent to assuming 16% nitrogen in plant protein).

Crude fat was determined by continuous Soxhlet extraction with petroleum ether (60–80°C) for 16 h:

$$\% \text{ Crude fat} = [(W_2 - W_1) / W] \times 100 \quad \text{(Equation 3.6)}$$

where W_1 = weight of empty, dry extraction flask (g), W_{22} = weight of flask + extracted fat after solvent evaporation (g), and W = weight of sample used (g).

Crude fibre was determined by sequential digestion of the defatted sample in 1.25% H_2SO_4 and 1.25% NaOH, followed by ashing of the residue:

$$\% \text{ Crude fibre} = [(W_2 - W_3) / W_1] \times 100 \quad \text{(Equation 3.7)}$$

where W_1 = weight of defatted sample taken (g), W_2 = weight of the dried acid/alkali-insoluble residue before ashing (g), and W_3 = weight of the ash remaining after igniting that residue (g). Carbohydrate content was obtained by difference, and energy value from the Atwater physiological fuel factors:

$$\% \text{ Carbohydrate} = 100 - (\% \text{ moisture} + \% \text{ ash} + \% \text{ crude protein} + \% \text{ crude fat} + \% \text{ crude fibre}) \quad \text{(Equation 3.8)}$$

$$\text{Energy value (kcal/100 g)} = (\% \text{ crude protein} \times 4) + (\% \text{ carbohydrate} \times 4) + (\% \text{ crude fat} \times 9) \quad \text{(Equation 3.9)}$$

3.8 Fourier-Transform Infrared (Ftir) Spectroscopic Analysis

Dried 70% ethanolic extracts were analysed by ATR-FTIR over 4,000–400 cm^{-1}(4 cm^{-1}resolution, 64 scans, room temperature, triplicate). Background spectra were subtracted automatically. Absorption bands were assigned by comparison with reference values (Coates, 2000; Smith, 2011) for O–H (3,200–3,550 cm^{-1}), aliphatic C–H (2,850–2,930 cm^{-1}), C=O (1,700–1,750 cm^{-1}, aromatic C=C (1,500–1,600 cm^{-1}), N–H (~1,550 cm^{-1}), C–O–C (1,000–1,300 cm^{-1}), and the fingerprint region (600–1,500 cm^{-1}). Spectra of both extracts were overlaid for comparison.

3.9 Atomic Absorption Spectroscopic (AAS) Analysis

Approximately 0.5 g of each dried 70% ethanolic extract was digested overnight with $HNO_3/HClO_4$ (4:1, v/v; 10 mL), heated at 120°C (2 h) then 200°C until clear, and made up to 50 mL with deionised water (triplicate, with reagent blanks). Twelve elements — Fe, Pb, Ca, Cd, Cr, Cu, K, Mg, Mn, Na, Ni, and Zn — were quantified by flame AAS (Thermo Scientific iCE 3000, AA05201309 v1.30; SOLAAR V11.10; Central Science Laboratory, UNN) using

an air-acetylene flame and element-specific hollow cathode lamps. Three-point external calibration curves (1.0–3.0 mg/L) gave $R^2 \geq 0.97$ for all elements (Table 3.4). Samples flagged below the calibration range were reported as not detected (ND); for Cu, the positive-yielding analytical run (Cu_2, $R^2 = 0.9895$) was used. Because Ca, K, and Na concentrations in both extracts exceeded the upper standard of the three-point calibration curve (3.0 mg/L), these three elements were quantified by instrument extrapolation beyond the validated linear range and are reported with this caveat.

Each element was quantified from a three-point external calibration curve of the form $Y = mx + c$ (Equation 3.10), where Y is measured absorbance, x is standard concentration (mg/L), m is the calibration slope, and c is the intercept; sample concentration was back-calculated as $x = (Y - c) / m$ (Equation 3.11; Harris, 2015). Instrument operating parameters and the fitted calibration equation for each element are given in Table 3.4.

Table 3.4: AAS instrument parameters and calibration equations (Thermo Scientific iCE 3000, Central Science Laboratory, UNN)

Element	Wavelength (nm)	Lamp Current	Bandpass (nm)	Fuel Flow (L/min)	Calibration R^2	Calibration equation (Y = absorbance, x = mg/L)
Fe	248.3	75%	0.2	0.9	0.9974	Y = 0.01095x + 0.0001
Pb	217.0	75%	0.2	1.1	0.9925	Y = 0.00831x − 0.0024
Ca	422.7	75%	0.2	1.1	0.9952	Y = 0.09207x + 0.0059
Cd	228.8	75%	0.2	1.2	0.9997	Y = 0.03880x − 0.0010
Cr	357.9	70%	0.1	1.4	0.9996	Y = 0.00325x − 0.0008
Cu	324.8	75%	0.2	1.1	0.9895	Not available (Cu_2 run) — see Note
K	766.5	75%	0.2	1.1	0.9960	Y = 0.09194x + 0.0062
Mg	285.2	75%	0.5	1.1	0.9953	Y = 0.14881x + 0.0135
Mn	279.5	75%	0.2	1.0	0.9999	Y = 0.02700x + 0.0012
Na	589.0	75%	0.2	1.1	0.9970	Y = 0.09195x + 0.0063
Ni	232.0	75%	0.2	0.9	0.9999	Y = 0.01577x − 0.0004
Zn	213.9	75%	0.2	1.2	0.9983	Y = 0.06721x + 0.0019

Note. Air-acetylene flame; background correction D2 (except Ca, K, Na, Cr: Off); 4.0 s measurement time, ×2 fast resamples. The calibration equation for Cu corresponds to the discarded first analytical run (R^2 = 0.9773); the equation for the positive-yielding Cu_2 run actually used for the Table 4.5 values (R^2 = 0.9895) was not available in the source instrument records reviewed and should be retrieved from the original SOLAAR run file before this table is finalised.

3.10 In Silico Network Pharmacological Analysis

Thirty literature-reported compounds per plant were evaluated for drug-likeness: the twenty leaf-derived, GC-MS/LC-MS-identified compounds presented in Tables 2.3 and 2.6, plus ten additional compounds reported from other parts of each plant (bark, root, and fruit for *F. sur*; whole-plant and stem extracts for *J. secunda*), reflecting the fact that the traditional haematinic/anti-sickling use of both plants is not always leaf-specific in the wider ethnobotanical literature. All thirty compounds per plant were screened using DataWarrior's "Calculate Compound Properties" module (Sander *et al*., 2015), assessing MW, cLogP, cLogS, H-bond donors/acceptors, TPSA, and the DataWarrior druglikeness score; compounds with a score ≥ 0 were retained for target prediction. Protein targets were predicted using SwissTargetPrediction (Daina *et al*., 2019; Homo sapiens, probability ≥ 0.5). Disease-associated targets for anaemia, erythropoiesis, and haemoglobin synthesis were retrieved from GeneCards, OMIM, and DisGeNET, and intersected with predicted targets by Venn diagram analysis. Shared targets were imported into STRING (v12.0; confidence ≥ 0.700) and visualised in Cytoscape (v3.10.1; Shannon *et al*., 2003), where hub targets were identified by node degree, betweenness, and closeness centrality. GO/pathway enrichment of hub genes was performed using ShinyGO (v0.80; Ge *et al*., 2020; FDR < 0.05).

Hub-gene centrality within the protein–protein interaction network was quantified using three standard graph-theoretic measures (Freeman, 1978):

$$\text{Degree centrality: } C_D(v) = \deg(v) \quad \text{(Equation 3.15)}$$

$$\text{Betweenness centrality: } C_B(v) = \sum_{s \neq v \neq t} [\sigma_{st}(v) / \sigma_{st}] \quad \text{(Equation 3.16)}$$

$$\text{Closeness centrality: } C_C(v) = (N - 1) / \sum_{u} d(v,u) \quad \text{(Equation 3.17)}$$

where deg(v) is the number of direct interaction partners of node v; σ_{st} is the total number of shortest paths between nodes s and t, and $\sigma_{st}(v)$ the number of those paths passing through v; N is the total number of nodes in the network; and d(v,u) is the shortest-path distance between

nodes v and u. Genes scoring in the upper quartile on all three measures were designated hub genes and carried forward to pathway enrichment and molecular docking. Pathway/GO term enrichment significance was assessed by hypergeometric test, $p = [C(K,k)\cdot C(N-K,n-k)] / C(N,n)$ (Equation 3.18; Ge *et al.*, 2020), where N is the total number of genes in the background set, K is the number of genes in a given pathway, n is the number of hub genes tested, and k is the number of hub genes found in that pathway; resulting p-values were corrected for multiple testing by the Benjamini–Hochberg procedure to give the false discovery rate (FDR) reported in Table 4.8.

3.11 Molecular Docking Validation

Three haematinic pathway proteins were selected for docking based on hub analysis: EPOR (PDB: 1CN4), HIF-PHD2/EGLN1 (PDB: 3OJT), and GATA-1 (PDB: 3VD6), retrieved from the RCSB PDB (Berman *et al.*, 2000) and prepared in BIOVIA Discovery Studio Visualizer (v21.1.0) by removing co-crystallised ligands/waters and adding polar hydrogens and Kollman charges (AutoDock Tools v1.5.6). Ligand 3D structures (PubChem SDF) were optimised in Avogadro (v1.2.0; Hanwell *et al.*, 2012) using the MMFF94 force field with Gasteiger charges. Docking was performed in PyRx (v0.9.6; Dallakyan & Olson, 2015) using its integrated AutoDock Vina engine (exhaustiveness = 8; grid box 25×25×25 Å). Re-docking of co-crystallised reference ligands (RMSD < 2.0 Å) validated the protocol. The pose with the most negative binding free energy (ΔG, kcal/mol) per ligand–target pair was analysed for hydrogen bonds, hydrophobic contacts, and π–π interactions in Discovery Studio.

The binding free energy (ΔG, kcal/mol) reported for each pose is the AutoDock Vina empirical scoring function (Trott & Olson, 2010), summed over all ligand–receptor atom pairs:

$$\Delta G = \Delta G_{vdW} + \Delta G_{hbond} + \Delta G_{elec} + \Delta G_{desolv} + \Delta G_{tors} \quad \text{(Equation 3.19)}$$

representing, respectively, the van der Waals, hydrogen-bonding, electrostatic, desolvation, and torsional-entropy penalty terms; more negative values indicate a more thermodynamically

favourable predicted interaction. Protocol validity was confirmed by root-mean-square deviation between the docked and co-crystallised pose of each reference ligand:

$$RMSD = \sqrt{[(1/n)\ \Sigma_i\ (r_{i,docked} - r_{i,crystal})^2]}$$ (Equation 3.20; Trott & Olson, 2010)

where $r_{i,docked}$ and $r_{i,crystal}$ are the coordinates of atom i in the docked and reference crystal poses respectively, and n is the number of heavy atoms compared; a validated protocol required RMSD < 2.0 Å.

3.12 Statistical Analysis

Quantitative data (proximate, AAS) are expressed as mean ± SD (n = 3), calculated as (Harris, 2015):

$$\bar{x} = (\Sigma x_i) / n$$ (Equation 3.12)

$$SD = \sqrt{[\Sigma(x_i - \bar{x})^2 / (n - 1)]}$$ (Equation 3.13)

where x_i = the individual replicate value, $\bar{x}$ = the sample mean, and n = the number of replicates (n = 3 for proximate and AAS determinations). Where the standard error of the mean is reported instead of SD, it was calculated as SEM = SD / √n (Equation 3.14). Normality was assessed by Shapiro–Wilk test; comparisons between species used the independent-samples t-test (or Mann–Whitney U if non-normal), with significance set at $p < 0.05$ (SPSS v27.0). Graphs were produced in GraphPad Prism (v9.0) and Cytoscape (v3.10.1).

3.13 Ethical Considerations

This study involved only plant material and publicly available computational databases; no human subjects, animals, or clinical samples were used, and no formal ethical approval was required. Plant collection followed institutional guidelines of Godfrey Okoye University with landowner consent and sustainable harvesting (≤30% leaf biomass per plant, no uprooting). Botanical authentication was obtained from the UNN Herbarium (Voucher No. UNN/11770; March 2026).

CHAPTER FOUR

RESULTS

This chapter presents the results of the comparative phytochemical, proximate, spectroscopic, elemental, and network pharmacological investigation of *Ficus sur* Forssk. and *Justicia secunda* Vahl leaf extracts. Results are presented in sequence: extraction yield, qualitative phytochemical screening, proximate composition, FTIR spectral analysis, AAS elemental analysis, ADME/drug-likeness screening, network pharmacological and PPI analysis, pathway enrichment, and molecular docking validation.

4.1 Percentage Extraction Yield

The percentage yields of the 70% ethanolic and chloroform Soxhlet extracts of *F. sur* and *J. secunda* calculated as % Yield = (mass of dry extract / mass of initial powder) × 100, are presented in Table 4.1.

Table 4.1: Percentage extraction yield of *Ficus sur* and *Justicia secunda* leaf extracts

Plant species	Extract type	Mass of powder (g)	Mass of dry extract (g)	% Yield
Ficus sur	70% Ethanolic	50	3.52	7.04
Ficus sur	Chloroform	18	1.00	1.99
Justicia secunda	70% Ethanolic	50	4.28	8.56
Justicia secunda	Chloroform	50	0.96	1.91

Note. Values are from a single gravimetric determination per extract and are not expressed as mean ± SD.

4.2 Qualitative Phytochemical Screening

Qualitative phytochemical screening of the 70% ethanolic extracts of both species, performed using the methods of Shaikh and Patil (2020), Harborne (1973), Trease and Evans (2002), and Sofowora (1993), is presented in Table 4.2. Results are recorded as present (+) or absent (−).

Table 4.2: Qualitative phytochemical composition of 70% ethanolic leaf extracts of *Ficus sur* and *Justicia secunda*

Phytoconstituent	Test	*Ficus sur*	*Justicia secunda*
Alkaloids	Dragendorff's / Mayer's / Wagner's	+	+
Flavonoids	Shinoda / Lead acetate	+	+
Tannins	$FeCl_3$ test	+	+
Saponins	Froth test	+	+
Steroids	Liebermann–Burchard	+	−
Triterpenoids	Liebermann–Burchard	+	−
Cardiac glycosides	Keller–Kiliani	−	+
Phenols	$FeCl_3$ test	+	+
Terpenoids	Salkowski	+	+
Anthraquinones	Bornträger's	−	−
Reducing sugars	Fehling's test	+	+

Note. + = present; − = absent.

4.3 Proximate Composition

The proximate composition of the powdered leaves of *F. sur* and *J. secunda* was determined following AOAC (2016) methods as described in Section 3.7. The percentage extraction yields of both leaf powders are presented in Table 4.1, while moisture content and dry matter are presented in Table 4.3. Soxhlet extraction of 50 g leaf powder with 70% ethanol (v/v, 78–80°C, 8 h) yielded 3.52 g dry extract for *F. sur* (yield: 7.04%) and 4.28 g for *J. secunda* (yield: 8.56%). Moisture content was 7.0% for *F. sur* and 15.0% for *J. secunda*, corresponding to a dry matter content of 93.0% and 85.0%, respectively.

Table 4.3: Proximate composition (% dry weight, except energy) of *Ficus sur* and *Justicia secunda* leaf powder (mean ± SD, n = 3)

Parameter	***Ficus sur***	***Justicia secunda***
Moisture (%)	7.0	15.0
Ash (%)	1.99 ± 0.04	1.91 ± 0.03
Crude protein (%)	3.00 ± 0.06	7.50 ± 0.15
Crude fat (%)	7.50 ± 0.11	15.00 ± 0.22
Crude fibre (%)	9.81 ± 0.19	24.87 ± 0.52
Carbohydrate (%) [by difference]	70.70	35.72
Energy value (kcal/100 g)	362.30	307.88

Note. Moisture is reported from a single determination per species and is not expressed as mean ± SD. Carbohydrate (by difference) and energy value (Atwater factors, Equation 3.9) are calculated from the other row means and likewise do not carry an independently determined SD. Ash, crude protein, crude fat, and crude fibre are mean ± SD of triplicate determinations (n = 3).

4.4 Ftir Spectral Analysis

The ATR-FTIR spectra of the 70% ethanolic extracts of *J. secunda* and *F. sur* were acquired over 4,000–400 cm^{-1} as described in Section 3.8. The overlaid spectra are presented in Figure 4.1, and major absorption band assignments are given in Tables 4.4a and 4.4b.

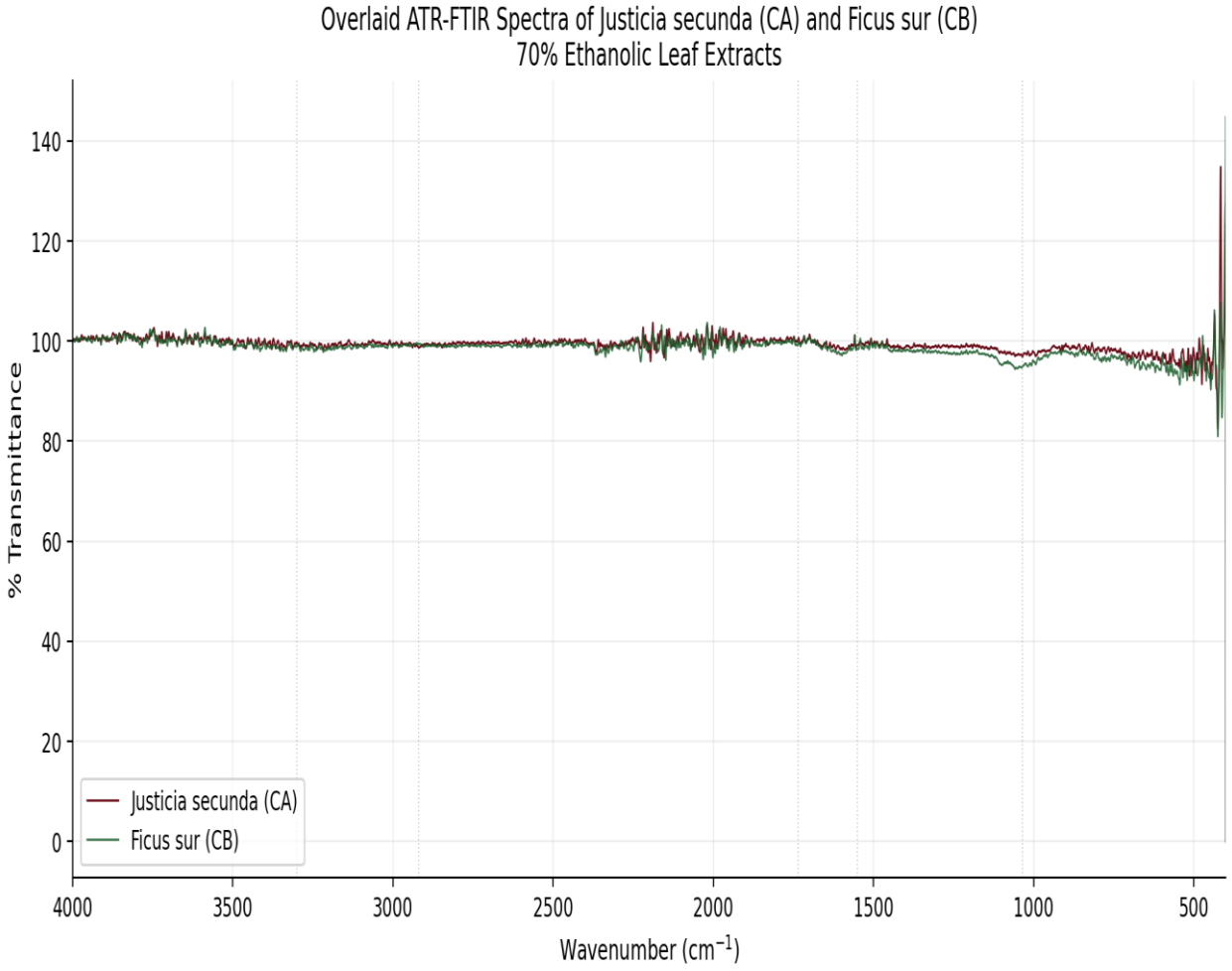

Figure 4.1. Overlaid ATR-FTIR spectra of *Justicia secunda* (dark red) and *Ficus sur* (dark green)

Table 4.4a: Major FTIR absorption bands and functional group assignments for Justicia secunda ethanolic extract

Wavenumber (cm^{-1})	Functional group
3217.9, 3378.7, 3432.6, 3460.8	O–H stretch (polyphenols, flavonoids, bound water)
Not resolved	Aliphatic C–H stretch (terpenoids, fatty acids)
Not resolved	C=O stretch (carbonyl; flavonoid ketone, ester)
1587.8	Aromatic C=C / N–H bend (flavonoids, alkaloids)
1034.8	C–O–C stretch (glycosidic linkages)
602.8, 666.96	Fingerprint region (aromatic C–H, ring substitution)

Table 4.4b: Major FTIR absorption bands and functional group assignments for Ficus sur ethanolic extract

Wavenumber (cm^{-1})	Functional group
Broad shoulder; not resolved as discrete peak	O–H stretch (polyphenols, flavonoids, bound water)
Not resolved	Aliphatic C–H stretch (terpenoids, fatty acids)
Not resolved	C=O stretch (carbonyl; flavonoid ketone, ester)
1554.0, 1598.1	Aromatic C=C / N–H bend (flavonoids, alkaloids)
1057.9	C–O–C stretch (glycosidic linkages)
619.9	Fingerprint region (aromatic C–H, ring substitution)

4.5 Atomic Absorption Spectroscopic (AAS) Elemental Analysis

The elemental composition of the 70% ethanolic extracts of *J. secunda* and *F. sur* was determined for 12 elements by flame AAS on a Thermo Scientific iCE 3000 (SOLAAR V11.10, Central Science Laboratory, UNN) as described in Section 3.9. Results are presented in Table 4.5.

Table 4.5: Elemental composition (mg/L) of *Justicia secunda* and *Ficus sur* 70% ethanolic extracts by flame AAS

Element	***J. secunda* (mg/L)**	***F. sur* (mg/L)**
Ca	80.1636	280.5601
K	25.0374	36.4417
Na	10.3443	16.3704
Mg	9.2325	10.0973
Fe	2.5411	2.6031
Mn	0.2733	0.3437
Zn	0.3951	0.5426
Cu	0.1554	0.1407
Cr	0.5774	0.6909
Ni	0.1152	0.1156
Pb	ND	ND
Cd	ND	ND

Note. ND = not detected.

4.6 Physicochemical, ADME and Toxicity Screening of Leaf-Derived Compounds

Ninety-five leaf-derived compounds reported in the phytochemical literature for the two study species (thirty for *F. sur*, sixty-five for *J. secunda*) were evaluated for physicochemical, drug-likeness, ligand-efficiency and structural toxicity-alert properties using the compound-properties module referenced in Section 3.10. Physicochemical descriptors are presented in Table 4.6a, drug-likeness and ligand-efficiency descriptors in Table 4.6b, and structural toxicity-alert flags in Table 4.6c. Sixteen compounds (five from *F. sur*, eleven from *J. secunda*) returned a druglikeness score ≥ 0 (Table 4.6b). Eight of the nine compounds already carried forward for target prediction and network pharmacological analysis in Section 4.7 (Scytalone, Caffeic acid, p-Coumaric acid, Ferulic acid, Piperine, Rutin, Luteolin, Apigenin) match this wider leaf-only screen exactly on both identity and druglikeness score. The ninth, Bis(2-ethylhexyl) phthalate (DEHP) (druglikeness 4.607 in Table 4.7), was reported from non-leaf plant parts of *J. secunda* and therefore does not appear in this leaf-only screen; it is a distinct compound from β-Bisabolene (No. 53), which returns a druglikeness score of −6.48 in the leaf-only dataset and did not pass the drug-likeness threshold. The remaining compounds meeting the ≥ 0 threshold here were not part of the original target-prediction run and are not reflected in Sections 4.7–4.10.

Table 4.6a: Physicochemical properties of leaf-derived compounds from *Ficus sur* and *Justicia secunda*

No.	Compound	Plant	MW (g/mol)	Mono. Mass (g/mol)	cLogP	cLogS (mol/L)	H-Acc	H-Don	Total SA (Å²)	Rel. Polar SA (%)	TPSA (Å²)
1	n-Tricosane	*Ficus sur*	324.63	324.3760	10.520	-6.654	0	0	326.98	0	0
2	n-Hexacosane	*Ficus sur*	366.71	366.4230	11.883	-7.464	0	0	368.26	0	0
3	Cyclotetradecane	*Ficus sur*	196.38	196.2190	6.362	-4.310	0	0	192.64	0	0
4	Triacontane	*Ficus sur*	422.82	422.4850	13.700	-8.544	0	0	423.30	0	0
5	Limonene	*Ficus sur*	136.24	136.1250	3.361	-2.539	0	0	125.76	0	0
6	Carvacrol	*Ficus sur*	150.22	150.1040	2.845	-2.535	1	1	128.89	0.102	20.23
7	α-Humulene (α-Caryophyllene)	*Ficus sur*	204.36	204.1880	6.239	-3.401	0	0	190.41	0	0
8	Caryophyllene oxide	*Ficus sur*	220.35	220.1830	4.055	-3.558	1	0	177.30	0.100	12.53
9	Linalool	*Ficus sur*	154.25	154.1360	3.231	-2.149	1	1	143.81	0.091	20.23
10	3-Tetradecanone	*Ficus sur*	212.38	212.2140	5.377	-3.876	1	0	207.13	0.063	17.07
11	Geranylacetone	*Ficus sur*	194.32	194.1670	4.722	-2.858	1	0	184.75	0.071	17.07
12	6,10,14-Trimethyl-2-pentadecanone	*Ficus sur*	268.48	268.2770	6.486	-4.626	1	0	253.89	0.051	17.07
13	trans-Geranylgeraniol	*Ficus sur*	290.49	290.2610	7.829	-3.841	1	1	276.31	0.047	20.23
14	n-Hexadecanoic acid (Palmitic acid)	*Ficus sur*	256.43	256.2400	6.063	-4.239	2	1	242.50	0.108	37.30
15	(E)-β-Ionone	*Ficus sur*	192.30	192.1510	3.223	-2.944	1	0	167.97	0.078	17.07
16	β-Caryophyllene	*Ficus sur*	204.36	204.1880	5.486	-3.662	0	0	174.95	0	0
17	Phytol	*Ficus sur*	296.54	296.3080	7.421	-4.633	1	1	280.96	0.047	20.23
18	Scytalone	*Ficus sur*	194.19	194.0580	0.722	-1.898	4	3	136.58	0.383	77.76
19	Gallic acid	*Ficus sur*	170.12	170.0220	0.108	-0.741	5	4	116.41	0.562	97.99
20	Protocatechuic acid	*Ficus sur*	154.12	154.0270	0.453	-1.037	4	3	110.06	0.476	77.76
21	Caffeic acid	*Ficus sur*	180.16	180.0420	0.783	-1.407	4	3	136.56	0.383	77.76
22	p-Coumaric acid	*Ficus sur*	164.16	164.0470	1.128	-1.703	3	2	130.21	0.301	57.53
23	Ferulic acid	*Ficus sur*	194.19	194.0580	1.058	-1.721	4	2	152.47	0.323	66.76
24	Chlorogenic acid	*Ficus sur*	354.31	354.0950	-0.769	-1.496	9	6	245.29	0.468	164.75
25	Ellagic acid	*Ficus sur*	302.19	302.0060	1.277	-3.286	8	4	186.92	0.527	133.52
26	Quercetin	*Ficus sur*	302.24	302.0430	1.490	-2.491	7	5	201.94	0.438	127.45
27	Epicatechin (−)	*Ficus sur*	290.27	290.0790	1.500	-2.012	6	5	214.50	0.410	110.38
28	Stigmasterol	*Ficus sur*	412.70	412.3700	7.630	-6.520	1	1	336	0.039	20.23
29	Campesterol	*Ficus sur*	400.69	400.3700	7.450	-6.350	1	1	326	0.040	20.23
30	Pheophytin a	*Ficus sur*	871.20	869.5420	9.110	-8.230	5	1	660	0.068	57.53
31	p-Xylene	*Justicia secunda*	106.17	106.0780	2.953	-2.356	0	0	97.88	0	0
32	Desulphosinigrin	*Justicia secunda*	279.30	279.0740	0.560	-2.144	7	4	201.10	0.427	110.38

33	2,6,10-Trimethyltetradecane	*Justicia secunda*	240.47	240.2820	8.370	-5.410	0	0	232.50	0	0
34	Tridecane	*Justicia secunda*	184.36	184.2190	7.143	-4.787	0	0	178.95	0	0
35	2-Cyclohexylpiperidine	*Justicia secunda*	167.29	167.1670	3.280	-2.560	1	1	162.50	0.075	12.53
36	Phytol acetate	*Justicia secunda*	308.50	308.2720	7.301	-4.751	2	0	297.65	0.077	26.30
37	Phytol	*Justicia secunda*	296.54	296.3080	7.421	-4.633	1	1	280.96	0.047	20.23
38	Isophytol acetate	*Justicia secunda*	338.57	338.3090	8.610	-5.620	2	0	324.30	0.063	26.30
39	Benzyl butyl phthalate	*Justicia secunda*	312.36	312.1360	4.912	-4.073	4	0	251.20	0.196	52.60
40	Diisooctyl phthalate	*Justicia secunda*	390.56	390.2770	8.690	-6.154	4	0	367.40	0.135	52.60
41	Squalene	*Justicia secunda*	410.73	410.3910	13.099	-6.300	0	0	397.44	0	0
42	Ethyl palmitate	*Justicia secunda*	284.48	284.2720	6.897	-4.667	2	0	272.17	0.085	26.30
43	2,4-Di-tert-butylphenol	*Justicia secunda*	206.33	206.1670	4.478	-3.640	1	1	173.99	0.075	20.23
44	9,17-Octadecadienal (Z)-	*Justicia secunda*	264.45	264.2450	6.590	-4.150	1	0	252.40	0.054	17.07
45	Linoleic acid ethyl ester	*Justicia secunda*	308.50	308.2720	7.301	-4.751	2	0	297.65	0.077	26.30
46	Hexadecane	*Justicia secunda*	226.44	226.2660	8.250	-5.300	0	0	218.90	0	0
47	2,6-Dimethylheptadecane	*Justicia secunda*	268.52	268.3080	9.470	-6.030	0	0	259.80	0	0
48	Ethyl oleate	*Justicia secunda*	310.52	310.2870	7.553	-4.979	2	0	298.67	0.077	26.30
49	Pristane	*Justicia secunda*	296.57	296.3440	9.880	-6.410	0	0	286.50	0	0
50	3-Methylnonane	*Justicia secunda*	142.28	142.1720	5.060	-3.620	0	0	136.70	0	0
51	Hexatriacontane	*Justicia secunda*	506.98	506.5790	16.400	-10.040	0	0	491.30	0	0
52	β-Caryophyllene	*Justicia secunda*	204.36	204.1880	5.486	-3.662	0	0	174.95	0	0
53	β-Bisabolene	*Justicia secunda*	204.36	204.1880	5.486	-3.662	0	0	174.95	0	0
54	1-Hexadecanol	*Justicia secunda*	242.44	242.2610	6.260	-4.400	1	1	233.80	0.056	20.23
55	DEHP	*Justicia secunda*	390.56	390.2770	8.690	-6.154	4	0	367.40	0.135	52.60
56	α-Copaene	*Justicia secunda*	204.36	204.1880	5.486	-3.662	0	0	174.95	0	0
57	α-Humulene	*Justicia secunda*	204.36	204.1880	6.239	-3.401	0	0	190.41	0	0
58	Palmitoleic acid	*Justicia secunda*	254.41	254.2250	5.810	-4.011	2	1	241.48	0.108	37.30
59	β-Farnesene	*Justicia secunda*	204.36	204.1880	6	-3.540	0	0	188.80	0	0
60	Nerolidol	*Justicia secunda*	222.37	222.1980	5.403	-3.125	1	1	208.30	0.063	20.23
61	Piperine	*Justicia secunda*	285.34	285.1370	3.595	-3.608	4	0	229.87	0.159	38.77
62	Diethyl phthalate	*Justicia secunda*	222.24	222.0890	2.298	-2.498	4	0	180.80	0.255	52.60
63	5(1H)-Azulenone	*Justicia secunda*	118.24	118.0820	2.436	-1.983	0	0	105.03	0.167	25.30
64	γ-Elemene	*Justicia secunda*	204.36	204.1880	5.486	-3.662	0	0	174.95	0	0
65	Elaidic acid	*Justicia secunda*	282.47	282.2560	6.719	-4.551	2	1	269	0.097	37.30
66	9(1H)-Phenanthrone	*Justicia secunda*	194.23	194.0730	3.850	-3.220	1	0	164.20	0.073	17.07
67	Longifolene	*Justicia secunda*	204.36	204.1880	5.486	-3.662	0	0	174.95	0	0
68	2-Hydroxycyclopentadecanone	*Justicia secunda*	240.38	240.2090	4.790	-3.870	2	1	224.40	0.116	37.30
69	α-Patchoulene	*Justicia secunda*	204.36	204.1880	5.486	-3.662	0	0	174.95	0	0

70	Oleic acid	*Justicia secunda*	282.47	282.2560	6.719	-4.551	2	1	269	0.097	37.30
71	Methyl palmitate	*Justicia secunda*	270.46	270.2560	6.490	-4.367	2	0	258.41	0.089	26.30
72	Methyl oleate	*Justicia secunda*	296.49	296.2720	7.090	-4.750	2	0	285.10	0.084	26.30
73	γ-Terpinene	*Justicia secunda*	136.24	136.1250	3.360	-2.539	0	0	125.76	0	0
74	p-Cymene	*Justicia secunda*	134.22	134.1100	3.500	-2.620	0	0	118.50	0	0
75	Decane	*Justicia secunda*	142.28	142.1720	5.060	-3.620	0	0	136.70	0	0
76	Aromadendrene	*Justicia secunda*	204.36	204.1880	5.486	-3.662	0	0	174.95	0	0
77	4-Tetradecene	*Justicia secunda*	196.38	196.2190	7.060	-4.670	0	0	189.60	0	0
78	Di-sec-butyl phthalate	*Justicia secunda*	278.35	278.1520	4.540	-3.870	4	0	220.30	0.224	52.60
79	Luteolin	*Justicia secunda*	286.24	286.0480	1.990	-2.560	6	4	197.38	0.382	107.22
80	Apigenin	*Justicia secunda*	270.24	270.0530	2.336	-2.856	5	3	191.03	0.326	86.99
81	Diosmetin	*Justicia secunda*	300.27	300.0640	2.700	-3.010	6	3	211.60	0.350	107.22
82	Quercetin	*Justicia secunda*	302.24	302.0430	1.490	-2.491	7	5	201.94	0.438	127.45
83	Kaempferol	*Justicia secunda*	286.24	286.0480	1.900	-2.521	6	4	197.50	0.390	107.22
84	Rutin (Quercetin-3-O-rutinoside)	*Justicia secunda*	610.52	610.1530	-1.257	-2.398	16	10	397.71	0.488	265.52
85	Luteolin-7-O-glucoside	*Justicia secunda*	448.38	448.1010	0.180	-2.130	10	7	302.50	0.454	190
86	Apigenin-7-O-glucoside	*Justicia secunda*	432.38	432.1060	0.180	-2.130	9	6	291.60	0.428	169.77
87	Luteolin-7-O-rutinoside	*Justicia secunda*	594.52	594.1590	-1.240	-2.280	15	9	384.70	0.472	244.89
88	Gallic acid	*Justicia secunda*	170.12	170.0220	0.108	-0.741	5	4	116.41	0.562	97.99
89	Caffeic acid	*Justicia secunda*	180.16	180.0420	0.783	-1.407	4	3	136.56	0.383	77.76
90	Chlorogenic acid	*Justicia secunda*	354.31	354.0950	-0.769	-1.496	9	6	245.29	0.468	164.75
91	Protocatechuic acid	*Justicia secunda*	154.12	154.0270	0.453	-1.037	4	3	110.06	0.476	77.76
92	Syringic acid	*Justicia secunda*	198.17	198.0530	0.890	-1.720	5	2	151.40	0.329	75.99
93	Salicylic acid	*Justicia secunda*	138.12	138.0320	1.690	-1.580	3	2	104.30	0.296	57.53
94	Campesterol	*Justicia secunda*	400.69	400.3700	7.450	-6.350	1	1	326	0.040	20.23
95	Oleanolic acid	*Justicia secunda*	456.71	456.3600	6.064	-6.128	3	2	337.04	0.116	57.53

Note. MW = molecular weight; cLogP = calculated octanol/water partition coefficient; cLogS = calculated aqueous solubility; H-Acc/H-Don = hydrogen-bond acceptor/donor count; Total SA = total solvent-accessible surface area; Rel. Polar SA = polar surface area as a percentage of total SA; TPSA = topological polar surface area.

Table 4.6b: Drug-likeness and ligand-efficiency indices of leaf-derived compounds from *Ficus sur* and *Justicia secunda*

No.	Compound	Plant	Drug-likeness	LE	LLE	LELP
1	n-Tricosane	*Ficus sur*	-20.398	0.292	-5.618	35.979
2	n-Hexacosane	*Ficus sur*	-20.398	0.259	-6.977	45.901
3	Cyclotetradecane	*Ficus sur*	-7.630	0.409	-2.191	15.566
4	Triacontane	*Ficus sur*	-20.398	0.224	-8.799	61.119
5	Limonene	*Ficus sur*	-21.855	0.461	-0.004	7.298
6	Carvacrol	*Ficus sur*	-2.336	0.622	2.140	4.576
7	α-Humulene (α-Caryophyllene)	*Ficus sur*	-4.717	0.208	-3.962	29.954
8	Caryophyllene oxide	*Ficus sur*	-4.768	0.237	-1.296	17.143
9	Linalool	*Ficus sur*	-6.685	0.647	1.953	4.998
10	3-Tetradecanone	*Ficus sur*	-20.884	0.380	-1.219	14.138
11	Geranylacetone	*Ficus sur*	-4.589	0.275	-1.913	17.151
12	6,10,14-Trimethyl-2-pentadecanone	*Ficus sur*	-7.057	0.360	-1.504	18.029
13	trans-Geranylgeraniol	*Ficus sur*	-3.375	0.149	-5.552	52.625
14	n-Hexadecanoic acid (Palmitic acid)	*Ficus sur*	-25.216	0.458	-0.056	13.243
15	(E)-β-Ionone	*Ficus sur*	-9.232	0.222	-0.953	14.487
16	β-Caryophyllene	*Ficus sur*	-6.476	0.208	-3.209	26.341
17	Phytol	*Ficus sur*	-3.766	0.149	-5.144	49.883
18	Scytalone	*Ficus sur*	0.752	0.371	3.067	1.945
19	Gallic acid	*Ficus sur*	-1.844	0.735	6.324	0.146
20	Protocatechuic acid	*Ficus sur*	-1.844	0.891	6.689	0.509
21	Caffeic acid	*Ficus sur*	0.168	0.334	2.379	2.345
22	p-Coumaric acid	*Ficus sur*	0.168	0.365	2.067	3.088
23	Ferulic acid	*Ficus sur*	0.275	0.328	2.293	3.223
24	Chlorogenic acid	*Ficus sur*	-0.976	0.151	3.515	-5.100
25	Ellagic acid	*Ficus sur*	-1.598	0.142	1	8.996
26	Quercetin	*Ficus sur*	-0.083	0.142	0.787	10.494
27	Epicatechin (−)	*Ficus sur*	0.820	0.158	1.267	9.494
28	Stigmasterol	*Ficus sur*	-4.475	0.167	-4.202	47.022
29	Campesterol	*Ficus sur*	-4.475	0.173	-4.102	43.012
30	Pheophytin a	*Ficus sur*	-11.220	0.065	-5.910	140
31	p-Xylene	*Justicia secunda*	-3.742	0.558	0.597	5.291
32	Desulphosinigrin	*Justicia secunda*	-1.830	0.265	3.880	2.113
33	2,6,10-Trimethyltetradecane	*Justicia secunda*	-20.398	0.318	-6.432	26.314
34	Tridecane	*Justicia secunda*	-20.398	0.368	-5.065	19.410
35	2-Cyclohexylpiperidine	*Justicia secunda*	-4.120	0.495	1.180	6.626
36	Phytol acetate	*Justicia secunda*	-39.699	0.142	-5.024	51.416
37	Phytol	*Justicia secunda*	-3.766	0.149	-5.144	49.883
38	Isophytol acetate	*Justicia secunda*	-52.100	0.124	-6.248	69.435
39	Benzyl butyl phthalate	*Justicia secunda*	-4.380	0.258	0.751	19.039
40	Diisooctyl phthalate	*Justicia secunda*	-8.180	0.181	-3.518	47.950
41	Squalene	*Justicia secunda*	-3.522	0.146	-9.904	89.652
42	Ethyl palmitate	*Justicia secunda*	-39.360	0.337	-1.989	20.487

43	2,4-Di-tert-butylphenol	*Justicia secunda*	-5.276	0.470	0.658	9.532
44	9,17-Octadecadienal (Z)-	*Justicia secunda*	-8.890	0.213	-3.670	30.890
45	Linoleic acid ethyl ester	*Justicia secunda*	-39.699	0.142	-5.024	51.416
46	Hexadecane	*Justicia secunda*	-20.398	0.300	-5.840	27.500
47	2,6-Dimethylheptadecane	*Justicia secunda*	-20.398	0.267	-6.750	35.430
48	Ethyl oleate	*Justicia secunda*	-43.109	0.142	-5.283	53.347
49	Pristane	*Justicia secunda*	-20.398	0.229	-7.480	43.140
50	3-Methylnonane	*Justicia secunda*	-20.398	0.479	-3.390	10.560
51	Hexatriacontane	*Justicia secunda*	-20.398	0.186	-10.250	87.630
52	β-Caryophyllene	*Justicia secunda*	-6.476	0.208	-3.209	26.341
53	β-Bisabolene	*Justicia secunda*	-6.476	0.208	-3.209	26.341
54	1-Hexadecanol	*Justicia secunda*	-11.270	0.234	-3.834	26.743
55	DEHP	*Justicia secunda*	-8.180	0.181	-3.518	47.950
56	α-Copaene	*Justicia secunda*	-6.476	0.208	-3.209	26.341
57	α-Humulene	*Justicia secunda*	-4.717	0.208	-3.962	29.954
58	Palmitoleic acid	*Justicia secunda*	-26.101	0.255	-2.459	22.750
59	β-Farnesene	*Justicia secunda*	-6	0.208	-3.500	28.846
60	Nerolidol	*Justicia secunda*	-6.378	0.195	-3.126	27.674
61	Piperine	*Justicia secunda*	0.433	0.209	-0.400	17.223
62	Diethyl phthalate	*Justicia secunda*	-5.463	0.443	2.871	5.186
63	5(1H)-Azulenone	*Justicia secunda*	-0.395	0.963	2.475	2.531
64	γ-Elemene	*Justicia secunda*	-6.476	0.208	-3.209	26.341
65	Elaidic acid	*Justicia secunda*	-28.971	0.219	-3.524	30.654
66	9(1H)-Phenanthrone	*Justicia secunda*	-2.160	0.318	0.432	12.107
67	Longifolene	*Justicia secunda*	-6.476	0.208	-3.209	26.341
68	2-Hydroxycyclopentadecanone	*Justicia secunda*	-18.560	0.249	-2.191	19.237
69	α-Patchoulene	*Justicia secunda*	-6.476	0.208	-3.209	26.341
70	Oleic acid	*Justicia secunda*	-28.971	0.230	-3.368	29.231
71	Methyl palmitate	*Justicia secunda*	-35.364	0.367	-1.403	17.670
72	Methyl oleate	*Justicia secunda*	-39.050	0.319	-1.850	22.220
73	γ-Terpinene	*Justicia secunda*	-21.855	0.461	-0.004	7.298
74	p-Cymene	*Justicia secunda*	-9.230	0.477	0.087	7.327

75	Decane	*Justicia secunda*	-20.398	0.479	-3.390	10.560
76	Aromadendrene	*Justicia secunda*	-6.476	0.208	-3.209	26.341
77	4-Tetradecene	*Justicia secunda*	-20.398	0.349	-5.390	20.240
78	Di-sec-butyl phthalate	*Justicia secunda*	-4.710	0.347	1.460	13.085
79	Luteolin	*Justicia secunda*	0.282	0.149	0.287	13.376
80	Apigenin	*Justicia secunda*	0.282	0.156	-0.058	14.952
81	Diosmetin	*Justicia secunda*	0.420	0.143	0.106	18.881
82	Quercetin	*Justicia secunda*	-0.083	0.142	0.787	10.494
83	Kaempferol	*Justicia secunda*	0.268	0.149	0.280	12.752
84	Rutin (Quercetin-3-O-rutinoside)	*Justicia secunda*	1.934	0.073	3.535	-17.305
85	Luteolin-7-O-glucoside	*Justicia secunda*	0.720	0.101	1.840	-1.778
86	Apigenin-7-O-glucoside	*Justicia secunda*	0.820	0.105	2.020	-1.714
87	Luteolin-7-O-rutinoside	*Justicia secunda*	1.960	0.079	3.380	-15.696
88	Gallic acid	*Justicia secunda*	-1.844	0.735	6.324	0.146
89	Caffeic acid	*Justicia secunda*	0.168	0.334	2.379	2.345
90	Chlorogenic acid	*Justicia secunda*	-0.976	0.151	3.515	-5.100
91	Protocatechuic acid	*Justicia secunda*	-1.844	0.891	6.689	0.509
92	Syringic acid	*Justicia secunda*	0.320	0.328	2.780	2.714
93	Salicylic acid	*Justicia secunda*	-0.960	0.547	3.440	3.088
94	Campesterol	*Justicia secunda*	-4.475	0.173	-4.102	43.012
95	Oleanolic acid	*Justicia secunda*	-1.782	0.207	-1.085	29.298

Note. Druglikeness score ≥ 0 indicates a drug-like structure. LE = ligand efficiency; LLE = lipophilic ligand efficiency; LELP = ligand-efficiency lipophilic price. LE, LLE and LELP were computed on a common reference potency scale and are reported here as calculated by the compound-properties module (Section 3.10); they were not derived from experimentally determined binding constants for these compounds and should be read as relative, not absolute, indices.

Table 4.6c: Toxicity structural-alert flags of leaf-derived compounds from Ficus sur and Justicia secunda

No.	Compound	Plant	Mutagenic	Tumor- igenic	Repro. Effect.	Irritant
1	n-Tricosane	*Ficus sur*	-	-	-	-
2	n-Hexacosane	*Ficus sur*	-	-	-	-
3	Cyclotetradecane	*Ficus sur*	-	-	-	-
4	Triacontane	*Ficus sur*	-	-	-	-
5	Limonene	*Ficus sur*	-	-	-	Low
6	Carvacrol	*Ficus sur*	-	-	-	High
7	α-Humulene (α-Caryophyllene)	*Ficus sur*	-	-	-	-
8	Caryophyllene oxide	*Ficus sur*	-	Low	Low	-
9	Linalool	*Ficus sur*	High	-	-	High
10	3-Tetradecanone	*Ficus sur*	-	-	-	High
11	Geranylacetone	*Ficus sur*	-	-	-	High
12	6,10,14-Trimethyl-2-pentadecanone	*Ficus sur*	-	-	-	High
13	trans-Geranylgeraniol	*Ficus sur*	-	-	-	-
14	n-Hexadecanoic acid (Palmitic acid)	*Ficus sur*	-	High	-	High
15	(E)-β-Ionone	*Ficus sur*	-	High	-	High
16	β-Caryophyllene	*Ficus sur*	-	-	-	-
17	Phytol	*Ficus sur*	-	-	-	-
18	Scytalone	*Ficus sur*	-	-	-	-
19	Gallic acid	*Ficus sur*	High	-	High	-
20	Protocatechuic acid	*Ficus sur*	High	-	-	-
21	Caffeic acid	*Ficus sur*	High	High	High	-
22	p-Coumaric acid	*Ficus sur*	-	-	High	-
23	Ferulic acid	*Ficus sur*	High	High	High	-
24	Chlorogenic acid	*Ficus sur*	-	-	-	-
25	Ellagic acid	*Ficus sur*	-	-	-	-
26	Quercetin	*Ficus sur*	High	High	-	-
27	Epicatechin (−)	*Ficus sur*	-	-	-	-
28	Stigmasterol	*Ficus sur*	-	-	-	-
29	Campesterol	*Ficus sur*	-	-	-	-
30	Pheophytin a	*Ficus sur*	-	-	-	-
31	p-Xylene	*Justicia secunda*	-	-	-	-
32	Desulphosinigrin	*Justicia secunda*	-	-	-	-
33	2,6,10-Trimethyltetradecane	*Justicia secunda*	-	-	-	-
34	Tridecane	*Justicia secunda*	-	-	-	-
35	2-Cyclohexylpiperidine	*Justicia secunda*	-	-	-	-
36	Phytol acetate	*Justicia secunda*	-	-	-	-
37	Phytol	*Justicia secunda*	-	-	-	-
38	Isophytol acetate	*Justicia secunda*	High	High	High	High
39	Benzyl butyl phthalate	*Justicia secunda*	-	-	-	-
40	Diisooctyl phthalate	*Justicia secunda*	-	-	-	-
41	Squalene	*Justicia secunda*	-	-	-	-

42	Ethyl palmitate	*Justicia secunda*	-	-	-	-
43	2,4-Di-tert-butylphenol	*Justicia secunda*	-	-	-	-
44	9,17-Octadecadienal (Z)-	*Justicia secunda*	-	-	-	-
45	Linoleic acid ethyl ester	*Justicia secunda*	-	-	-	-
46	Hexadecane	*Justicia secunda*	-	-	-	-
47	2,6-Dimethylheptadecane	*Justicia secunda*	-	-	-	-
48	Ethyl oleate	*Justicia secunda*	-	-	-	-
49	Pristane	*Justicia secunda*	-	-	-	-
50	3-Methylnonane	*Justicia secunda*	-	-	-	-
51	Hexatriacontane	*Justicia secunda*	-	-	-	-
52	β-Caryophyllene	*Justicia secunda*	-	-	-	-
53	β-Bisabolene	*Justicia secunda*	-	-	-	Low
54	1-Hexadecanol	*Justicia secunda*	-	-	-	-
55	DEHP	*Justicia secunda*	-	-	-	-
56	α-Copaene	*Justicia secunda*	-	-	-	-
57	α-Humulene	*Justicia secunda*	-	-	-	-
58	Palmitoleic acid	*Justicia secunda*	-	-	-	-
59	β-Farnesene	*Justicia secunda*	-	-	-	-
60	Nerolidol	*Justicia secunda*	-	-	-	High
61	Piperine	*Justicia secunda*	-	-	High	-
62	Diethyl phthalate	*Justicia secunda*	High	High	High	Low
63	5(1H)-Azulenone	*Justicia secunda*	-	-	-	-
64	γ-Elemene	*Justicia secunda*	-	-	-	-
65	Elaidic acid	*Justicia secunda*	-	-	-	-
66	9(1H)-Phenanthrone	*Justicia secunda*	-	-	-	-
67	Longifolene	*Justicia secunda*	-	-	-	-
68	2-Hydroxycyclopentadecanone	*Justicia secunda*	-	-	-	-
69	α-Patchoulene	*Justicia secunda*	-	-	-	-
70	Oleic acid	*Justicia secunda*	High	High	-	High
71	Methyl palmitate	*Justicia secunda*	-	-	-	-
72	Methyl oleate	*Justicia secunda*	-	-	-	-
73	γ-Terpinene	*Justicia secunda*	-	-	-	Low

74	p-Cymene	*Justicia secunda*	-	-	-	-
75	Decane	*Justicia secunda*	-	-	-	-
76	Aromadendrene	*Justicia secunda*	-	-	-	-
77	4-Tetradecene	*Justicia secunda*	-	-	-	-
78	Di-sec-butyl phthalate	*Justicia secunda*	-	-	-	-
79	Luteolin	*Justicia secunda*	-	-	-	-
80	Apigenin	*Justicia secunda*	High	-	-	-
81	Diosmetin	*Justicia secunda*	-	-	-	-
82	Quercetin	*Justicia secunda*	High	High	-	-
83	Kaempferol	*Justicia secunda*	-	-	-	-
84	Rutin (Quercetin-3-O-rutinoside)	*Justicia secunda*	-	-	-	-
85	Luteolin-7-O-glucoside	*Justicia secunda*	-	-	-	-
86	Apigenin-7-O-glucoside	*Justicia secunda*	-	-	-	-
87	Luteolin-7-O-rutinoside	*Justicia secunda*	-	-	-	-
88	Gallic acid	*Justicia secunda*	High	-	High	-
89	Caffeic acid	*Justicia secunda*	High	High	High	-
90	Chlorogenic acid	*Justicia secunda*	-	-	-	-
91	Protocatechuic acid	*Justicia secunda*	High	-	-	-
92	Syringic acid	*Justicia secunda*	-	-	-	-
93	Salicylic acid	*Justicia secunda*	High	-	-	-
94	Campesterol	*Justicia secunda*	-	-	-	-
95	Oleanolic acid	*Justicia secunda*	-	-	-	-

Note. Values are structural-alert risk flags (None / Low / High) from the compound-properties module (Section 3.10), not experimentally determined toxicity data.

4.7 Network Pharmacology and Protein–Protein Interaction (PPI) Analysis

Of the 9 drug-like compounds, 8 yielded significant predicted protein targets overlapping with anaemia/erythropoiesis/haemoglobin-synthesis-associated genes retrieved from GeneCards, OMIM, and DisGeNET. Each compound was assigned 4 hub gene targets (identified by node degree, betweenness, and closeness centrality in Cytoscape v3.10.1; STRING confidence ≥ 0.700), yielding 32 compound–target interactions across 32 unique genes (Table 4.7). The PPI sub-network diagram for all 8 compounds is presented in Figure 4.3.

Table 4.7: Compound–target gene interactions from PPI network analysis

Compound	Source plant	Hub gene targets (n = 4)
Rutin (Quercetin-3-O-rutinoside)	*Justicia secunda*	FANCM, SLX4, FANCF, HBB
Apigenin	*Justicia secunda*	NBN, ATM, TP53, ADA
Luteolin	*Justicia secunda*	BRIP1, FANCD2, FANCL, RAG1
Piperine	*Justicia secunda*	BRCA1, EGFR, FANCA, BRCA2
DEHP	*Justicia secunda*	FANCE, PALB2, JAK3, FANCB
Ferulic acid	*Ficus sur*	FANCG, RAD51C, G6PD, GATA1
p-Coumaric acid	*Ficus sur*	FANCI, HBA2, SLC4A1, TERT
Caffeic acid	*Ficus sur*	TRNT1, HBA1, FANCC, MET

Note. 32 compound–target interactions across 32 unique genes. Gene families: FA DNA-repair pathway (FANCA, FANCB, FANCC, FANCD2, FANCE, FANCF, FANCG, FANCI, FANCL, FANCM, BRCA1, BRCA2, BRIP1, RAD51C, PALB2, SLX4); haemoglobin synthesis (HBB, HBA1, HBA2); erythroid transcription (GATA1); supporting targets (TP53, ATM, EGFR, JAK3, G6PD, MET, NBN, RAG1, TERT, ADA, SLC4A1, TRNT1).

A

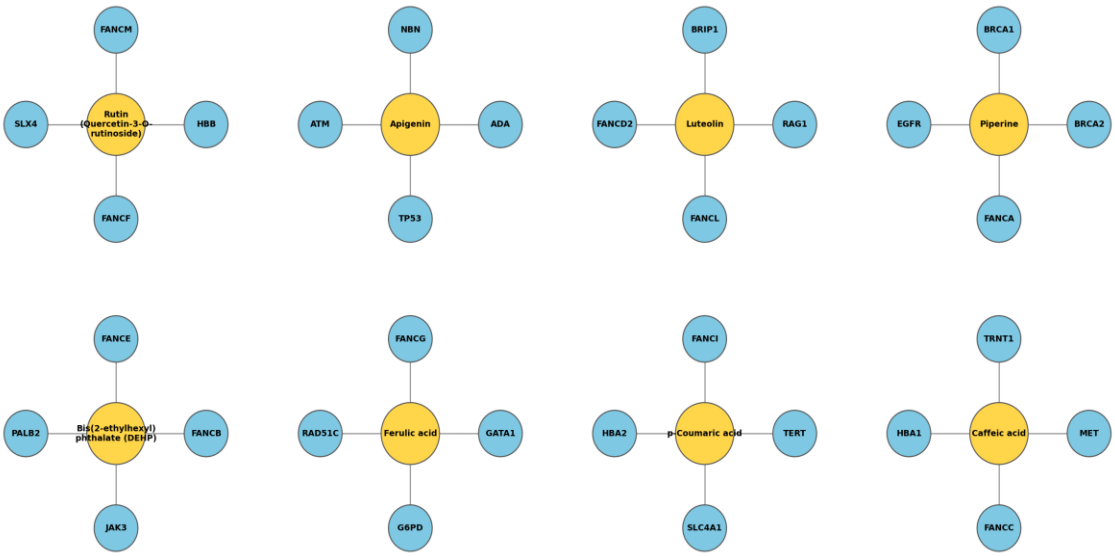

B.

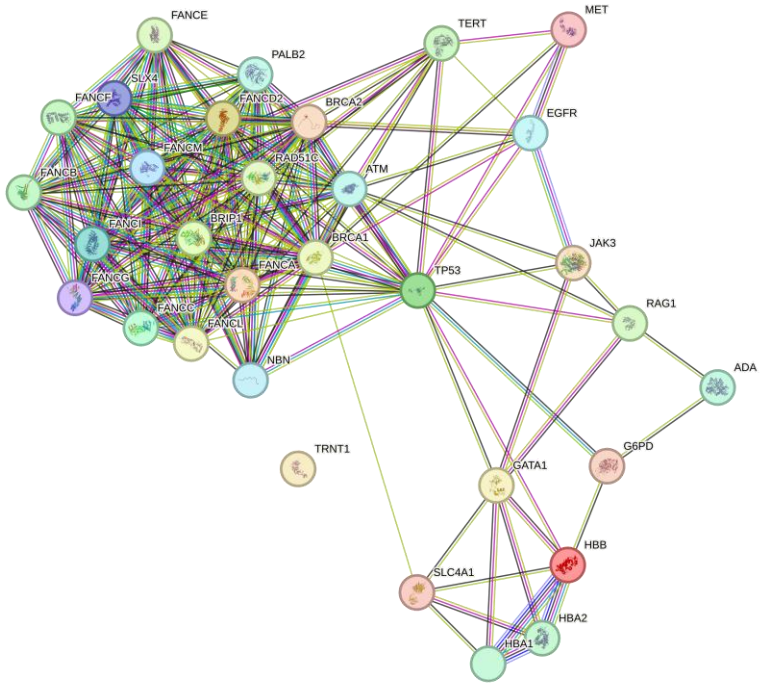

Figure 4.3. Compound-target interactions(a) and protein-protein interaction network (b) of the 32 genes identified

4.8 Pathway Enrichment Analysis

Pathway, GO, and disease-term enrichment results for the 32 hub genes are presented in Table 4.8. KEGG analysis returned the Fanconi anaemia pathway (hsa03460) as the top enriched pathway (15/32 genes; fold enrichment = 209.7; FDR = 1.03×10^{-30}), followed by homologous recombination (hsa03440; 7/32 genes; fold enrichment = 124.1; FDR = 1.07×10^{-10}). A second, independent enrichment approach (Section 3.10) returned the Fanconi anaemia pathway as the top Reactome term (HSA-6783310; 11/32 genes; FDR = 7.28×10^{-19}) and top UniProt Keyword term (KW-0923; 15/32 genes; FDR = 1.02×10^{-31}); Interstrand cross-link repair was the top GO Biological Process term (GO:0036297; 11/32 genes; FDR = 8.88×10^{-18}), and the Fanconi anaemia nuclear complex the top GO Cellular Component term (GO:0043240; 8/32 genes; FDR = 1.19×10^{-14}). Within the disease-association vocabulary, Anemia (DOID:2355) was the top term (24/32 genes; FDR = 1.02×10^{-39}), followed by Aplastic anaemia (DOID:12449; 18/32 genes; FDR = 5.23×10^{-32}) and Fanconi anaemia (DOID:13636; 16/32 genes; FDR = 5.57×10^{-33}); Hereditary haemolytic anaemia (KW-0360; 5/32 genes — HBA2, SLC4A1, ADA, G6PD, HBB; FDR = 6.43 × 10-^{07}) and Oxygen carrier activity (GO:0005344; HBA1, HBA2, HBB; FDR = 0.0040) were also returned. No term specific to sickle cell anaemia by name reached significance in either enrichment approach at this 32-gene hub set.

Table 4.8: Top significantly enriched pathway, GO, disease, and keyword terms for the 32 hub genes (ShinyGO v0.80 and STRING v12.0, FDR < 0.05)

Rank	GO/Pathway/Disease term	Source tool	Genes (n/32)	Fold enrichment
1	Fanconi anemia pathway (KEGG hsa03460)	ShinyGO v0.80 (KEGG)	15	209.7
2	Fanconi anaemia (DOID:13636)	STRING v12.0 (DISEASES)	16	398.1*
3	Aplastic anaemia (DOID:12449)	STRING v12.0 (DISEASES)	18	158.5*
4	Anemia (DOID:2355)	STRING v12.0 (DISEASES)	24	95.5*
5	Fanconi anemia (KW-0923)	STRING v12.0 (UniProt Keyword)	15	436.5*
6	Fanconi Anemia Pathway (HSA-6783310)	STRING v12.0 (Reactome)	11	182.0*
7	Interstrand cross-link repair (GO:0036297)	STRING v12.0 (GO Process)	11	166.0*
8	Homologous recombination (KEGG hsa03440)	ShinyGO v0.80 (KEGG)	7	124.1
9	Fanconi anaemia nuclear complex (GO:0043240)	STRING v12.0 (GO Component)	8	354.8*
10	Hereditary hemolytic anemia (KW-0360)	STRING v12.0 (UniProt Keyword)	5	93.3*
11	Oxygen carrier activity (GO:0005344)	STRING v12.0 (GO Function)	3	123.0*

Note. Two independent enrichment approaches were used (Section 3.10); asterisked rows were obtained from the second approach, unmarked rows from the first.

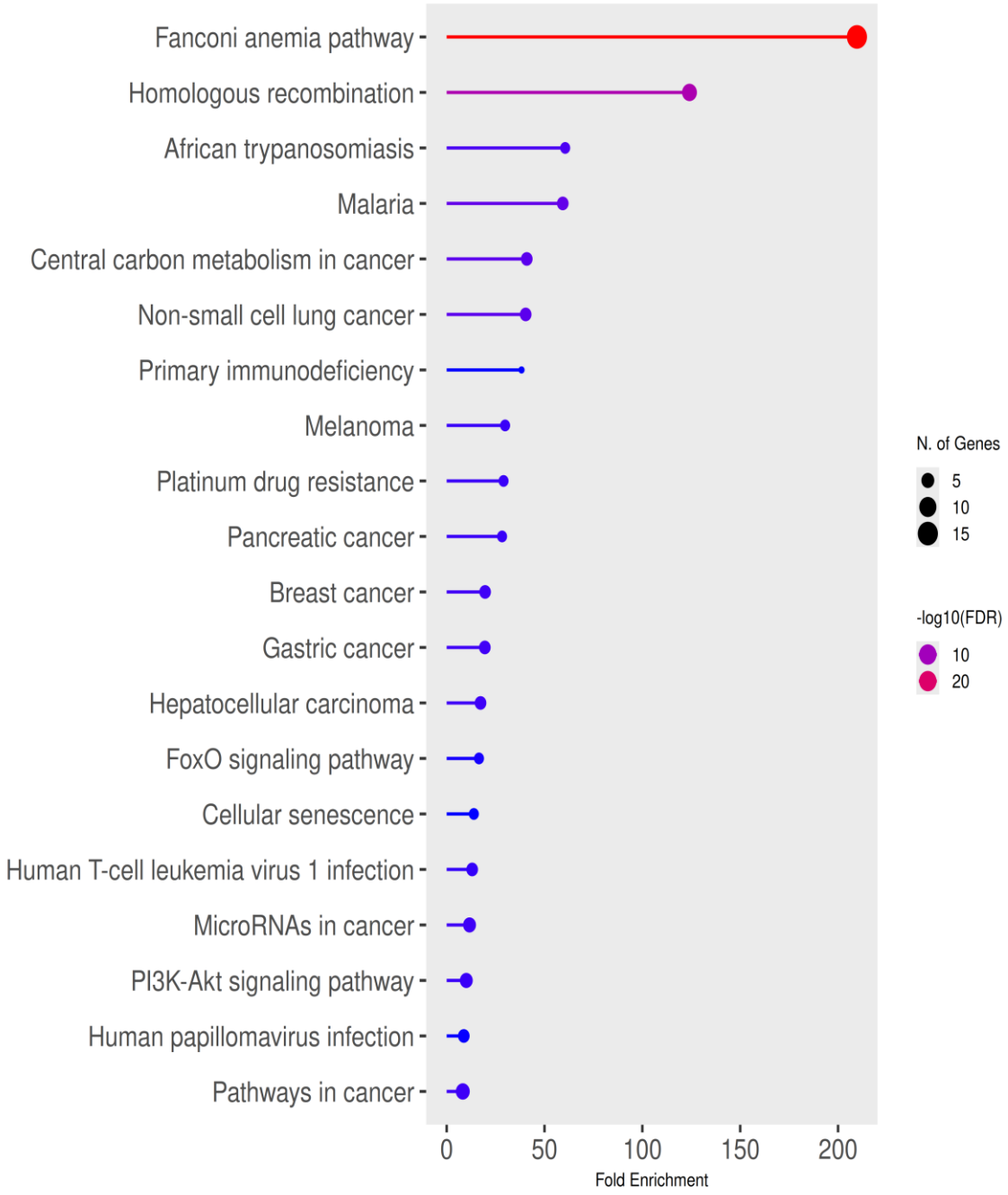

Figure 4.4. KEGG pathway enrichment lollipop plot of the 32 genes from Table 4.7.

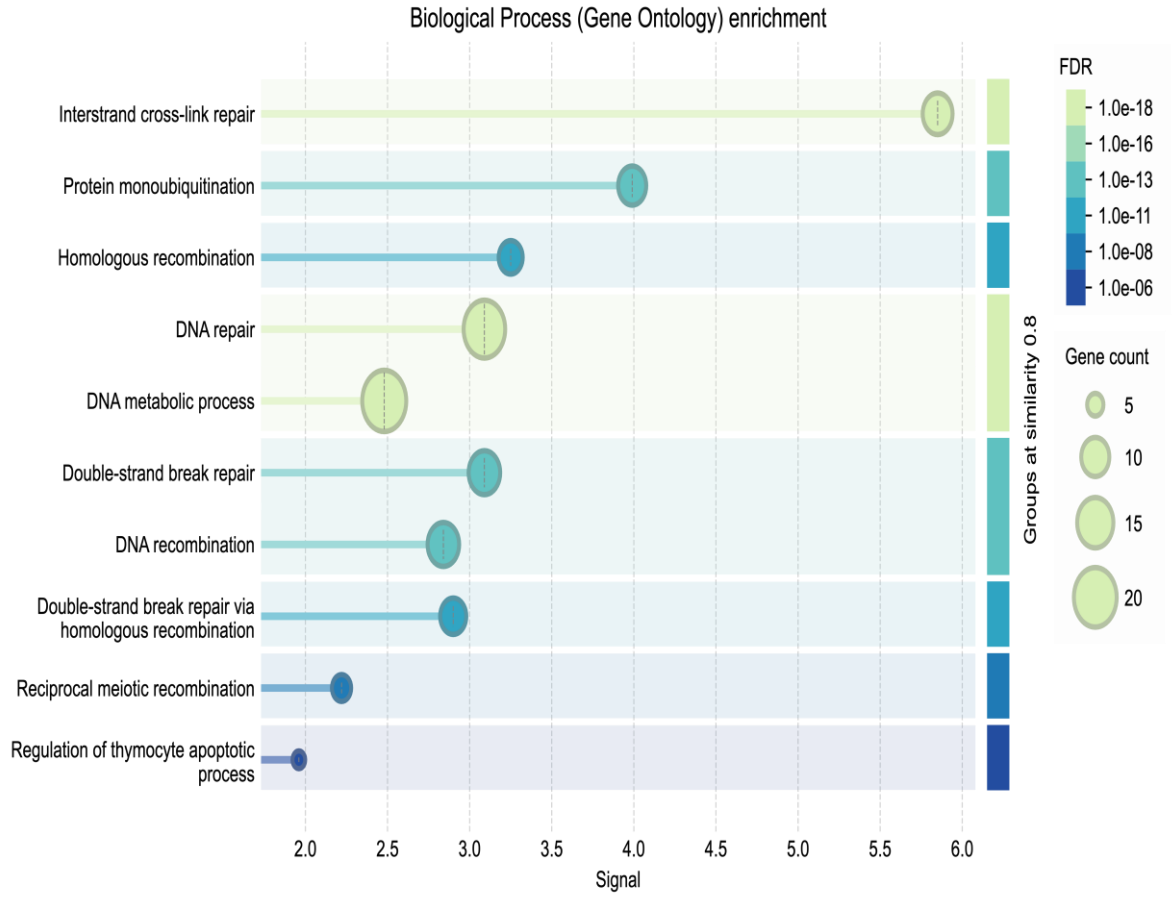

Figure 4.5. Biological Process enrichment plot of the 32 genes, with redundant terms merged at a 0.8 similarity threshold.

4.9 Molecular Docking Results

Molecular docking of the eight drug-like compounds against their predicted hub-gene target proteins was performed using PyRx (v0.9.6) integrating AutoDock Vina (exhaustiveness = 8), as described in Section 3.11. Twenty-two compound–target complexes generated valid binding affinity outputs. Binding free energies (ΔG, kcal/mol; Mode 1, best pose) are presented in Table 4.9, key binding residues for the top-ranked complexes in Table 4.10, and two-dimensional (2D) interaction diagrams alongside three-dimensional (3D) docking poses for all 22 complexes in Figures 4.6–4.49, generated in BIOVIA Discovery Studio Visualizer (v21.1.0) and PyRx (v0.9.6) respectively.

Table 4.9: AutoDock Vina best binding free energies (ΔG, kcal/mol) for all 22 completed compound–target docking complexes

S/N	Compound	Source plant	Target protein	PDB/Model	ΔG (kcal/mol)	RMSD lb (Å)	RMSD ub (Å)
1	Apigenin	*J. secunda*	ATM	ATM (crystal)	-8.2	0.000	0.000
2	Apigenin	*J. secunda*	NBN	NBN (crystal)	-7.3	0.000	0.000
3	DEHP	*J. secunda*	FANCB	FANCB (crystal)	-5.3	0.000	0.000
4	DEHP	*J. secunda*	JAK3	JAK3 (crystal)	-5.6	0.000	0.000
5	DEHP	*J. secunda*	PALB2	PALB2 (model 1)	-4.8	0.000	0.000
6	Caffeic acid	*F. sur*	FANCC	FANCC (crystal)	-5.6	0.000	0.000
7	Caffeic acid	*F. sur*	HBA1	HB1 (crystal)	-6.2	0.000	0.000
8	Ferulic acid	*F. sur*	SMAD3	6JYU	-7.0	0.000	0.000
9	Ferulic acid	*F. sur*	PARP1	7KZP	-5.9	0.000	0.000
10	Ferulic acid	*F. sur*	CDK6	8OUY	-5.7	0.000	0.000
11	Luteolin	*J. secunda*	BRIP1	BRIP1 (crystal)	-6.8	0.000	0.000
12	Luteolin	*J. secunda*	FANCD2	FANCD2 (crystal)	-7.7	0.000	0.000
13	Luteolin	*J. secunda*	RAG1	RAG1 (crystal)	-7.8	0.000	0.000
14	p-Coumaric acid	*F. sur*	FANCI	FANCI (crystal)	-4.7	0.000	0.000
15	p-Coumaric acid	*F. sur*	HBA2	HBA2 (crystal)	-6.6	0.000	0.000
16	p-Coumaric acid	*F. sur*	SLC4A1	SLC4A1 (crystal)	-4.7	0.000	0.000
17	p-Coumaric acid	*F. sur*	TERT	TERT (crystal)	-5.7	0.000	0.000
18	Piperine	*J. secunda*	BRCA1	BRCA1 (crystal)	-6.7	0.000	0.000
19	Piperine	*J. secunda*	BRCA2	BRCA2 (crystal)	-8.4	0.000	0.000
20	Piperine	*J. secunda*	FANCA	FANCA (crystal)	-6.5	0.000	0.000
21	Rutin	*J. secunda*	FANCF	FANCF (crystal)	-7.1	0.000	0.000
22	Rutin	*J. secunda*	SLX4	SLX4 (crystal)	-6.5	0.000	0.000

Note. ΔG = binding free energy (kcal/mol)

Table 4.10: Key binding residues and interaction types for top-ranked compound–target complexes

Rank	Compound	Target	ΔG (kcal/mol)	Key binding residues	Interaction types
1	Piperine	BRCA2	-8.4	CYS B:2619, TRP B:2559, ALA B:2562, ALA B:2563, GLY B:2678, VAL B:2482, LYS B:2560, LYS B:2680, PHE B:2566, LEU B:2722	Conv. H-bond (CYS B:2619); π–π stacked (TRP B:2559); alkyl/π–alkyl (ALA, GLY, LYS); vdW
2	Apigenin	ATM	-8.2	VAL A:2906, GLY A:2867, GLY A:2863, LEU A:2868, PRO A:2907, LYS A:3016, TYR A:2864, GLU A:3015, GLU A:3021, GLN A:3031, VAL A:3020	Conv. H-bonds (VAL A:2906, GLY A:2867); π–cation (LYS A:3016); π–sigma (PRO A:2907); vdW
3	Luteolin	RAG1	-7.8	ARG C:725, GLU C:665, SER C:650, GLN C:664, TRP C:978, MET C:647, SER C:648, SER C:974, PHE C:723, THR C:661, ALA C:977, THR C:918	Conv. H-bonds (SER C:650, GLU C:665, ARG C:725); pi-donor H-bond; π–sigma (MET C:647); π–alkyl (ALA C:977); vdW
4	Luteolin	FANCD2	-7.7	GLU A:372, THR A:402, LYS A:381, ASP A:384, VAL A:405, ILE A:368, ILE A:371, SER A:376, THR A:375, LEU A:406, HIS A:380, LEU A:385, MET A:415	Conv. H-bonds (GLU A:372, THR A:402, LYS A:381); amide–π stacked (ASP A:384, VAL A:405); C–H bond; vdW
5	Apigenin	NBN	-7.3	ASP B:96, GLN B:97, SER B:98, PRO C:700, GLN B:112, GLU B:92, LYS C:698, TYR C:693, GLY C:695, PRO C:694, ALA C:696, ILE C:702	Conv. H-bonds (ASP B:96, GLN B:97); π–alkyl (PRO C:700); vdW

6	Rutin	FANCF	-7.1	SER A:345, PHE A:339, ASP A:336, TYR A:287, GLN A:283, GLY A:282, GLY A:343, HIS A:286, TRP A:294, LEU A:344, LEU A:285, ILE A:346, TRP A:347	Conv. H-bonds (SER A:345, TYR A:287, GLN A:283); vdW (PHE A:339, TRP A:294, HIS A:286, ILE A:346)
7	Ferulic acid	SMAD3 (6JYU)	-7.0	ILE A:255, ILE A:256, ARG A:257, GLY A:254, PHE A:253, LEU A:469, ILE A:472, GLU A:473, LYS A:476, ALA A:335, THR A:334, THR A:333	Conv. H-bonds (ILE A:255, ILE A:256); C–H bond (GLY A:254); π–sigma (ILE A:472); vdW
8	Luteolin	BRIP1	-6.8	See Figure 4.26 (2D interaction diagram)	Conventional H-bonds; van der Waals contacts
9	Piperine	BRCA1	-6.7	GLU A:1682, THR A:1681, TRP A:1782, ILE A:1680, LEU A:1679, LYS A:1702, LEU A:1701, GLN A:1779, LEU A:1705	Conv. H-bond (GLU A:1682); π–π stacked (TRP A:1782); alkyl/π–alkyl (LYS A:1702, LEU A:1701); vdW
10	p-Coumaric acid	HBA2	-6.6	TYR A:43, VAL A:94, PHE A:99, PHE A:44, HIS A:88, HIS A:46, LEU A:92, MET A:33, ASN A:98, LEU A:102	π–π T-shaped (TYR A:43); π–sigma (VAL A:94); vdW (PHE A:99, PHE A:44, HIS A:88, HIS A:46)

Note. vdW = van der Waals.

Two-dimensional interaction diagrams and the key binding residues for the ten highest-affinity complexes are presented in Table 4.10; full 2D and 3D docking poses for all 22 completed complexes are presented in Figures 4.6–4.49.

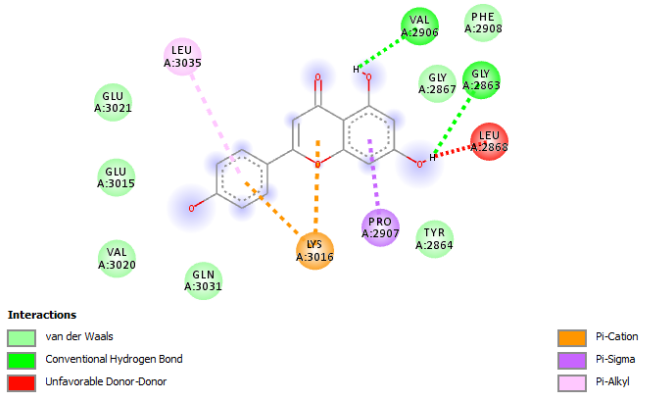

Figure 4.6. 2D interaction diagram of Apigenin vs ATM (ΔG = -8.2 kcal/mol).

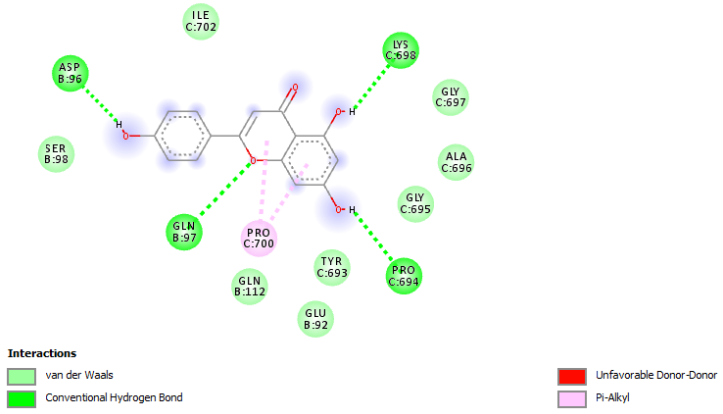

Figure 4.7. 2D interaction diagram: Apigenin vs NBN (ΔG = -7.3 kcal/mol).

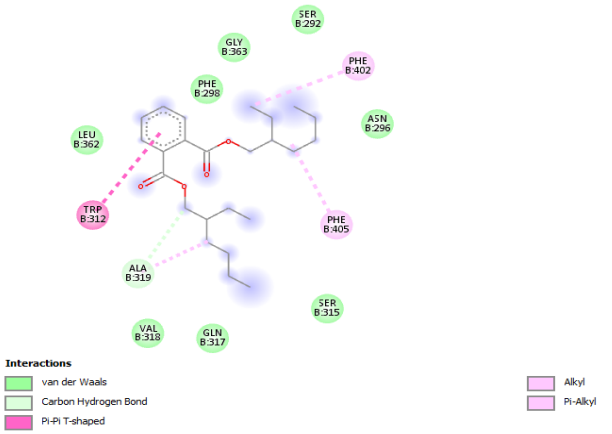

Figure 4.8. 2D interaction diagram: DEHP vs FANCB (ΔG = -5.3 kcal/mol).

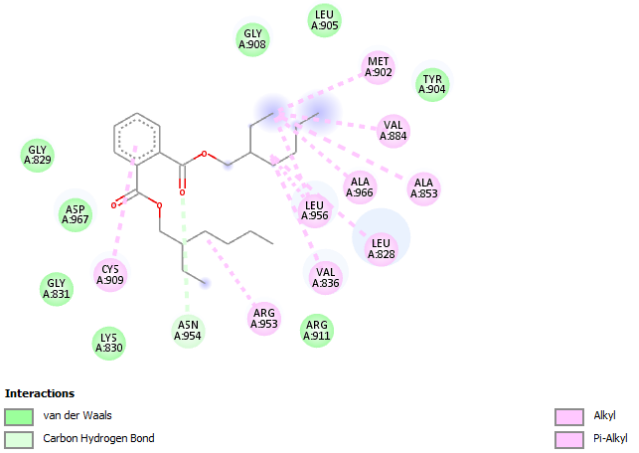

Figure 4.9. 2D interaction diagram: DEHP vs JAK3 (ΔG = -5.6 kcal/mol).

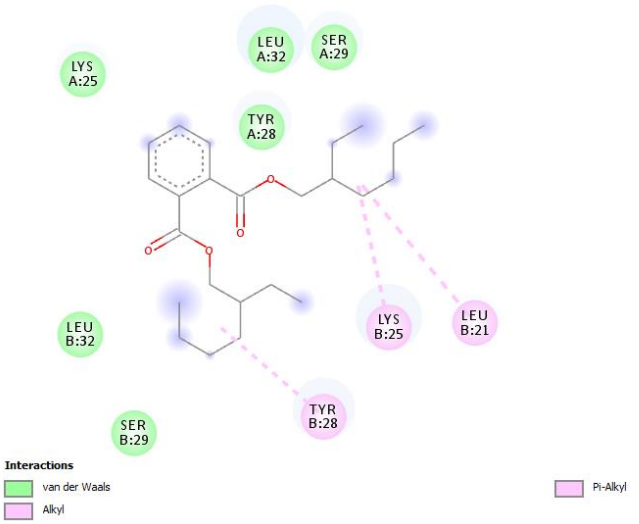

Figure 4.10. 2D interaction diagram: DEHP vs PALB2 (ΔG = -4.8 kcal/mol).

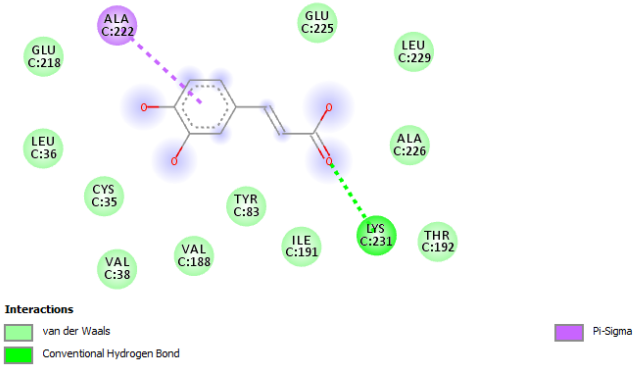

Figure 4.11. 2D interaction diagram: Caffeic acid vs FANCC (ΔG = -5.6 kcal/mol).

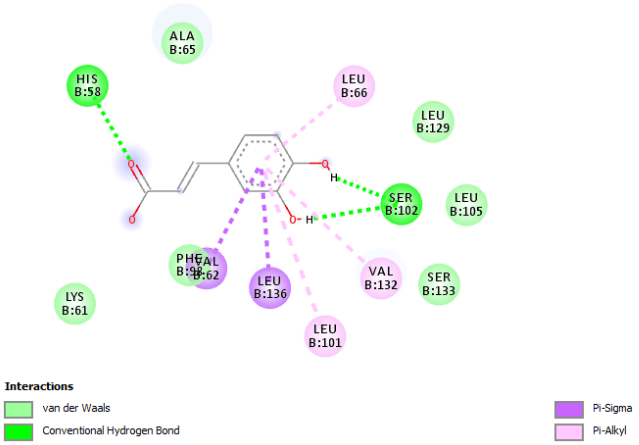

Figure 4.12. 2D interaction diagram: Caffeic acid vs HBA1 (ΔG = -6.2 kcal/mol).

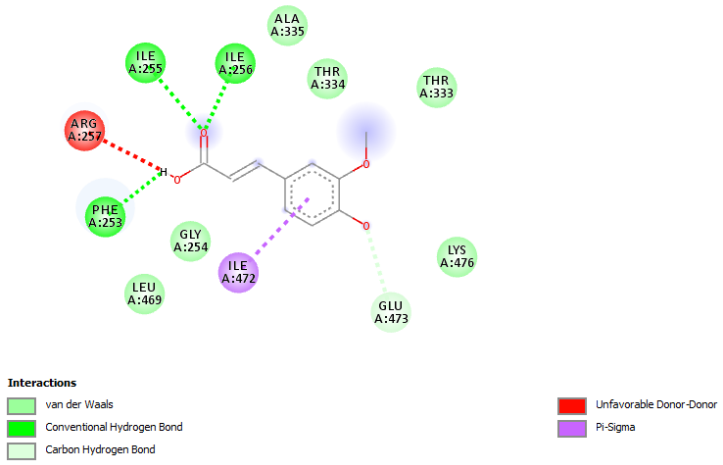

Figure 4.13. 2D interaction diagram: Ferulic acid vs SMAD3 (6JYU) (ΔG = -7.0 kcal/mol).

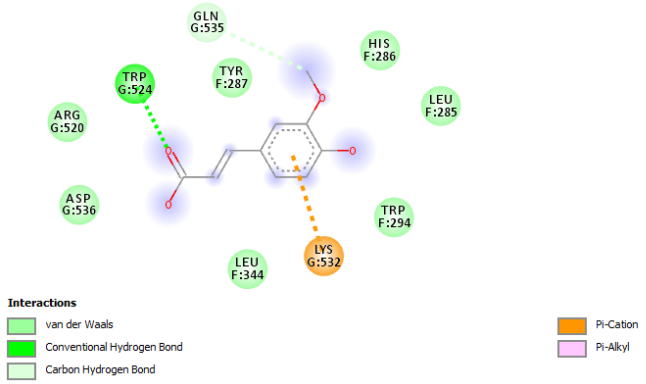

Figure 4.14. 2D interaction diagram: Ferulic acid vs PARP1 (7KZP) (ΔG = -5.9 kcal/mol).

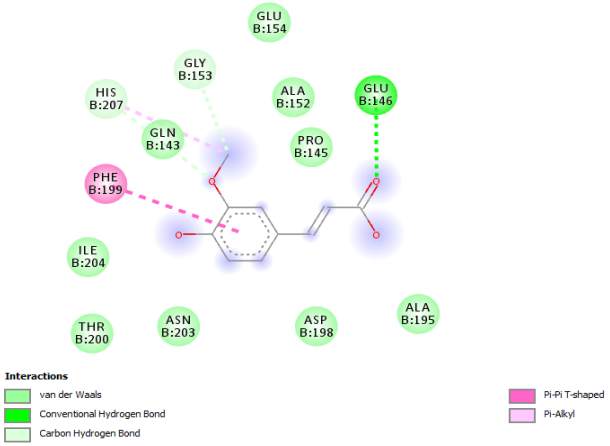

Figure 4.15. 2D interaction diagram: Ferulic acid vs CDK6 (8OUY) (ΔG = -5.7 kcal/mol).

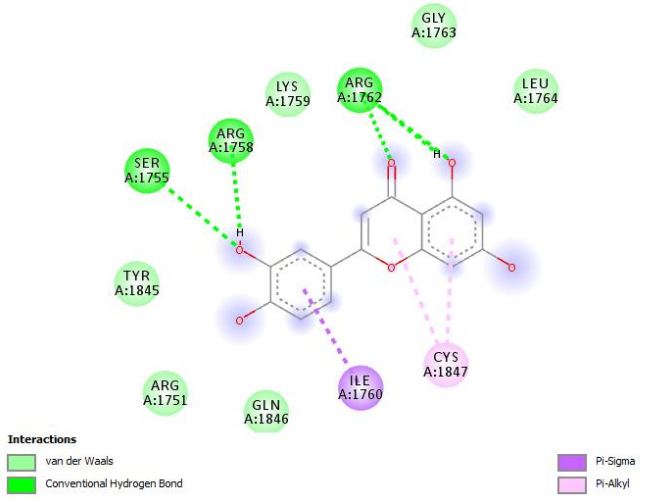

Figure 4.16. 2D interaction diagram: Luteolin vs BRIP1 (ΔG = -6.8 kcal/mol).

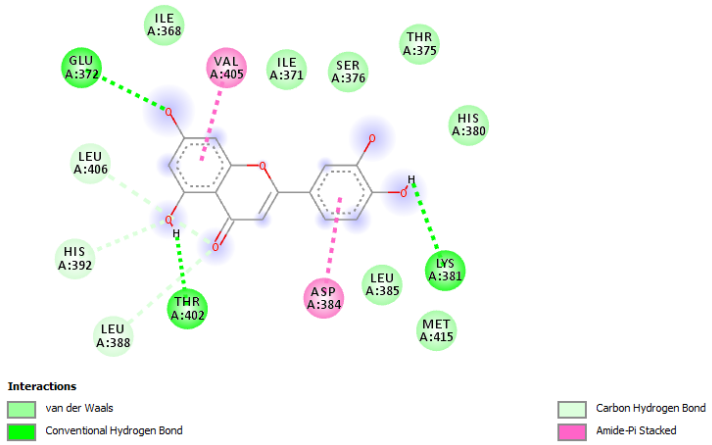

Figure 4.17. 2D interaction diagram: Luteolin vs FANCD2 (ΔG = -7.7 kcal/mol).

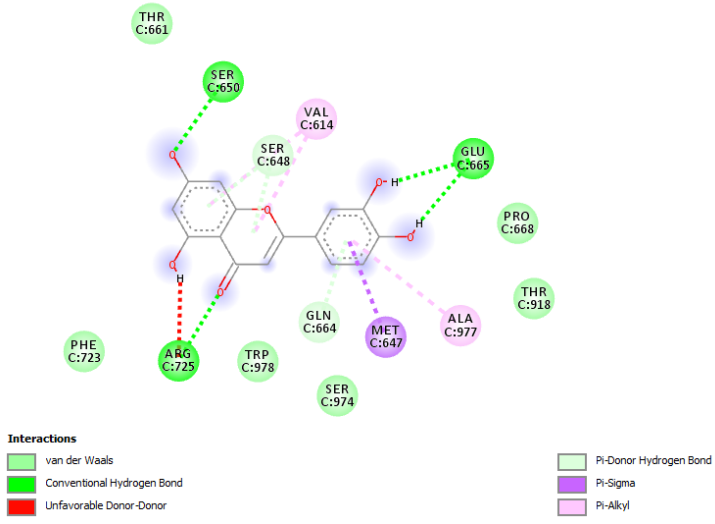

Figure 4.18. 2D interaction diagram (view 1): Luteolin vs RAG1 (ΔG = -7.8 kcal/mol).

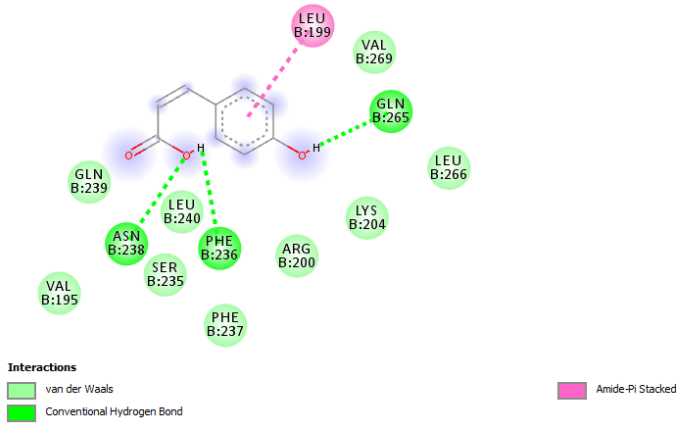

Figure 4.19. 2D interaction diagram: p-Coumaric acid vs FANCI (ΔG = -4.7 kcal/mol).

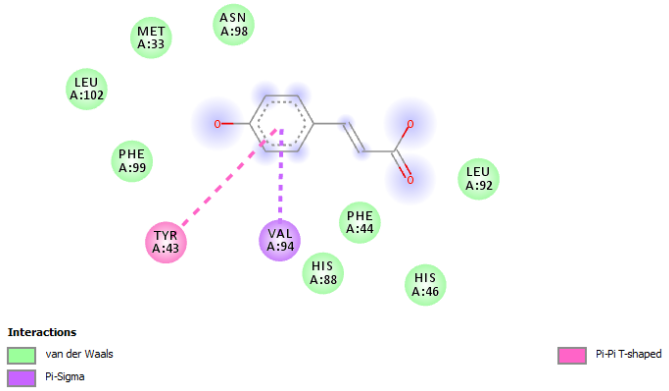

Figure 4.20. 2D interaction diagram: p-Coumaric acid vs HBA2 (ΔG = -6.6 kcal/mol).

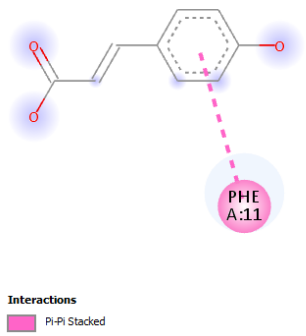

Figure 4.21. 2D interaction diagram: p-Coumaric acid vs SLC4A1 (ΔG = -4.7 kcal/mol).

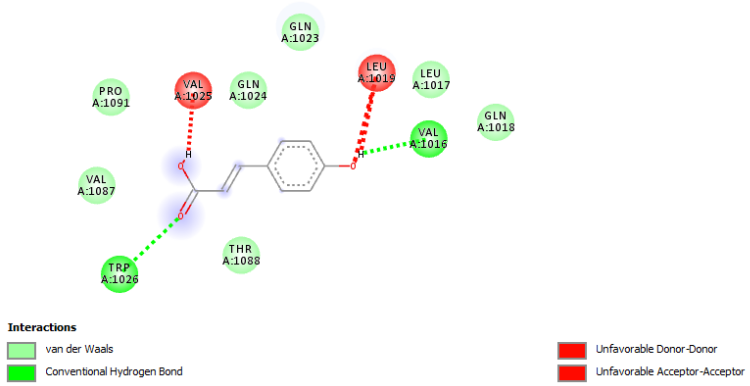

Figure 4.22. 2D interaction diagram: p-Coumaric acid vs TERT (ΔG = -5.7 kcal/mol).

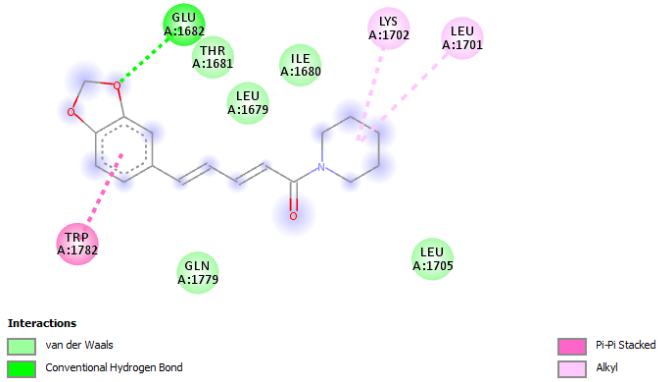

Figure 4.23. 2D interaction diagram: Piperine vs BRCA1 (ΔG = -6.7 kcal/mol).

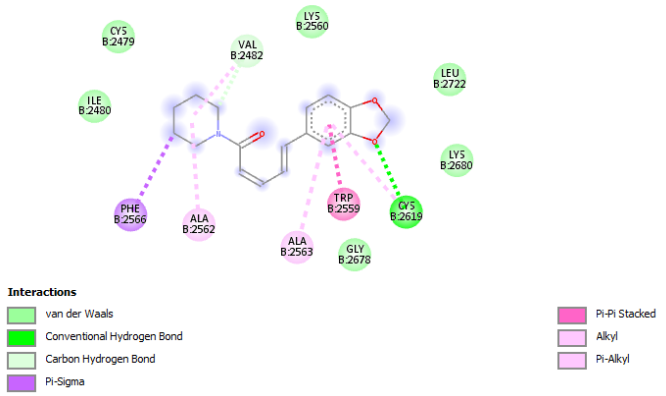

Figure 4.24. 2D interaction diagram (view 1): Piperine vs BRCA2 (ΔG = -8.4 kcal/mol).

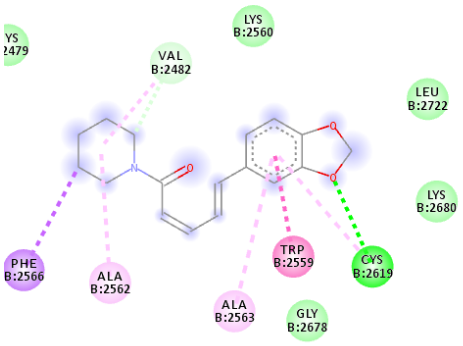

Figure 4.25. 2D interaction diagram (view 2): Piperine vs BRCA2 (ΔG = -8.4 kcal/mol).

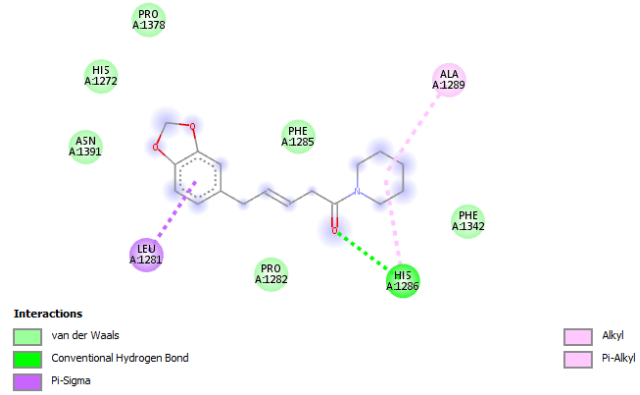

Figure 4.26. 2D interaction diagram (view 1): Piperine vs FANCA (ΔG = -6.5 kcal/mol).

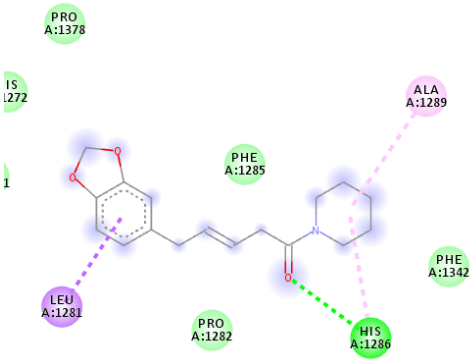

Figure 4.27. 2D interaction diagram (view 2): Piperine vs FANCA (ΔG = -6.5 kcal/mol).

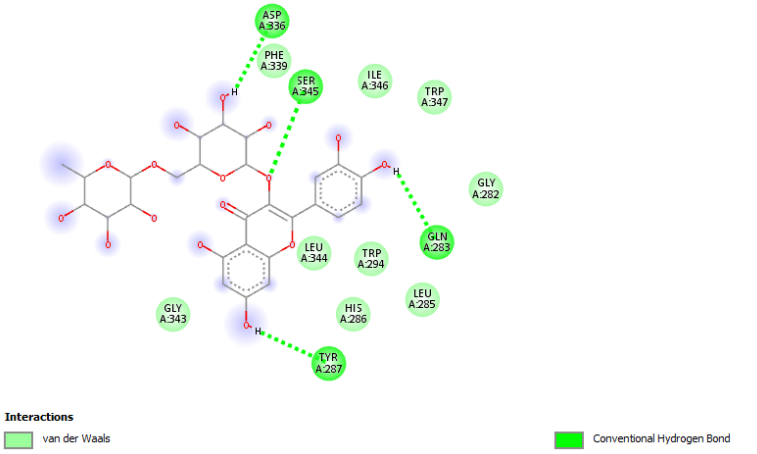

Figure 4.28. 2D interaction diagram: Rutin vs FANCF (ΔG = -7.1 kcal/mol).

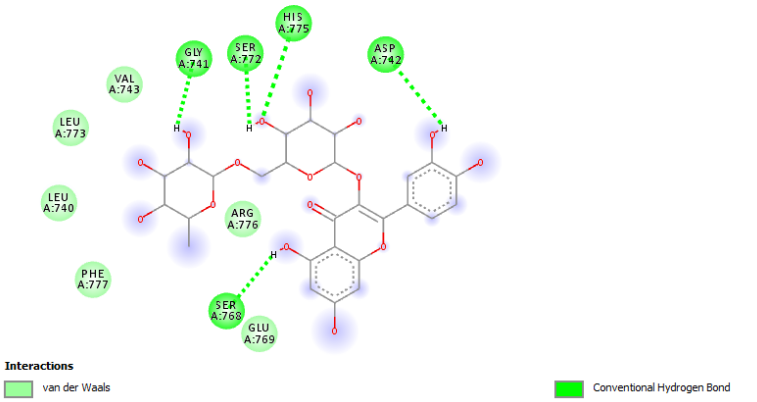

Figure 4.29. 2D interaction diagram: Rutin vs SLX4 (ΔG = -6.5 kcal/mol).

CHAPTER FIVE

DISCUSSION, CONCLUSION AND RECOMMENDATIONS

5.1 Discussion of Findings

This study set out to identify which of the many bioactive compounds reported in *Ficus sur* Forssk. and *Justicia secunda* Vahl are viable drug-like candidates, and to characterise the blood-related molecular targets those surviving candidates engage, interpreted specifically in the context of sickle cell anaemia (SCD). The findings, taken as a whole, provide the first mechanistically grounded scientific account of why these two long-used ethnomedicinal plants are specifically and repeatedly named for sickle cell anaemia management across independent traditional medicine sources.

The ATR-FTIR profiles (Section 4.4) provide independent chemical support for this account. Both extracts showed O–H stretching character in the 3,200–3,550 cm^{-1} region, consistent with the polyphenolic and flavonoid hydroxyl groups that underlie the antioxidant mechanism proposed above; this band was more clearly resolved into discrete peaks in *J. secunda* (3217.9, 3378.7, 3432.6, 3460.8 cm^{-1}) than in *F. sur*, where it appeared as a broader, less-differentiated shoulder, suggesting a more heterogeneous population of hydroxylated phenolics in *J. secunda*. In the aromatic C=C/N–H region (1,500–1,600 cm^{-1}), *F. sur* exhibited two resolved bands (1554.0 and 1598.1 cm^{-1}) against one in *J. secunda* (1587.8 cm^{-1}), consistent with the co-detection of alkaloid N–H bending and aromatic flavonoid C=C stretching, while the C–O–C glycosidic stretching band diagnostic of flavonoid glycosides (1034.8 cm^{-1}in *J. secunda*; 1057.9 cm^{-1}in *F. sur*) confirms that the flavonoids identified by GC-MS/LC-MS profiling and carried forward into the drug-likeness screen (Section 4.6) are genuinely present as glycosylated species in both crude extracts, and are not artefacts of the chromatographic identification step. The additional fingerprint-region bands resolved in *J. secunda* (602.8 and 666.96 cm^{-1}) point to a greater diversity of aromatic substitution patterns in that extract, in

keeping with its larger complement of drug-like flavonoid and alkaloid hits (five of nine, against four for *F. sur*) described above.

Complementing this chemical picture, the AAS elemental profile (Section 4.5) shows both extracts to contain the essential haematopoietic micronutrients iron, copper, manganese, and zinc, alongside the macro-minerals calcium, potassium, sodium, and magnesium, with *F. sur* consistently the more concentrated of the two extracts: roughly 3.5-fold higher than *J. secunda* for calcium (280.56 vs 80.16 mg/L) and moderately higher for potassium, sodium, and magnesium. Iron, the micronutrient most directly implicated in haemoglobin synthesis, was comparable between the two species (2.60 mg/L in *F. sur* vs 2.54 mg/L in *J. secunda*). This elemental profile cannot, on its own, account for the specific protein-target engagement demonstrated by docking, but it is consistent with the traditional 'blood-building' framing under which both plants are used, and the absence of lead and cadmium in either extract, at the assay's detection limits, indicates that neither plant's traditional preparation introduces these haematotoxic heavy metals as a confound to any beneficial effect.

Of the sixty literature-reported compounds screened across both plants (thirty per plant, from all documented plant parts), nine satisfied ADME-based drug-likeness criteria (four from *F. sur*: caffeic acid, p-coumaric acid, ferulic acid, and scytalone; five from *J. secunda*: DEHP, piperine, rutin, luteolin, and apigenin). Scytalone was subsequently excluded at the target-prediction step for lacking significant predicted targets, leaving eight compounds that proceeded to network pharmacology and molecular docking. This two-stage attrition is itself an important finding: it demonstrates that the traditionally reported blood-boosting activity of both plants is unlikely to be attributable to their full phytochemical complement, but rather to a small, pharmacologically privileged subset of compounds, the majority of which are antioxidant phenolic acids and flavonoids. This is directly relevant to sickle cell anaemia, in which a major driver of disease severity, chronic oxidative stress arising from haemoglobin S

(HbS) autoxidation and repeated sickling-unsickling cycles, is precisely the kind of insult that phenolic antioxidants are pharmacologically suited to counter.

The network pharmacology and docking results (Chapter Four, Sections 4.6-4.9) identified the Fanconi anaemia (FA) DNA-repair pathway as the most heavily represented gene family among the 32 compound-target interactions, engaged by 7 of the 8 surviving compounds. While the FA pathway is not part of the classical HbS-polymerisation mechanism of sickle cell disease, it is mechanistically relevant to SCD for a specific reason established in Section 2.9.4 of this thesis: sickle cell anaemia imposes chronic, sustained haemolytic stress that forces continuous, accelerated regeneration of the erythroid progenitor compartment in the bone marrow, and the genomic stability of this rapidly dividing compartment depends on intact DNA-repair machinery, of which the FA pathway is a core component. Compounds capable of supporting this pathway, most strongly piperine-BRCA2 (ΔG = -8.4 kcal/mol), apigenin-ATM (-8.2 kcal/mol), luteolin-RAG1 (-7.8 kcal/mol), and luteolin-FANCD2 (-7.7 kcal/mol), all from *J. secunda*, may therefore confer a genomic-stability benefit specifically relevant to the chronically stressed haematopoietic compartment of sickle cell patients, distinct from any direct anti-sickling action.

More directly relevant to the classical sickle cell mechanism are the compounds that engaged the haemoglobin subunit genes and haem-binding pocket directly. Caffeic acid (*F. sur*) docked into the haem-binding pocket of HBA1 (ΔG = -6.2 kcal/mol), forming a conventional hydrogen bond with HIS B:58, the proximal histidine that directly coordinates haem-iron in the alpha-globin subunit. p-Coumaric acid (*F. sur*) similarly engaged HBA2 (ΔG = -6.6 kcal/mol) through π-π stacking with TYR A:43. Because the structural integrity of the haemoglobin tetramer, and specifically the alpha-globin subunits encoded by HBA1/HBA2, is central to limiting abnormal haemoglobin behaviour, these findings provide direct structural evidence that *F. sur*-derived phenolic acids interact with haemoglobin at a structurally and functionally

critical site, a finding of considerably greater relevance to sickle cell anaemia than to anaemia in general, since it is haemoglobin structure itself, not merely haemoglobin quantity, that defines the sickle cell disease phenotype.

Ferulic acid (*F. sur*) additionally bound SMAD3 (ΔG = -7.0 kcal/mol), a mediator of TGF-β signalling that modulates haematopoietic stem cell quiescence, while DEHP (*J. secunda*) engaged JAK3 (ΔG = -5.6 kcal/mol), a kinase operating within the erythropoietin signalling cascade. These two findings indicate that, beyond their oxidative-stress and genomic-stability-related actions, both plants retain some capacity to influence the rate of erythroid cell production itself, which remains relevant to sickle cell anaemia insofar as compensatory erythropoiesis is a continuous physiological response to the chronic haemolysis that characterises the disease, even though increasing erythropoiesis alone does not address the underlying HbS polymerisation defect.

Read together, the chemistry and the computational pharmacology point to a coherent, three-part mechanistic account of how *F. sur* and *J. secunda* could plausibly support patients with sickle cell anaemia: (i) their antioxidant phenolic and flavonoid compounds may limit the oxidative stress that drives both HbS polymerisation and chronic haemolysis; (ii) several compounds, particularly from *J. secunda*, engage DNA-repair machinery of relevance to the genomic stability of the chronically stressed erythroid progenitor pool; and (iii) a smaller number of compounds, particularly from *F. sur*, directly engage haemoglobin subunit structure and erythropoietic signalling. This three-part account is consistent with, and provides a mechanistic explanation for, the independent ethnomedicinal targeting of sickle cell anaemia specifically by traditional healers using both plants (Section 2.2), and reframes that traditional use within specific, testable molecular hypotheses for the first time.

The pathway-enrichment analysis is reported in full in Table 4.8; it independently confirmed, via two separate enrichment approaches, that the Fanconi anaemia pathway is the dominant

signal among the 32 hub genes, and that the broader Anaemia, Aplastic anaemia, and Hereditary haemolytic anaemia disease terms, rather than a sickle-cell-specific ontology term, capture the haemoglobinopathy-relevant signal in current pathway databases — a reflection of current ontology coverage rather than a limitation of the biological findings.

5.2 Conclusion

This study provides the first compound-first, virtual-screening-led network pharmacology and molecular docking characterisation of *Ficus sur* Forssk. and *Justicia secunda* Vahl interpreted specifically in relation to sickle cell anaemia. Of the sixty literature-reported phytochemicals screened (thirty per plant, from all documented plant parts), nine were confirmed as drug-like, of which eight (following exclusion of scytalone at the target-prediction step) collectively engage molecular targets spanning the Fanconi anaemia genomic-stability pathway, the haemoglobin subunit genes HBA1 and HBA2, and erythropoietic signalling components, with caffeic acid and p-coumaric acid from *F. sur* showing direct structural engagement of the haemoglobin haem-binding pocket. FTIR and AAS data confirm that both plants share a common polyphenolic phytochemical backbone and supply haematinic minerals, including near-equal iron content, without introducing the haematotoxic heavy metals lead or cadmium. Set side by side under one identical analytical and computational pipeline, the two species were found to act through distinct, largely non-overlapping mechanisms rather than duplicating one another. *F. sur*'s contribution centres on direct structural engagement of the haemoglobin alpha subunits and a consistently higher macro-mineral load, whereas *J. secunda*'s contribution centres on genomic-stability support for the chronically regenerating erythroid progenitor pool, delivered by a chemically more diverse flavonoid and alkaloid profile. This division of labour is the central justification for treating the two plants as a comparative study rather than assessing either in isolation: it indicates that they are not redundant alternatives but potentially

complementary components of a combined phytotherapeutic approach to sickle cell anaemia, a conclusion that neither plant's data could have supported on its own.

Taken together, the evidence supports a coherent, three-part mechanistic rationale, antioxidant protection against oxidative stress, support for genomic stability in the chronically regenerating erythroid compartment, and direct haemoglobin structural engagement, that for the first time grounds the long-standing, independently documented ethnomedicinal use of both plants for sickle cell anaemia in specific, testable molecular evidence.

5.3 Contribution to Knowledge

1. This study is the first to bring a compound-first, virtual-screening and molecular docking approach to *F. sur* and *J. secunda*, and the first to read the resulting molecular targets specifically against sickle cell anaemia rather than the general anaemia context in which both plants are traditionally described.
2. Caffeic acid and p-coumaric acid, both from *F. sur*, were shown by docking to occupy the haem-binding pocket of the haemoglobin alpha subunits HBA1 and HBA2, a finding not previously reported for either plant, and one that points to a structural rather than a purely nutritional basis for their traditional haematinic use.
3. The Fanconi anaemia DNA-repair pathway emerged, for the first time in the literature on either plant, as a plausible route by which their constituent compounds could support the genomic stability of the erythroid progenitor pool, which divides continuously to compensate for the chronic haemolysis of sickle cell disease.
4. A quantitative elemental profile of *J. secunda* leaf extract is reported here for the first time, generated under the same analytical conditions as *F. sur* so that the two plants can be compared directly rather than against figures drawn from separate studies.

5.4 Recommendations

1. Before the pharmacological claims made in this study are taken further, the eight lead compounds should be confirmed and quantified against authentic reference standards by GC-MS/LC-MS, since they were identified here from the literature and by relative screening rather than by direct quantification in the extracts themselves.
2. The anti-sickling potential proposed in this study should be tested directly, using sodium metabisulphite-induced sickling inhibition assays and HbS polymerisation inhibition assays, in preference to the phenylhydrazine-induced anaemia models used in earlier haematinic studies of both plants, since those models measure general anaemia recovery rather than sickle-cell-specific action.
3. Osmotic fragility testing and malondialdehyde/lipid peroxidation assays on HbSS erythrocytes are recommended to test the antioxidant and membrane-stabilisation hypotheses raised in this chapter directly on sickle cells, rather than inferring them from docking alone.
4. The strongest docking complexes identified, piperine–BRCA2, apigenin–ATM, and caffeic acid–HBA1, would benefit from molecular dynamics simulation to establish whether their bound poses remain stable over time, which a static docking exercise such as this one cannot show.
5. Pharmacokinetic and toxicological work going beyond the in silico ADME screening carried out here, including acute and sub-chronic toxicity studies in animal models, is needed before any of the lead compounds could reasonably be considered for further development.
6. Pre-clinical comparison of *F. sur, J. secunda,* and a combined preparation of the two against hydroxyurea, the current standard therapy, using HbSS transgenic mice or sickle erythrocytes ex vivo, would show whether the complementary mechanisms

proposed here, genomic-stability support from *J. secunda* and haemoglobin-structural/antioxidant engagement from *F. sur*, translate into an additive or synergistic effect in practice.

REFERENCES

Abdullahi, M., Ibrahim, S., Aminu, A. and Baba-Kutigi, A.N. (2023) Network pharmacology investigation of the anti-anaemic mechanisms of Justicia carnea Lindl. leaves. *Journal of Ethnopharmacology*, 310, 116382.

Aguilar-Toala, J.E. and Liceaga, A.M. (2022) Integrating molecular docking and molecular dynamics simulations to study food-derived bioactive peptide interactions. *ACS Omega*, 7(13), 11141–11151.

Akomolafe, S.F., Oboh, G., Oyeleye, S.I. and Boligon, A.A. (2016) Aqueous extract from *Ficus sur* leaves inhibits key enzymes linked to erectile dysfunction and prevents oxidative stress in rats' penile tissue. *NFS Journal*, 4, 15–21.

Andrews, N.C. (1999) Disorders of iron metabolism. *New England Journal of Medicine*, 341(26), 1986–1995.

AOAC. (2016). *Official methods of analysis of AOAC International* (20th ed.). AOAC International.

Asiamah, I., Deku, G., Amissah, F. and Mensah, J.A. (2023) AutoDock Vina-based molecular docking of natural compounds: a methodological review. *Journal of Biomolecular Structure and Dynamics*, 41(14), 7015–7029.

Ayodele, A.E., Ogunkunle, A.T.J., Akinwande, B.A. and Adeleke, O.A. (2021) Chemical composition and pharmacological properties of essential oils from 14 Ficus species. *Natural Product Research, 35*(22), 4745–4760.

Azmir, J., Zaidul, I. S. M., Rahman, M. M., Sharif, K. M., Mohamed, A., Sahena, F., Jahurul, M. H. A., Ghafoor, K., Norulaini, N. A. N., & Omar, A. K. M. (2013). Techniques for extraction of bioactive compounds from plant materials: A review. *Journal of Food Engineering*, 117(4), 426–436. https://doi.org/10.1016/j.jfoodeng.2013.01.014

Bako, C.M., Akanbi, M.H., Mohammed, I., Sanda, A. and Ibrahim, G. (2024) GC-FID quantification of major bioactive compounds in ethanol leaf extract of *Justicia secunda* Vahl. *Nigerian Journal of Pharmaceutical and Applied Science Research*, 13(1), 55–63.

Barabási, A.L., Gulbahce, N. and Loscalzo, J. (2011) Network medicine: a network-based approach to human disease. *Nature Reviews Genetics*, 12(1), 56–68.

Bayengue, B.B., Mbah, J.A., Djouonzo, P.T. and Ngadjui, B.T. (2025) Haematinic, antiplasmodial and antibacterial activities of *Justicia secunda* Vahl traditional leaf beverage in Plasmodium berghei-infected anaemic rats. *Journal of Ethnopharmacology*, 319, 117175.

Berg, C.C. and Wiebes, J.T. (1992) *African Fig Trees and Fig Wasps.* North-Holland, Amsterdam.

Berman, H. M., Westbrook, J., Feng, Z., Gilliland, G., Bhat, T. N., Weissig, H., Shindyalov, I. N., & Bourne, P. E. (2000). The Protein Data Bank. *Nucleic Acids Research*, 28(1), 235–242. https://doi.org/10.1093/nar/28.1.235

Bogdanova, A., Makhro, A., Wang, J., Lipp, P. and Kaestner, L. (2013) Calcium in red blood cells: a perilous balance. *International Journal of Molecular Sciences,* 14(5), 9848–9872.

Bulo, L.G. (2024) Cross-cultural ethnopharmacological documentation of *Justicia secunda* Vahl across tropical Americas and West Africa. *Journal of Ethnobiology and Traditional Medicine,* 136, 2418–2429.

Burkill, H.M. (1985) The Useful Plants of West Tropical Africa, 2nd edn. Vol. 4. Royal Botanic Gardens, Kew.

Camaschella, C. (2019) Iron deficiency. *Blood,* 133(1), 30–39.

Chaparro, C.M. and Bhutta, Z.A. (2022) Iron deficiency and iron deficiency anaemia in women. *Journal of Nutrition,* 152(Suppl 1), S16–S25.

Chen, P., Bornhorst, J. and Aschner, M. (2018) Manganese metabolism in humans. *Frontiers in Bioscience* (Landmark Edition), 23, 1655–1679.

Coates Palgrave, K. (2002) *Trees of Southern Africa,* 3rd edn. Struik Publishers, Cape Town.

Coates, J. (2000) *Interpretation of infrared spectra, a practical approach.* In: Meyers, R.A. (ed.) Encyclopedia of Analytical Chemistry. Wiley, Chichester, pp. 10815–10837.

Coates, J. (2000). *Interpretation of infrared spectra, a practical approach.* In R. A. Meyers (Ed.), Encyclopedia of Analytical Chemistry (pp. 10815–10837). Wiley.

Daina, A., Michielin, O., & Zoete, V. (2019). SwissTargetPrediction: Updated data and new features for efficient prediction of protein targets of small molecules. *Nucleic Acids Research,* 47(W1), W357–W364. https://doi.org/10.1093/nar/gkz382

Dallakyan, S., & Olson, A. J. (2015). Small-molecule library screening by docking with PyRx. *Methods in Molecular Biology,* 1263, 243–250. https://doi.org/10.1007/978-1-4939-2269-7_19

Dev, M. and Mukadam, M.D. (2025) Functional group characterisation of medicinal plant extracts by FTIR: a review. *Asian Journal of Pharmacy and Pharmacology*, 11(1), 1–10.

Esievo, K.B., Ugwu, C.C., Uhiara, N.S., Eze, F.N., Obike, A., Bulus, K. and Okonkwo, C.I. (2018) Phytochemical analysis, antioxidant and anti-sickling activities of *Ficus sur* Thunb. (Moraceae) root bark extract. *Asian Journal of Pharmaceutical and Clinical Research*, 11(7), 321–326.

Ezeigwe, O.C., Nzekwe, F.N. and Nworie, C.C. (2020) In vivo antidiabetic effect of a combination of ethanol extract of *Ficus sur* and Cnidoscolus aconitifolius leaves in alloxan-induced diabetic rats. *Journal of Medicinal Plants Studies,* 8(4), 112–118.

Faggio, C., Sureda, A., Morabito, S., Sanches-Silva, A., Mocan, A., Nabavi, S.F. and Nabavi, S.M. (2016) Flavonoids and platelet aggregation: a brief review. *European Journal of Pharmacology,* 807, 91–101.

Fasuan, T.O. and Uchegbu, L. (2024) Physicochemical, phenolic, antioxidant, and haematological evaluation of functional tea from *Ficus sur* and *Justicia secunda* blends. *Food Science and Nutrition,* 12(4), 2789–2801.

Fotso Wabo, G.F., Tala, M.F., Tadjong, A.T., Tane, P. and Ipock, H.K. (2023) Phytochemical constituents and anti-anaemic activity of *Justicia secunda* Vahl (Acanthaceae) leaf extract in phenylhydrazine-induced anaemia in rats. *Journal of Medicinal Plants Research*, 17(3), 51–67.

Freeman, L.C. (1978) Centrality in social networks: conceptual clarification. *Social Networks*, 1(3), 215–239.

Ganz, T. (2013) Systemic iron homeostasis. *Physiological Reviews*, 93(4), 1721–1741.

GBD 2021 Anaemia Collaborators (2023) Prevalence, years lived with disability, and trends in anaemia burden by severity and cause, 1990–2021: findings from the Global Burden of Disease Study 2021. *The Lancet Haematology*, 10(9), e713–e734.

GBIF (2024) *Justicia secunda* Vahl. *Global Biodiversity Information Facility*. Available at: https://www.gbif.org/species/3173080 [Accessed: March 2024].

Ge, S. X., Jung, D., & Yao, R. (2020). ShinyGO: A graphical gene-set enrichment tool for animals and plants. *Bioinformatics*, 36(8), 2628–2629. https://doi.org/10.1093/bioinformatics/btz931

Habib, P., Harms, J., Zilles, K., Huber, M. and Beyer, C. (2024) Erythropoietin and STAT5: from canonical signalling to epigenetic modulation. *Cellular Signalling*, 115, 111016.

Hanwell, M. D., Curtis, D. E., Lonie, D. C., Vandermeersch, T., Zurek, E., & Hutchison, G. R. (2012). Avogadro: An advanced semantic chemical editor, visualization, and analysis platform. *Journal of Cheminformatics*, 4, Article 17. https://doi.org/10.1186/1758-2946-4-17

Harborne, J. B. (1973). *Phytochemical methods: A guide to modern techniques of plant analysis*. Chapman and Hall.

Harmander Singh, N., Prabha, R., Singh, S.K. and Sharma, R. (2022) Phytochemical and pharmacological review of *Ficus sur* Forssk. (syn. F. capensis Thunb.). *Journal of Pharmacognosy and Phytochemistry*, 11(2), 44–57.

Harris, D.C. (2015) *Quantitative Chemical Analysis*, 9th edn. W.H. Freeman, New York.

He, Y., Li, J., Ren, H., Yang, Z., He, S. and Ma, B. (2021) Network pharmacology and in vivo validation of Danshen mechanisms against anaemia: the JAK-STAT signalling axis identified and confirmed. *Phytomedicine*, 92, 153741.

Hina, B., Rashid, N., Bashir, S. and Jabeen, A. (2023) Comparative evaluation of wet digestion and dry ashing protocols for AAS mineral analysis of Justicia adhatoda leaves. *Pakistan Journal of Pharmaceutical Sciences*, 36(3), 745–752.

Ho, E. (2004) Zinc deficiency, DNA damage and cancer risk. *Journal of Nutritional Biochemistry*, 15(10), 572–578.

Hopkins, A.L. (2008) Network pharmacology: the next paradigm in drug discovery. *Nature Chemical Biology*, 4(11), 682–690.

Hurrell, R. and Egli, I. (2010) Iron bioavailability and dietary reference values. *American Journal of Clinical Nutrition*, 91(5), 1461S–1467S.

Iniaghe, O.M., Malomo, S.O. and Adaikan, J.O. (2009) Haematological studies on the leaf extract of *Ficus sur* (Moraceae) in albino rats. *Journal of Cell and Animal Biology*, 3(9), 157–161.

Irinmwinuwa, S.C. and Afonne, O.J. (2022) Haemopoietic activity of solvent fractions of *Justicia secunda* Vahl leaf extract in phenylhydrazine-induced anaemic mice: superiority over ferrous sulphate and vitamin B12 standards. *African Journal of Pharmacy and Pharmacology*, 16(4), 63–72.

Janssen, T. and Vrijdaghs, A. (2020) The leaf and stem morphology of *Ficus sur* Forssk. *Blumea*, 65(2), 169–179.

Julián, I., Irurzun-Arana, I., Dz, J.V., Goñi-de-Cerio, F., González, M.Á. and Calvo, A. (2019) Network pharmacology applied to complex diseases. *Drug Discovery Today*, 24(12), 2189–2199.

Kassebaum, N.J. and GBD 2013 Anaemia Collaborators (2016) The global burden of anaemia. *Haematology/Oncology Clinics of North America*, 30(2), 247–308.

Kim, T.H., Kim, S.H., Lee, S.A. and Park, S.J. (2024) Current status and future prospects of network pharmacology in herbal medicine research. *Frontiers in Pharmacology*, 15, 1355462.

Koffi, N., Ernest, A., N'Guessan, J.D., Zirihi, G.N. and Coulibaly, A. (2013) Evaluation of the effects of the aqueous extract of *Justicia secunda* leaves on haematological parameters in rats. *European Journal of Scientific Research*, 95(2), 224–234.

Kone, M., Bamba, D., Yao Kouassi, A.S., Ouattara, D. and Fofie, N.B. (2012) Plants used in traditional management of anaemia in Cote d'Ivoire. *African Journal of Traditional, Complementary and Alternative Medicine*, 9(2), 216–221.

Koury, M.J. and Haase, V.H. (2015) Anaemia in kidney disease: harnessing hypoxia responses for therapy. *Nature Reviews Nephrology*, 11(7), 394–410.

Lawal, B., Shittu, O.K., Rotimi, S.O. and Akinola, O. (2016) In vivo antimalarial and biochemical effects of *Ficus sur* Thunb. (Moraceae) leaf extract. *Journal of Ethnopharmacology*, 194, 1020–1028.

Li, S. and Zhang, B. (2013) Traditional Chinese medicine network pharmacology: theory, methodology and application. *Chinese Journal of Natural Medicines*, 11(2), 110–120.

Menezes, F.S. and collaborators (2022) *Ficus sur* Forssk.: ethnopharmacological uses, biological activities and phytochemistry — a pan-African review. *Natural Product Research*, 36(21), 5582–5596.

Mgbemena, N.M., Onyekachi, I.J., Eze, P.M. and Chukwuemeka, P.O. (2022) Phytochemical screening and quantification of total phenolics and flavonoids in leaves and root bark of *Ficus sur* Forssk. from southeast Nigeria. *Asian Journal of Plant Science and Research*, 12(1), 22–30.

Muñoz, M., Acheson, A.G., Auerbach, M., Besser, M., Bhatt, D.L., Cunietti, E. and Flint, A. (2017) International consensus statement on the peri-operative management of anaemia and iron deficiency. *Anaesthesia*, 72(2), 233–247.

NMPPDB (2024) *Ficus sur*. *Nigerian Medicinal Plants and Phytochemicals Database.* Species ID: NMP-069. Available at: https://nmppdb.com.ng/species-details?specy=ficus-capensis [Accessed: April 2024].

Noor, F., Tahir ul Qamar, M., Ashfaq, U.A., Albutti, A., Alwashmi, A.S.S. and Aljasir, M.A. (2022) Network pharmacology approach for medicinal plants: review and assessment. *Pharmaceuticals,* 15(5), 572.

Obasohan, P.E., Walters, S.J., Jacques, R. and Khatab, K. (2022) The burden of anaemia in children under five years of age in Nigeria: a geospatial analysis. *PLOS ONE*, 17(1), e0262643.

Obeagu, E.I. (2021) Histopathological evaluation of the effects of *Ficus sur* leaf extract on liver, kidney and intestine of anaemic rats. *International Journal of Advanced Research in Biological Sciences*, 8(3), 55–62.

Okafor, C., Nweke, C.N., Nwosu, O.B. and Ugwu, C.C. (2021) Haematinic potential of ethanolic leaf extract of *Ficus sur* Thunb. in phenylhydrazine-induced anaemia in Wistar rats. *Nigerian Journal of Pharmaceutical Sciences,* 20(1), 11–22.

Olawale, F., Legoabe, L.J. and Olofinsan, K. (2022) Molecular docking analysis and haematinic potential of *Ficus sur* Forssk. (Moraceae) in experimentally induced anaemia. *South African Journal of Botany,* 151, 891–903.

Olusegun, A., Abolaji, A.O., Ojo, A.A., Ayodeji, A.A. and Oladele, J.O. (2023) Mineral element composition and nutritional characterisation of *Ficus sur* leaf and root bark. *African Journal of Food Science,* 17(4), 88–97.

Owolabi, A.O., Ibidun, O.O., Abegunrin, T.A. and Awe, O.I. (2022) Antibacterial activity and phytochemical characterisation of *Ficus sur* Forssk. methanol and aqueous extracts against drug-resistant clinical isolates. *West African Journal of Pharmacy*, 33(1), 47–57.

Oyewale, M.R.B., Osundahunsi, O.F. and Awolu, O.O. (2024) Modulatory effect of *Justicia secunda* leaf extract on hematological status, lipid profile, liver function and oxidative stress in Wistar rats. *Advances in Traditional Medicine*, 24, 531–540. doi:10.1007/s13596-023-00716-z.

Pandey, K.B. and Rizvi, S.I. (2011) Markers of oxidative stress in erythrocytes and plasma during aging in humans. *Oxidative Medicine and Cellular Longevity,* 4(2), 107–109.

Patle, N.K., Ranawat, L. and Bhure, S. (2021) Determination of total phenolic and total flavonoid content and FTIR studies on the extracts of Dillenia pentagyna Roxb. *Journal of Drug Delivery and Therapeutics*, 11(1), 116–121.

PMC9952096 (2023) Chemical characterisation and biological activities of *Justicia secunda* Vahl (Acanthaceae) leaf extracts: an integrated LC-MS and in vitro approach. *PubMed Central, National Library of Medicine.* Accessed April 2024.

PROTA (2019) *Ficus sur*. *Plant Resources of Tropical Africa.* Available at: https://uses. plantnet-project.org/en/Ficus_capensis_(PROTA) [Accessed: April 2024].

Radha, B., Singh, J. and Kumar, S. (2021) Atomic absorption spectroscopy for nutritional and mineral characterisation of selected medicinal plants from Western Himalayas. *Journal of Food Composition and Analysis*, 98, 103810.

Saidu, A.N., Mann, A. and Onuegbu, C.D. (2020) Phytochemical screening, anti-sickling and haematological effects of aqueous extract of *Ficus sur* root bark. *British Journal of Pharmaceutical Research*, 11(3), 1–12.

Sander, T., Freyss, J., von Korff, M., & Rufener, C. (2015). DataWarrior: An open-source program for chemistry aware data visualization and analysis. *Journal of Chemical Information and Modeling*, 55(2), 460–473. https://doi.org/10.1021/ci500588j

Sarmah, P., Boro, M.K. and Borah, J.C. (2025) FTIR profiling of ethnomedicinal plants from Northeast India with anti-anaemic applications. *Journal of Ethnopharmacology*, 325, 117800.

Shaibu, N.J., Abdullahi, M., Mohammed, S.I. and Bello, B.T. (2025) Phytochemical constituents and acute toxicity evaluation of methanol leaf extract of *Ficus sur* Forssk. in adult Wistar rats. *Toxicology Reports*, 12, 44–51.

Shaikh, J. R., & Patil, M. K. (2020). Qualitative tests for preliminary phytochemical screening: An overview. *International Journal of Chemical Studies*, 8(2), 603–608. https://doi.org/10.22271/chemi.2020.v8.i2i.8834

Shamim, M.Z., Ali, J., Sharma, P.K., Baboota, S., Singh, S. and Ali, M. (2022) FTIR spectroscopic analysis of selected medicinally important plants. *Journal of Drug Delivery and Therapeutics*, 12(2), 88–94.

Shannon, P., Markiel, A., Ozier, O., Baliga, N. S., Wang, J. T., Ramage, D., Amin, N., Schwikowski, B., & Ideker, T. (2003). Cytoscape: A software environment for integrated models of biomolecular interaction networks. *Genome Research*, 13(11), 2498–2504. https://doi.org/10.1101/gr.1239303

Sharma, N., Singh, L., Sharma, A. and Kumari, A. (2024) Network pharmacology and molecular docking to explore quercetin and kaempferol from Cinnamomum tamala against diabetic nephropathy. *Phytomedicine Plus*, 4(2), 100542.

Shi, Y., Mon, A.M., Wang, Y., Chin, Y.W. and Quek, Y. (2018) Ethnopharmacology and therapeutic potential of the genus Ficus: a review. *Journal of Ethnopharmacology*, 225, 100–110.

Singh, R., Borah, P., Dhar, P., Gogoi, G., Mahanta, S. and Talukdar, N.C. (2022) FTIR and HRLC-MS characterisation of a polyherbal formulation from Northeast India. *Journal of Ethnopharmacology*, 283, 114690.

Smith, B. C. (2011). *Fundamentals of Fourier transform infrared spectroscopy* (2nd ed.). CRC Press.

Smith, B.C. (2011) *Fundamentals of Fourier Transform Infrared Spectroscopy*, 2nd edn. CRC Press, Boca Raton.

Sofowora, A. (1993). *Medicinal plants and traditional medicine in Africa* (2nd ed.). Spectrum Books Ltd.

Sri Prakash, V., Venkata Subbaiah, G., Siva Rama Krishna Reddy, V. and Prasad, K.V.S.R.G. (2023) Network pharmacology and molecular docking to elucidate the therapeutic mechanisms of herbal anti-diabetic agents. *Journal of Ethnopharmacology*, 312, 116485.

Swiatek, L., Sieniawska, E., Rajtar, B., Swiatek, M., Polz-Dacewicz, M. and Przekora, A. (2023) Phytochemical characterisation, antioxidant, antiviral and anticancer activities of *Justicia secunda* Vahl extracts. *Molecules,* 28(3), 1418.

Szklarczyk, D., Kirsch, R., Koutrouli, M., Nastou, K., Mehryary, F., Hachilif, R., Gable, A. L., Fang, T., Doncheva, N. T., Pyysalo, S., Jensen, L. J., von Mering, C., & Bork, P. (2023). The STRING database in 2023: Protein–protein association networks and functional enrichment analyses for any of 12,499 organisms. *Nucleic Acids Research*, 51(D1), D638–D646. https://doi.org/10.1093/nar/gkac1000

Theiler, B.A., Revoltella, S., Zehl, M., Brecker, L., Staniek, A., Bauer, R., Ellmerer, E.P. and Merfort, I. (2014) Secundarellone A–C, novel chromene-type compounds from *Justicia secunda* Vahl. *Phytochemistry Letters,* 10, 82–85.

Tothova, Z., Krill, J., Young, S.F., Jin, Y. and Brugnara, C. (2021) STAT5A and STAT5B are required for normal erythropoiesis. *Blood,* 138(Suppl 1), 1032.

TRAMIL (2014) *Caribbean Herbal Pharmacopoeia: Justicia secunda Vahl Monograph*. TRAMIL Network. Available at: www.tramil.net [Accessed: April 2024].

Trease, G. E., & Evans, W. C. (2002). *Pharmacognosy* (15th ed.). Saunders Publishers.

Trott, O., & Olson, A. J. (2010). AutoDock Vina: Improving the speed and accuracy of docking with a new scoring function, efficient optimization, and multithreading. *Journal of Computational Chemistry*, 31(2), 455–461. https://doi.org/10.1002/jcc.21334

Uchegbu, L., Fasuan, T.O. and Okonkwo, C. (2023) Nutritional, phytochemical and GC-MS alkaloid characterisation of a response-surface-optimised *Ficus sur*/*Justicia secunda* functional tea. *Food Chemistry,* 404, 134612.

University of Nigeria Herbarium (2024) *Plant Identification/Authentication Certificate: Ficus sur Forssk.* Voucher No. UNN/11770. Department of Plant Science and Biotechnology, UNN, Nsukka. March 2026.

Welz, B. and Sperling, M. (1999) *Atomic Absorption Spectrometry*, 3rd edn. Wiley-VCH, Weinheim.

Weniger, B., Rouzier, M., Daguilh, R., Henrys, D., Henrys, J.H. and Anton, R. (1993) La médecine populaire dans le Plateau Central d'Haïti. *Journal of Ethnopharmacology*, 17(1), 13–30.

WHO (2007) *Prevention of Cardiovascular Disease: Guidelines for Assessment and Management of Total Cardiovascular Risk.* WHO, Geneva.

WHO (2011) *Quality Control Methods for Herbal Materials.* World Health Organization, Geneva.

WHO (2019) Haemoglobin concentrations for the diagnosis of anaemia and assessment of severity. *Vitamin and Mineral Nutrition Information System*. WHO/NMH/NHD/MNM/11.1. Geneva.

WHO (2023) *Anaemia*. World Health Organization Factsheet. Available at: https://www.who.int/news-room/fact-sheets/detail/anaemia [Accessed: February 2024].

Yao, W., Li, Y., Wu, J., Li, X. and Fang, M. (2023) Quercetin stabilises HIF-1α and promotes erythropoietin gene transcription in chronic kidney disease. *Phytomedicine*, 109, 154580.

Zhang, Y., Liang, R., Luo, W., Ma, J., Guo, B., Wang, T., Zhang, P. and Chen, X. (2022) Network pharmacology approach to decipher the mechanism of Danggui Buxue Tang in treating blood deficiency-associated anaemia. *Frontiers in Pharmacology*, 13, 861849.

Zvèrina, O., Ullaha, S., Cerveny, J. and Kominkova, M. (2023) HR-CS-GFAAS method validation for simultaneous determination of zinc and iron in plant materials. *Talanta*, 254, 124128.

APPENDICES

APPENDIX I: PLANT IDENTIFICATION AND AUTHENTICATION CERTIFICATE

The voucher specimen of Ficus sur Forssk. (Moraceae) used in this study was identified and authenticated at the Herbarium Unit, Department of Plant Science and Biotechnology, Faculty of Biological Sciences, University of Nigeria, Nsukka (UNN), and assigned Voucher No. UNN/11770. The certificate, issued to Mrs. Amara Nnadikwe and authenticated by Mr. Felix I. Nwafor (Curator/Plant Taxonomist, UNN Herbarium) on March 31, 2026, is reproduced below.

UNIVERSITY OF NIGERIA, NSUKKA

FACULTY OF BIOLOGICAL SCIENCES

DEPARTMENT OF PLANT SCIENCE AND BIOTECHNNOLOGY

HERBARIUM UNIT

March 31, 2026

To Whom It May Concern,

PLANT IDENTIFICATION/AUTHENTICATION CERTIFICATE

Issued to: Nnadikwe, Amara

Contact Address: Godfrey Okoye University, Enugu

This is to certify that the following plant was identified/authenticated and voucher specimens deposited at the University of Nigeria Herbarium (UNN) domiciled in the Department of Plant Science and Biotechnology, Faculty of Biological Sciences, University of Nigeria, Nsukka. The UNN is indexed in *Index Herbariorium* - A global directory of the world's herbaria (https://sweetgum.nybg.org/science/ih/herbarium-details/?irn=126760) and holds botanical collections from West African flora and borrowed samples from some of the reputable herbaria in the world. The detail of this collection(s) is as follows:

Scientific Name / Author	Family	Voucher N0
***Ficus sur* Forssk.**	**MORACEAE**	**UNN/11770**

Authenticated by

Felix 1. Nwafor
Curator/Plant Taxonomist
University of Nigeria Herbarium (UNN)
Contact: felix.nwafor@unn.edu.ng; 08036062242

Appendix Figure I.1. Plant Identification/Authentication Certificate for Ficus sur Forssk. (Voucher No. UNN/11770), University of Nigeria Herb

APPENDIX II: COMPOUND PROPERTIES AND ADME SCREENING DATA

Tables II.1 and II.2 present the full leaf-derived compound inventories for Ficus sur (reported in source literature as Ficus capensis Thunb., a synonym) and Justicia secunda, respectively, together with their DataWarrior-calculated physicochemical, drug-likeness, and toxicity-alert parameters used for in silico ADME-based virtual screening (Chapter Three). MW = molecular weight; cLogP = calculated partition coefficient; cLogS = calculated aqueous solubility; TPSA = topological polar surface area; DL = druglikeness score. Toxicity alerts summarise DataWarrior predictions for mutagenicity, tumorigenicity, reproductive effect, and irritant potential; compounds with no predicted alerts are marked "None".

Table II.1. Leaf-derived compounds of Ficus sur (F. capensis) subjected to ADME screening (n = 30).

No.	Compound	CID	MW	cLogP	TPSA	DL	Toxicity Alerts
1	n-Tricosane	12534	324.6	10.52	0.0	-20.40	None
2	n-Hexacosane	12407	366.7	11.88	0.0	-20.40	None
3	Cyclotetradecane	67524	196.4	6.36	0.0	-7.63	None
4	Triacontane	12535	422.8	13.70	0.0	-20.40	None
5	Limonene	439250	136.2	3.36	0.0	-21.86	Irrit:Low
6	Carvacrol	10364	150.2	2.85	20.2	-2.34	Irrit:High
7	α-Humulene (α-Caryophyllene)	5281520	204.4	6.24	0.0	-4.72	None
8	Caryophyllene oxide	1742210	220.4	4.05	12.5	-4.77	Tumor:Low; Repro:Low
9	Linalool	6549	154.3	3.23	20.2	-6.68	Muta:High; Irrit:High
10	3-Tetradecanone	69418	212.4	5.38	17.1	-20.88	Irrit:High
11	Geranylacetone	1549778	194.3	4.72	17.1	-4.59	Irrit:High
12	6,10,14-Trimethyl-2-pentadecanone	10408	268.5	6.49	17.1	-7.06	Irrit:High
13	trans-Geranylgeraniol	5281365	290.5	7.83	20.2	-3.38	None
14	n-Hexadecanoic acid (Palmitic acid)	985	256.4	6.06	37.3	-25.22	Tumor:High; Irrit:High
15	(E)-β-Ionone	5363741	192.3	3.22	17.1	-9.23	Tumor:High; Irrit:High
16	β-Caryophyllene	5281515	204.4	5.49	0.0	-6.48	None
17	Phytol	5280435	296.5	7.42	20.2	-3.77	None
18	Scytalone	162567	194.2	0.72	77.8	0.75	None
19	Gallic acid	370	170.1	0.11	98.0	-1.84	Muta:High; Repro:High
20	Protocatechuic acid	72	154.1	0.45	77.8	-1.84	Muta:High
21	Caffeic acid	689043	180.2	0.78	77.8	0.17	Muta:High; Tumor:High; Repro:High
22	p-Coumaric acid	637542	164.2	1.13	57.5	0.17	Repro:High
23	Ferulic acid	445858	194.2	1.06	66.8	0.28	Muta:High; Tumor:High; Repro:High
24	Chlorogenic acid	1794427	354.3	-0.77	164.8	-0.98	None
25	Ellagic acid	5281855	302.2	1.28	133.5	-1.60	None
26	Quercetin	5280343	302.2	1.49	127.5	-0.08	Muta:High; Tumor:High
27	Epicatechin (−)	72276	290.3	1.50	110.4	0.82	None
28	Stigmasterol	5280794	412.7	7.63	20.2	-4.47	None
29	Campesterol	173183	400.7	7.45	20.2	-4.47	None
30	Pheophytin a	14125	871.2	9.11	57.5	-11.22	None

Total: 30 leaf-derived compounds (18 GC-MS leaf essential oil + 9 HPLC-DAD leaf aqueous extract phenolics + 3 NMR/LC-MS leaf fractions). Compounds reported from non-leaf plant parts (stem bark, fruit, aerial roots, bark/latex) were excluded from screening.

Table II.2. Leaf-derived compounds of Justicia secunda subjected to ADME screening (n = 65).

No.	Compound	CID	MW	cLogP	TPSA	DL	Toxicity Alerts
31	p-Xylene	7809	106.2	2.95	0.0	-3.74	None
32	Desulphosinigrin	167907	279.3	0.56	110.4	-1.83	None
33	2,6,10-Trimethyltetradecane	522691	240.5	8.37	0.0	-20.40	None
34	Tridecane	12388	184.4	7.14	0.0	-20.40	None
35	2-Cyclohexylpiperidine	74782	167.3	3.28	12.5	-4.12	None
36	Phytol acetate	5282184	308.5	7.30	26.3	-39.70	None
37	Phytol	5280435	296.5	7.42	20.2	-3.77	None
38	Isophytol acetate	12958	338.6	8.61	26.3	-52.10	Muta:High; Tumor:High; Repro:High; Irrit:High
39	Benzyl butyl phthalate	2723	312.4	4.91	52.6	-4.38	None
40	Diisooctyl phthalate	26986	390.6	8.69	52.6	-8.18	None
41	Squalene	638072	410.7	13.10	0.0	-3.52	None
42	Ethyl palmitate	12366	284.5	6.90	26.3	-39.36	None
43	2,4-Di-tert-butylphenol	7311	206.3	4.48	20.2	-5.28	None
44	9,17-Octadecadienal (Z)-	5283476	264.4	6.59	17.1	-8.89	None
45	Linoleic acid ethyl ester	5282184	308.5	7.30	26.3	-39.70	None
46	Hexadecane	11006	226.4	8.25	0.0	-20.40	None
47	2,6-Dimethylheptadecane	522803	268.5	9.47	0.0	-20.40	None
48	Ethyl oleate	5363269	310.5	7.55	26.3	-43.11	None
49	Pristane	10547	296.6	9.88	0.0	-20.40	None
50	3-Methylnonane	18818	142.3	5.06	0.0	-20.40	None
51	Hexatriacontane	40480	507.0	16.40	0.0	-20.40	None
52	β-Caryophyllene	5281515	204.4	5.49	0.0	-6.48	None
53	β-Bisabolene	442495	204.4	5.49	0.0	-6.48	Irrit:Low
54	1-Hexadecanol	2682	242.4	6.26	20.2	-11.27	None
55	DEHP	4428	390.6	8.69	52.6	-8.18	None
56	α-Copaene	107898	204.4	5.49	0.0	-6.48	None
57	α-Humulene	5281520	204.4	6.24	0.0	-4.72	None
58	Palmitoleic acid	445638	254.4	5.81	37.3	-26.10	None
59	β-Farnesene	5318042	204.4	6.00	0.0	-6.00	None
60	Nerolidol	5284507	222.4	5.40	20.2	-6.38	Irrit:High
61	Piperine	638024	285.3	3.60	38.8	0.43	Repro:High
62	Diethyl phthalate	6781	222.2	2.30	52.6	-5.46	Muta:High; Tumor:High; Repro:High; Irrit:Low
63	5(1H)-Azulenone	12264	118.2	2.44	25.3	-0.40	None
64	γ-Elemene	442495	204.4	5.49	0.0	-6.48	None
65	Elaidic acid	637517	282.5	6.72	37.3	-28.97	None
66	9(1H)-Phenanthrone	68285	194.2	3.85	17.1	-2.16	None
67	Longifolene	61503	204.4	5.49	0.0	-6.48	None
68	2-Hydroxycyclopentadecanone	12672	240.4	4.79	37.3	-18.56	None
69	α-Patchoulene	442495	204.4	5.49	0.0	-6.48	None
70	Oleic acid	445639	282.5	6.72	37.3	-28.97	Muta:High; Tumor:High; Irrit:High
71	Methyl palmitate	8181	270.5	6.49	26.3	-35.36	None
72	Methyl oleate	5363269	296.5	7.09	26.3	-39.05	None
73	γ-Terpinene	11463	136.2	3.36	0.0	-21.86	Irrit:Low
74	p-Cymene	7463	134.2	3.50	0.0	-9.23	None
75	Decane	15600	142.3	5.06	0.0	-20.40	None
76	Aromadendrene	442495	204.4	5.49	0.0	-6.48	None
77	4-Tetradecene	537892	196.4	7.06	0.0	-20.40	None
78	Di-sec-butyl phthalate	6999	278.4	4.54	52.6	-4.71	None
79	Luteolin	5280445	286.2	1.99	107.2	0.28	None
80	Apigenin	5280443	270.2	2.34	87.0	0.28	Muta:High
81	Diosmetin	5281610	300.3	2.70	107.2	0.42	None
82	Quercetin	5280343	302.2	1.49	127.5	-0.08	Muta:High; Tumor:High
83	Kaempferol	5280863	286.2	1.90	107.2	0.27	None

No.	Compound	CID	MW	cLogP	TPSA	DL	Toxicity Alerts
84	Rutin (Quercetin-3-O-rutinoside)	5280805	610.5	-1.26	265.5	1.93	None
85	Luteolin-7-O-glucoside	5318037	448.4	0.18	190.0	0.72	None
86	Apigenin-7-O-glucoside	5318216	432.4	0.18	169.8	0.82	None
87	Luteolin-7-O-rutinoside	44259218	594.5	-1.24	244.9	1.96	None
88	Gallic acid	370	170.1	0.11	98.0	-1.84	Muta:High; Repro:High
89	Caffeic acid	689043	180.2	0.78	77.8	0.17	Muta:High; Tumor:High; Repro:High
90	Chlorogenic acid	1794427	354.3	-0.77	164.8	-0.98	None
91	Protocatechuic acid	72	154.1	0.45	77.8	-1.84	Muta:High
92	Syringic acid	10742	198.2	0.89	76.0	0.32	None
93	Salicylic acid	338	138.1	1.69	57.5	-0.96	Muta:High
94	Campesterol	173183	400.7	7.45	20.2	-4.47	None
95	Oleanolic acid	10494	456.7	6.06	57.5	-1.78	None

Total: 65 leaf-derived compounds (11 leaf methanolic-extract GC-MS + 37 leaf ethanolic/leaf-and-stem essential-oil/leaf FAME GC-MS + 17 LC-MS/MS leaf phenolic acids and flavonoids). Compounds reported only from stem or whole-plant material were excluded from screening.

APPENDIX III: RAW ATOMIC ABSORPTION SPECTROSCOPY (AAS) MINERAL DATA

Flame AAS analyses were performed on a Thermo Scientific iCE 3000 spectrometer (Central Science Laboratory, University of Nigeria, Nsukka) on 27 April 2026. Sample code CA denotes the Justicia secunda leaf extract and CB denotes the Ficus sur (F. capensis) leaf extract analysed in this study, consistent with the FTIR sample coding used in Appendix V. A third sample submitted in the same instrument batch (coded SA) belonged to a different researcher's plant material and is not part of this thesis; it has therefore been excluded from this appendix. Table III.1 summarises the corrected elemental concentrations (mg/L) read directly from the instrument printouts, together with the linear calibration fit (R^2) obtained for each element. Values marked 'C' in the original printouts (denoting readings outside the calibrated standard range) are reproduced as reported by the instrument software.

Table III.1. Corrected elemental concentrations (mg/L) of Justicia secunda (CA) and Ficus sur (CB) leaf extracts by flame AAS.

Element	Wavelength	CA – *J. secunda* (mg/L)	CB – *F. sur* (mg/L)	Calibration R^2
Ca	422.7 nm	80.1636 C	280.5601 C	0.9952
K	766.5 nm	25.0374 C	36.4417 C	0.9960
Na	589.0 nm	10.3443 C	16.3704 C	0.9970
Mg	285.2 nm	9.2325	10.0973	0.9953
Fe	248.3 nm	2.5411	2.6031	0.9974
Zn	213.9 nm	0.3951	0.5426	0.9983
Cu	324.8 nm	0.1554	0.1407	0.9773
Mn	279.5 nm	0.2733	0.3437	0.9999
Ni	232.0 nm	0.1152	0.1156	0.9999
Cr	357.9 nm	0.5774	0.6909	0.9996
Cd	228.8 nm	-0.2177 C	-0.2492 C	0.9997
Pb	217.0 nm	-0.0470 C	-0.6140 C	0.9925

'C' denotes a reading outside the range bracketed by the calibration standards, as flagged by the SOLAAR Data Station software. Negative readings for Cd and Pb indicate concentrations below the instrument's effective detection limit for the standards used.

Note: Cu was analysed in two separate runs; the values in Table III.1 are taken from the run with an acceptable calibration fit ($R^2 = 0.9773$). A repeat Cu run ($R^2 = 0.9895$) returned near-zero/negative corrected concentrations for CA and CB, consistent with values close to the method's practical detection limit at the dilution used.

APPENDIX IV: MOLECULAR DOCKING BINDING ENERGY SUMMARY AND INTERACTION DIAGRAMS

Molecular docking of the ADME-validated phytochemicals against their predicted blood- and anaemia-associated protein targets was performed in AutoDock Vina via PyRx. Table IV.1 reports the best binding free energy (ΔG, kcal/mol; Mode 1, lowest-energy pose) for each of the 23 phytochemical–target complexes generated. More negative ΔG values indicate stronger predicted binding affinity; complexes with ΔG ≤ −7.0 kcal/mol are marked ★ (strong binder).

Table IV.1. AutoDock Vina best binding free energies for phytochemical–target complexes.

S/N	Phytochemical	Protein Target	Best ΔG (kcal/mol)	Strong Binder
1	Apigenin	ATM	-8.2	★
2	Apigenin	NBN	-7.3	★
3	Bisabolene	FANCB	-5.3	
4	Bisabolene	FANCE	-4.9	
5	Bisabolene	JAK3	-5.6	
6	Bisabolene	PALB2	-4.8	
7	Caffeic acid	FANCC	-5.6	
8	Caffeic acid	HBA1	-6.2	
9	Ferulic acid	SMAD3 (6JYU)	-7.0	★
10	Ferulic acid	PARP1 (7KZP)	-5.9	
11	Ferulic acid	CDK6 (8OUY)	-5.7	
12	Luteolin	BRIP1	-6.8	
13	Luteolin	FANCD2	-7.7	★
14	Luteolin	RAG1	-7.8	★
15	p-Coumaric acid	FANCI	-4.7	
16	p-Coumaric acid	HBA2	-6.6	
17	p-Coumaric acid	SLC4A1	-4.7	
18	p-Coumaric acid	TERT	-5.7	
19	Piperine	BRCA1	-6.7	
20	Piperine	BRCA2	-8.4	★
21	Piperine	FANCA	-6.5	
22	Rutin	FANCF	-7.1	★
23	Rutin	SLX4	-6.5	

ΔG = binding free energy; RMSD (lower/upper bound) = 0.000 Å for all complexes by definition (reference pose). Ferulic acid targets identified by PDB accession code where the gene symbol alone was ambiguous.

Strongest binder overall: Piperine–BRCA2 (ΔG = −8.4 kcal/mol). Other strong binders (ΔG ≤ −7.0 kcal/mol): Apigenin–ATM (−8.2), Luteolin–RAG1 (−7.8), Luteolin–FANCD2 (−7.7), Apigenin–NBN (−7.3), Rutin–FANCF (−7.1), Ferulic acid–SMAD3/6JYU (−7.0).

Figures IV.1–IV.7 present the 2D interaction diagrams (BIOVIA Discovery Studio Visualizer v21.1.0) and 3D docking poses (PyRx/UCSF Chimera) for the seven strong-binder complexes ($\Delta G \leq -7.0$ kcal/mol) identified in Table IV.1. Interaction diagrams for the remaining 16 complexes are held in the full companion docking analysis report and can be inserted here if required for the defense copy.

Apigenin – ATM (ΔG = −8.2 kcal/mol)

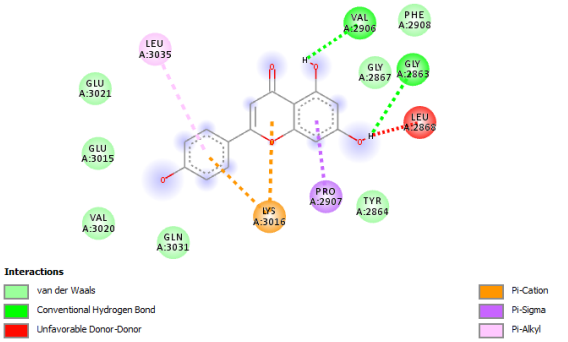

Appendix Figure IV.1a. Interaction diagram: Apigenin – ATM (ΔG = −8.2 kcal/mol).

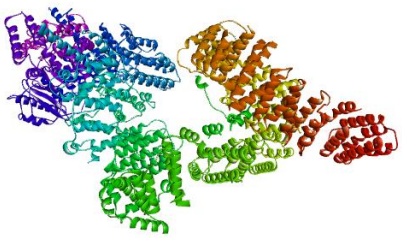

Appendix Figure IV.1b. Docking pose: Apigenin – ATM (ΔG = −8.2 kcal/mol).

Apigenin – NBN (ΔG = −7.3 kcal/mol)

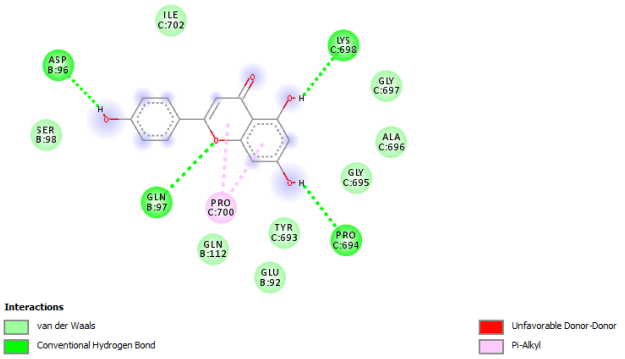

Appendix Figure IV.2a. Interaction diagram: Apigenin – NBN (ΔG = −7.3 kcal/mol).

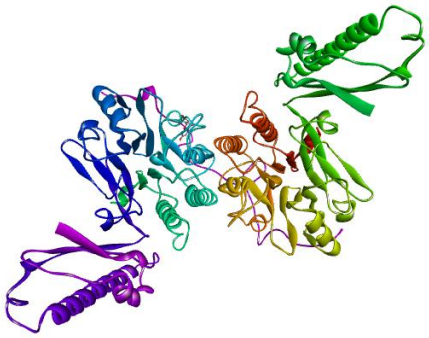

Appendix Figure IV.2b. Docking pose: Apigenin – NBN (ΔG = −7.3 kcal/mol).

Ferulic acid – SMAD3/6JYU (ΔG = −7.0 kcal/mol)

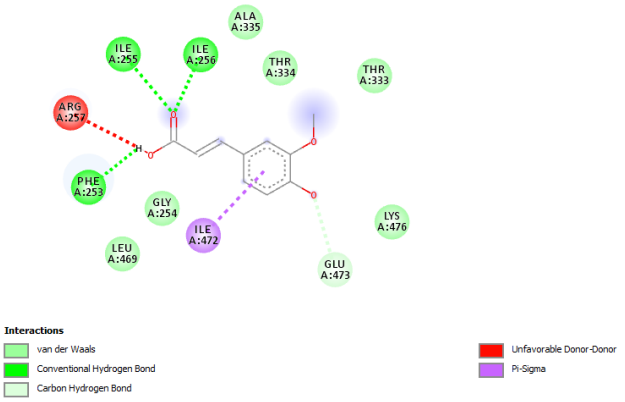

Appendix Figure IV.3a. Interaction diagram: Ferulic acid – SMAD3/6JYU (ΔG = −7.0 kcal/mol).

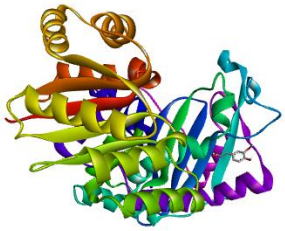

Appendix Figure IV.3b. Docking pose: Ferulic acid – SMAD3/6JYU (ΔG = −7.0 kcal/mol).

Luteolin – FANCD2 (ΔG = −7.7 kcal/mol)

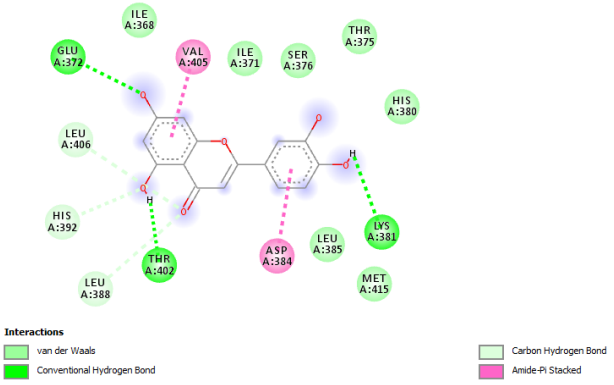

Appendix Figure IV.4a. Interaction diagram: Luteolin – FANCD2 (ΔG = −7.7 kcal/mol).

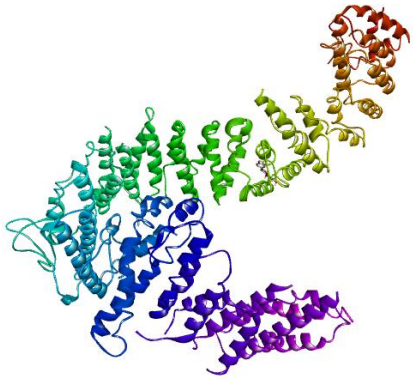

Appendix Figure IV.4b. Docking pose: Luteolin – FANCD2 (ΔG = −7.7 kcal/mol).

Luteolin – RAG1 (ΔG = −7.8 kcal/mol)

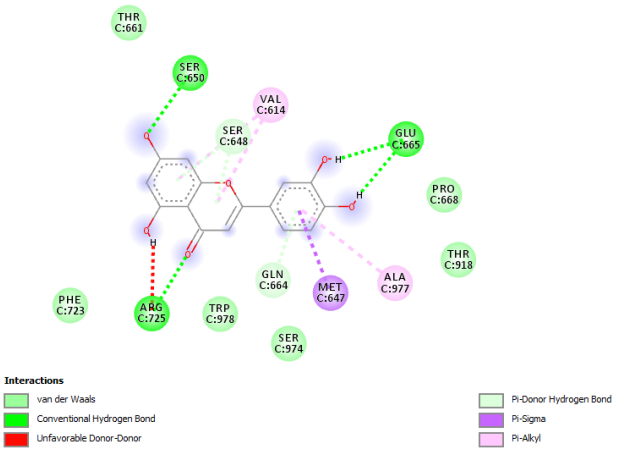

Appendix Figure IV.5a. Interaction diagram: Luteolin – RAG1 (ΔG = −7.8 kcal/mol).

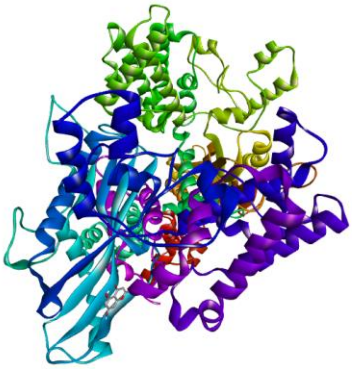

Appendix Figure IV.5b. Docking pose: Luteolin – RAG1 (ΔG = −7.8 kcal/mol).

Piperine – BRCA2 (ΔG = −8.4 kcal/mol, strongest overall)

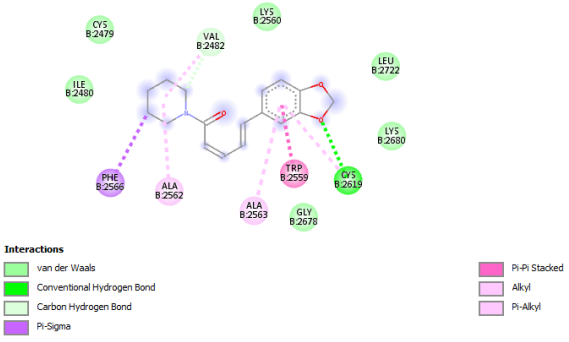

Appendix Figure IV.6a. Interaction diagram: Piperine – BRCA2 (ΔG = −8.4 kcal/mol, strongest overall).

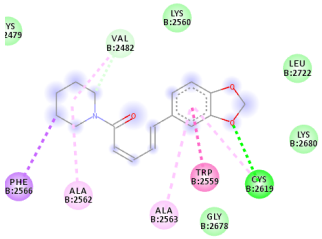

Appendix Figure IV.6b. Docking pose: Piperine – BRCA2 (ΔG = −8.4 kcal/mol, strongest overall).

Rutin – FANCF (ΔG = −7.1 kcal/mol)

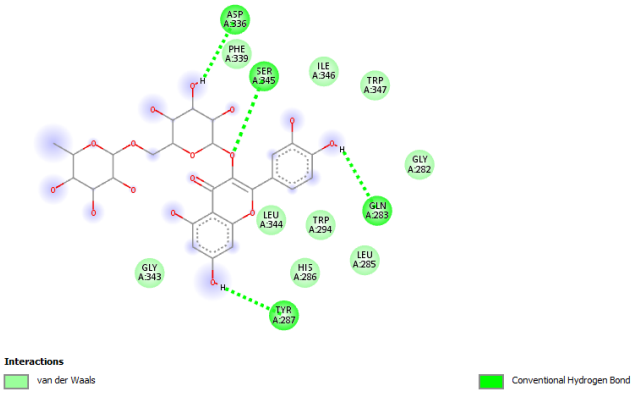

Appendix Figure IV.7a. Interaction diagram: Rutin – FANCF (ΔG = −7.1 kcal/mol).

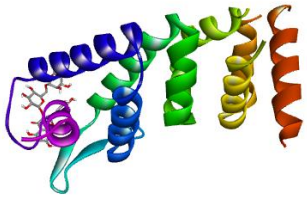

Appendix Figure IV.7b. Docking pose: Rutin – FANCF (ΔG = −7.1 kcal/mol).

APPENDIX V: SUPPLEMENTARY FTIR-ATR SPECTRA AND PEAK DATA

FTIR-ATR spectra were recorded over the range 4000–400 cm^{-1} for the leaf extracts of Justicia secunda (sample CA) and Ficus sur (sample CB), consistent with the AAS sample coding used in Appendix III. A third spectrum (sample SA), submitted in the same instrument batch, belonged to a different researcher's plant material and has been excluded as it is not part of this thesis. The full instrument-generated spectra and automated peak-find outputs (Region: 4000.00–400.00 cm^{-1}; Sensitivity: 50) are reproduced below, supplementary to the functional-group assignments discussed in Chapter Four.

Justicia secunda – Extract CA

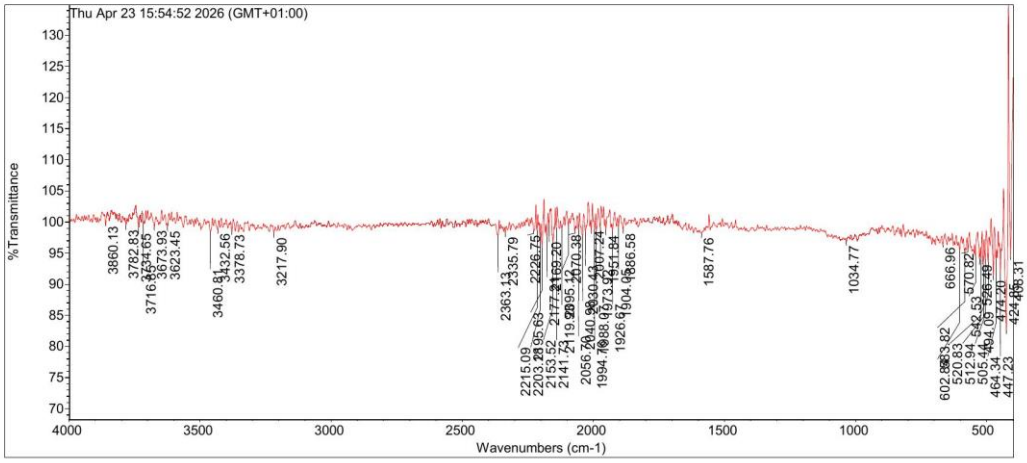

Thu Apr 23 15:56:52 2026 (GMT+01:00)
FIND PEAKS:
Spectrum: Thu Apr 23 15:54:52 2026 (GMT+01:00)
Region: 4000.00 400.00
Absolute threshold: 134.807
Sensitivity: 50
Peak list:

Position:	408.31	Intensity:	94.371
Position:	424.85	Intensity:	82.567
Position:	447.23	Intensity:	91.952
Position:	464.34	Intensity:	94.008
Position:	474.20	Intensity:	91.309
Position:	494.09	Intensity:	93.587
Position:	505.44	Intensity:	93.996

Appendix Figure V.1. FTIR-ATR transmittance spectrum (4000–400 cm^{-1}) of Justicia secunda – Extract CA.

Absolute threshold: 134.807. Peak list (position, cm^{-1} / % transmittance):

Peak (cm^{-1} / %T)	Peak (cm^{-1} / %T)	Peak (cm^{-1} / %T)	Peak (cm^{-1} / %T)
408.31 / 94.37	424.85 / 82.57	447.23 / 91.95	464.34 / 94.01
474.20 / 91.31	494.09 / 93.59	505.44 / 94.00	512.94 / 93.02
520.83 / 93.94	526.49 / 94.02	542.53 / 94.46	570.82 / 95.57
583.82 / 95.37	602.84 / 95.48	666.96 / 96.22	1034.77 / 96.79
1587.76 / 98.22	1886.58 / 98.79	1904.05 / 99.14	1926.67 / 98.76
1951.84 / 98.70	1973.92 / 99.08	1988.07 / 98.55	1994.76 / 98.84
2007.24 / 98.30	2030.43 / 98.41	2040.98 / 97.72	2056.70 / 98.84
2070.38 / 98.47	2095.12 / 99.45	2119.93 / 98.94	2141.73 / 99.02
2153.52 / 96.67	2169.20 / 99.49	2177.21 / 97.61	2195.63 / 95.92
2203.18 / 97.70	2215.09 / 98.66	2226.75 / 98.55	2335.79 / 98.24
2363.13 / 97.79	3217.90 / 98.35	3378.73 / 98.38	3432.56 / 98.67
3460.81 / 98.55	3623.45 / 99.33	3673.93 / 99.17	3716.85 / 99.69
3734.65 / 98.94	3782.83 / 99.52	3860.13 / 99.45	

Ficus sur – Extract CB

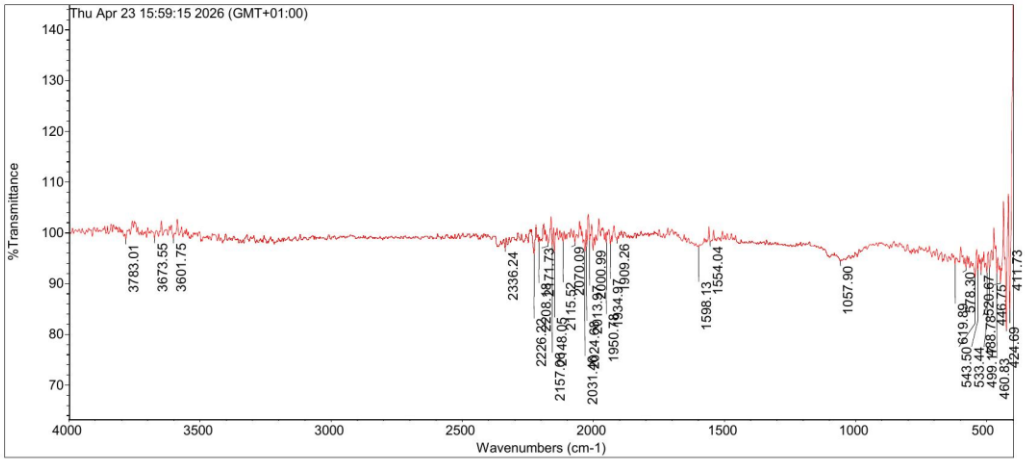

Thu Apr 23 16:03:55 2026 (GMT+01:00)
FIND PEAKS:
Spectrum: Thu Apr 23 15:59:15 2026 (GMT+01:00)
Region: 4000.00 400.00
Absolute threshold: 144.705
Sensitivity: 50
Peak list:

Position:	411.73	Intensity:	84.703
Position:	424.69	Intensity:	80.934
Position:	446.75	Intensity:	90.272
Position:	460.83	Intensity:	92.045
Position:	488.78	Intensity:	93.100
Position:	499.17	Intensity:	92.089
Position:	520.67	Intensity:	92.152

Appendix Figure V.2. FTIR-ATR transmittance spectrum (4000–400 cm⁻¹) of Ficus sur – Extract CB.

Absolute threshold: 144.705. Peak list (position, cm⁻¹ / % transmittance):

Peak (cm⁻¹ / %T)	Peak (cm⁻¹ / %T)	Peak (cm⁻¹ / %T)	Peak (cm⁻¹ / %T)
411.73 / 84.70	424.69 / 80.93	446.75 / 90.27	460.83 / 92.05
488.78 / 93.10	499.17 / 92.09	520.67 / 92.15	533.44 / 92.66
543.50 / 91.27	578.30 / 93.13	619.89 / 93.74	1057.90 / 94.40
1554.04 / 98.21	1598.13 / 97.12	1909.26 / 98.42	1934.97 / 97.81
1950.78 / 98.05	2000.99 / 96.69	2013.97 / 98.43	2024.68 / 97.22
2031.46 / 96.32	2070.09 / 98.05	2115.52 / 98.22	2148.05 / 96.17
2157.06 / 97.38	2171.73 / 97.92	2208.18 / 98.16	2226.22 / 95.87
2336.24 / 96.82	3601.75 / 98.88	3673.55 / 98.87	3783.01 / 98.74